Effect of Wavelength Tuning Material and CO_2 Supply On *Dunaliella Salina* Growth in Photobioreactor

By

Hatice BURAK

BSc, in Chemical Engineering, Izmir Institute of Technology, Turkey, 2010

MSc, in Chemical and Biological Engineering, University of Sheffield, UK, 2013

Thesis submitted in part fulfilment of the requirement for the degree of Doctor of Philosophy

Department of Chemical and Biological Engineering

Department of Molecular Biology and Biotechnology

The University of Sheffield, UK

June, 2018

Declaration

This is the declaration to confirm that all the work in this thesis my own effort. Other sourced used in the thesis have been acknowledged.

Signed by:

Hatice BURAK

Acknowledgments

"Being a candle is not easy: In order to give light one must first burn" Mevlana (Rumi)

The completion of this undertaken course could not have been possible without the participation and assistance of so many kind hearted people whose names may not all be numerated. I really appreciate to my supervisors; Dr. Alan Dunbar and Dr. James Gilmour with their excessive guidance, constant encouragements and invaluable contributions throughout the course are so great that, even my most profound gratitude is not enough. I also owe to my deepest gratitude to my sponsor, Turkish Government and Educational Ministry giving this opportunity to me. I am really fortunate that I have had a preciously great technical experience in the University of Sheffield, the Department of Chemical and Biological Engineering and the kind Algae Research Group. Furthermore, a massive thanks to molecular biology lab members and Alan Dunbar's group friends; Adnan Al-Mousawi, Abdullah Al-Temaimi, Chankyu Kwak, Murtakab Al-Hejjaj, and CBE lab technicians for their immense support for my project.

Last but not least, have such a lovely family who always keeps a good eye on me in every step of my life to reach this point, is always become an irreplaceable treasure for me and makes me feel like the luckiest person in the world. Therefore, I could not find an appropriate word to express my feelings how truly grateful I am to every one of you. I am honoured to say my gratitudes to my husband Fatih Burak, my mom, my dad, and my brother.

To my beloved daughter BILGE CANAN…

Abstract

The purpose of this research project is to investigate the limitations to algal growth, *Dunaliella salina* CCAP 19-30, by overcoming photosynthetic parameters such as CO_2 supply, O_2 accumulation and light intensity. Therefore, this project aims to enhance *D. salina* growth by combining wavelength tuning material and supplying an optimum CO_2 gas to the system. A breakthrough wavelength shifting material technology will help to increase the amount of light utilized by chlorophyll pigments.

Wavelength tuning can be performed using fluorophores which will absorb the unutilised light at a certain wavelength and re-emit it at a longer wavelength as useful light; therefore, Coumarin 1 and 1,2-Diphenylacetylene were selected for UV to blue light conversion; whereas, Bestoil Red 5B and Bestoil Orange 2G were chosen for green to red light conversion. Wavelength tuning materials were generated by mixing different concentration of these organic dyes with various solvents (THF, toluene, chloroform and chlorobenzene), polymer (PMMA) or PDMS which will give robustness to generated material.

Upon testing, using a Coumarin 1 film resulted in more efficient than 1,2-Diphenylacetylene at absorbing between 320 -400 nm and emitting between 400-550 nm. Also, Bestoil Orange 2G exhibited better mixing and absorption property than Bestoil Red 5B. It absorbed green light and re-emit red light between 620 nm and 780 nm. These two dyes give better results since *D. salina* absorbs the light between 400-500 nm and 630-680 nm.

Incorporating these wavelength tuning materials into the system increases the algal growth by 17.6% and 11.2% with UV to blue light conversion and green to red light conversion, respectively, for small scale (50 ml cell culture flasks) algae growth. Moreover, using fine-bubble raises the mass transfer and mixing; hence the growth increases by more than double the amount compared to non-aerated system.

D. salina growth in designed 3L photobioreactor was divided into two group as air supply and CO_2 supply in order to compare the effect of wavelength shifting material

and CO_2 amount, respectively. According to the air supplied algae growth results, reactor coated with Coumarin wavelength shifting materials produced the highest biomass with a final O

D_{595nm} value of 1.01 (26 days) among all other growth conditions as well as the Nile Red analysis and the fluorescent microscope images of *Dunaliella* cells supports this highest growth. Moreover, produced the most neutral lipid is also highest for the reactor with Coumarin shifting material applied at 0.31 µg ml^{-1} which is about 31.42% lipid.

Different CO_2 (air i.e.0.03% CO_2, 0.5%, 1%, 5% and 10%) supplied reactor showed a similar growth pattern for individual wavelength shifting material at diverse CO_2 concentration. However, Coumarin material demonstrated the highest OD_{595nm} growth in each dose as 0.931, 0.914, 0.939 and 0.936 at 595nm for 0.5%, 1%, 5% and 10%, respectively. Moreover, the growth period was decreased by half compared to the air supplied *D. salina* cultures. Apart from the 1% CO_2 dosed culture, the reactor with Coumarin shifting material applied indicated the highest Nile Red fluorescence intensity as well as dry cell weight lipid percentage.

Consequently, it was concluded that the Coumarin wavelength tuning material was demonstrated the best performance in terms of OD and the high density achieved in the *D. salina* cultures can be seen from the before and after photographs of the reactors for each experiment. *D. salina* produces β-carotene under stressed conditions and this is seen as green lipid dots inside the cells in fluorescence microscope images. UV light has detrimental effect on *D. salina* cell which was observed both in small and large scale algae growth.

Table of Contents

Acknowledgments iii

Abstract 1

CHAPTER 1: LITERATURE REVIEW 16

1.1. Introduction 17

1.1.1. Objectives of the Project 18

1.2. What Are Microalgae? 18

1.2.1. Photosynthesis in Microalgae 20

1.2.2. Limitations of Photosynthesis 25

1.2.3. *Dunaliella salina* as Algal Species 27

1.3. Utilising Solar Radiation 29

1.3.1. Wavelength Tuning Films 31

1.3.1.1. Quantum Dots 35

1.3.1.2. Organic Fluorophores 36

1.3.2. Working Principle of Wavelength Tuning Films 36

1. 4. Algae Growth Systems 38

1.4.1. A Brief Overview of Algae Growth Systems 38

1.4.2. Open Raceway Ponds 39

1.4.3. Closed Photobioreactors 40

1.4.4. Airlift Loop Photobioreactors as Proposed Reactor 43

CHAPTER 2.
FABRICATION OF WAVELENGTH TUNING MATERIALS 46

2.1. Introduction 47

2.2. Materials and Methods 48

2.2.1. Fabrication of Wavelength Tuning Materials 48

2.3. Results and Discussion 57

2.3.1. Wavelength Tuning Material Analysis 57

2.4. Conclusion 71

CHAPTER 3.
DESIGNING PHOTOBIOREACTOR FOR *DUNALIELLA SALINA* GROWTH 72
3.1. Photobioreactor Design 73
3.4.1. Small scale reactor and its coating process 74
3.4.2. Fine bubble addition to the small culture reactors 76
3.4.3. 3L flat plate photobioreactor 77
3.2. Conclusion 81
CHAPTER 4.
MATERIALS AND METHODS FOR DUNALIELLA SALINA GROWTH 82
4.1. *Dunaliella salina* Medium 83
4.2. pH measurements 85
4.3. CELL DENSITY MEASUREMENT 85
4.3.1. Spectrophotometer 85
4.3.2. Dry weight calculations versus OD concentration 86
4.4. LIPID DETERMINATION 88
4.4.1. Nile Red fluorescence for neutral lipid quantification 88
4.4.2. TRIOLEIN CALIBRATION CURVE 95
4.5. FLUORESCENT LIGHT MICROSCOPE IMAGING 97
4.6. CULTURE CONDITIONS AND MAINTENANCE 99
4.6.1. CULTURE MAINTENANCE 99
4.6.2. MBB H-FLOOR GROWTH ROOM 100
4.7. EXPERIMENTAL SET-UP AND MATERIALS 101
4.7.1 SPECTRAL MEASUREMENTS LIGHT SOURCES 101
4.7.2. COATING OF REACTORS 102
4.7.3. PHOTOBIOREACTOR CLEANING 102
4.7.4. ALGAL GROWTH SYSTEM SET-UP 103
CHAPTER 5: ALGAE GROWTH WITH AIR SUPPLY 107
5.1. Introduction 108
5.2. Results of *Dunaliella salina* growth with air supply 110
5.2.1. *D. salina* growth in small scale using cell culture flasks 111

5.2.2. *D. salina* growth in large scale - 3L photobioreactor 117
5.2.3. Determination of Neutral Lipid in 3L photobioreactor cultures using Nile Red 121
5.2.3.4. Correlation between OD and Cell Dry weight 126
5.2.4. Fluorescence Microscope images to monitor lipid droplets 128
5.3. Discussion 129
CHAPTER 6: ALGAE GROWTH WITH CO_2 SUPPLY 133
6.1. Introduction 134
6.2. Results of *Dunaliella salina* growth with CO_2 supply 135
6.2.1. *D. salina* growth in 3L photobioreactor with 1% CO_2 supply 136
6.2.2. *D. salina* growth in 3L photobioreactor with 5% CO_2 supply 139
6.2.3. *D. salina* growth in 3L photobioreactor with 10% CO_2 supply 145
6.2.4. *D. salina* growth in 3L photobioreactor with 0.5% CO_2 supply 149
6.3. Discussion 154
CHAPTER 7: CONCLUSIONS AND FUTURE WORK 157
7.1. CONCLUSION 158
7.2. Future Work 162
REFERENCES 166
APPENDIX 174
Appendix 1. 174
Appendix 2. 176
Appendix 3. 176
Appendix 4 177
Appendix 5 178
Appendix 6. 179

List of Figures

Figure 1. 1. Calvin cycle. Image is adapted from 'Photosynthesis' book written by. (Kohen et al., 1995)..... 21
Figure 1. 2. 13a - *D. salina* spp. *salina* fo. *salina*; 13b - *D. salina* spp. *salina* fo. *magna*; 13c - *D. salina* ssp. *salina* fo. *oblonga*; 13d - *D. salina* spp. *salina* spp. *sibirica* (Ben-Amotz and Avron, 1992)..... 27
Figure 1. 3. Images of various *D.* salina species, isolated by Teodoresco, grown at different salinities; A – 1.5 M NaCl, B and C – 4.5 M NaCl (Ben-Amotz et al., 2009) 29
Figure 1. 4. Direct Normal Spectral Irradiance on 37° Tilted Sun-Facing Surface (ASTM, 2012)..... 30
Figure 1. 5. Pathways of (1) incident photons (2) re-emitted directly with higher quantum yield (3); reflected through back to edge (4) and may exit through the sides (5). Without entering the material, it may reflect from surface (6). Transmit directly through another surface (7). Escape regarding Brewster angle (8) or absorbed by the host matrix (9) (Rowan et al., 2008, Mohsenpour et al., 2012) 34
Figure 1. 6. The schematic representation of Stokes Shift; a photon is absorbed and atom jumps to exited state (S_2), and then relaxes to intermediate (S_1) before returning ground state (S_0) (Lakowicz, 2006) 37
Figure 1. 7. Several photobioreactors for algae growth; (a) flat plate, (b) tubular, (c) bubble column and (d) air-lift (ALB) (Duan and Shi, 2014) 41
Figure 1. 8. Representative image of ALB associated with wavelength shifting material and bubbling technology proposed by Dr. Alan Dunbar. 43
Figure 1. 9. Illustration of light and dark zones inside the photobioreactor as a result of high cell concentration (Ben-Amotz et al., 2009)..... 45

Figure 2. 1. Direct and global spectral irradiance on 37^o tilted sun-facing surface (ASTM, 2012) and absorbance spectrum of chlorophylls inside *D. salina*. 47
Figure 2. 2. Spin coating apparatus – Laurell Technologies Corporation used for the coating the microscope slides with prepared dye/solvent solutions..... 49

Figure 2. 3. Construsted PDMS mould used to cure the PDMS/dye mixtures. The base of the mould is a thick clear glass and the edges of the mould is made using microscope slides. The slides were stuck to the base glass using Parafilm paraffin (melted inside the oven). 52
Figure 2. 4. Spectral test instruments Ocean Optics used for the absorption measurements of the produced wavelength shifting materials. 55
Figure 2. 5. Optical layout of FluoroMax 4 machine where; 1- Xenon lamp, 1a- Xenon lamp power supply, 1b – Xenon flash lamp, 2- Excitation monochromator, 3- Sample holder, 4- Emission monochromator, 5- Signal detector, 6- Reference detector and 7- Instrument controller. (Image is adapted from user manual of FluoroMax 4)..... 56
Figure 2. 6. Absorption spectra of Coumarin1 solutions at different Coumarin 1(C) /THF ratios 58
Figure 2. 7. Absorption spectra of 1,2-Diphenylacetylene solutions at diverse 1,2-Diphenylacetylene (D) / THF ratios 58
Figure 2. 8. Absorption patterns of Coumarin 1(C) /PMMA (P) and 1,2-Diphenylacetylene (D)/PMMA (P) mixtures at discrete rates. 60
Figure 2. 9. Absorption result of coating (film) of Coumarin 1 - toluene - PMMA mixture with different Coumarin 1/PMMA percentages 61
Figure 2. 10. (A) Absorption and (B) emission spectra of different Coumarin/PDMS mixtures. C represents Coumarin 1; and initial concentrations (0.1, 0.5, and 1) represent Coumarin 1/THF ratios..... 62
Figure 2. 11. Fabricated Coumarin 1/ PDMS shifting materials at different mixture percentages..... 63
Figure 2. 12. Absorption graphs of Bestoil Orange 2G and Bestoil Red 5B mixtures with THF as solution..... 64
Figure 2. 13. Absorption curves of PMMA (P) mixtures with Bestoil Orange 2G (O) and Bestoil Red 5B (R) as solution..... 65
Figure 2. 14. (A) Absorption and (B) emission pattern of Bestoil Red 5B (R) mixtures with PDMS. Initial concentrations (1 and 1.5) represent Bestoil Red 5B/THF ratios. 66
Figure 2. 15. Mixture sample of Bestoil Red 5B with PDMS 67

Figure 2. 16. (A) Absorption and (B) emission pattern of Bestoil Orange 2G (O) mixtures with PDMS. Initial concentrations (0.5 and 1) represent Bestoil Orange 2G/THF ratios. 68
Figure 2. 17. Fabricated Bestoil Orange 2G (O) / PDMS shifting materials at different mixture percentages 69
Figure 2. 18. Absorption/ emission graph of Bestoil Orange 2G (O) /Chlorobenzene mixed with PDMS. Initial concentrations (0.5 and 1) represent Bestoil Orange 2G (O) /Chlorobenzene ratios..... 70
Figure 2. 19. Absorption/ emission graph of Bestoil Orange 2G (O)/ Chloroform mixed with PDMS. Initial concentrations (0.5 and 1) represent Bestoil Orange 2G(O) /Chloroform ratios. 70

Figure 3. 1. Algae growth systems (a) UV light box, (b) visible light filter to cut the light 400nm over and (c) scheme of UV light box..... 73
Figure 3. 2. Intensities of UV lights inside UV light box (old and new replacements) and black box (long wave and short wave) and absorbance of *D. salina* 74
Figure 3. 3. Intensities of white lights in UV light box (old and new replacements) and H-floor growth room and absorbance of *D. salina* 75
Figure 3. 4. (a) The wavelength tuning materials and their arrangement inside; (b) the UV light box (transilluminator) 76
Figure 3. 5. Introducing microbubble technology to algal growth system (a) growth set-up and (b) sparger used in the experiment 77
Figure 3. 6. Technical drawing of 3L flat plate photo-bioreactor design. (Bangert, 2013) 78
Figure 3. 7. Scheme of experimental set-up for *Dunaliella salina* growth (a) Design of the growth chamber showing the dark enclosure, baffles to allow air circulation. Note the front is shown as transparent and only one light box is shown for clarity. (b) Plan view of the reactor and light source positioning within growth chamber. For control experiments no wavelength shifting material was present..... 79
Figure 3. 8. Emission spectra of the white and UV light inside the light box 80

Figure 4. 1Dry weight vs OD concentration calibration curve of *Dunaliella salina*. 88

Figure 4. 2. Standard addition Triolein concentration versus Nile Red fluorescence intensity calibration curve 97
Figure 4. 3. MBB H-Floor Growth room is used to keep subcultures and sample flasks after each experimental run 99
Figure 4. 4. Intensities of lights in UV light box (old and new replacements) and H-floor growth room and absorbance of *D. salina* 100
Figure 4. 5. Culture flask and the 3L photobioreactor used in the experiments 103
Figure 4. 6. Algae growth systems (a) UV light box, (b) closed system black box, (c) H-floor growth room and (d) scheme of large growth chamber and wavelength shifting orientations inside the chamber 104
Figure 4. 7. Introducing fine-bubble technology to algal growth system (a) growth set-up and (b) sparger used in the experiment 105

Figure 5. 1. Absorption/ emission spectra of the wavelength tuning materials used in the algae growth in cell culture flasks. C coating means that Coumarin- THF mixture was coated on the glass. C+ PDMS means that mixture of Coumarin and THF was combined and cured together with PDMS. O+PDMS means that mixture of Bestoil Orange 2G and THF was combined and cured together with PDMS. 109
Figure 5. 2. Growth rate of *D. salina* under 24 h (A) only UV light and (B) both UV and white light illumination with and without wavelength shifting material 112
Figure 5. 3. Growth pattern of *D. salina* under 24h UV and white light illumination using double amount of $NaHCO_3$. C coating means that Coumarin- THF mixture was coated on the glass. C+ PDMS means that mixture of Coumarin and THF was combined and cured together with PDMS. O+PDMS means that mixture of Bestoil Orange 2G and THF was combined and cured together with PDMS. 113
Figure 5. 4. Influence of high temperature on *D. salina* growth 114
Figure 5. 5. Microscopic images of *D. salina* at different salinity. The image was taken using a Nikon Eclipse E400 Microscope (phase 2 – 40X) endowed with a Nikon DXM1200 Digital Camera. The camera was attached to a software programme named LUCIA G Software and images were saved using this software with parameters; Red: 44, Green: 68, Blue: 72, Gain: 0, Gamma: 1, Offset:0, Exposure: 64ms. Sample

preparation method was the same as explained for the Fluorescence light microscope in Section 4.5 Materials and methods Chapter..... 115
Figure 5. 6. Effect of fine bubbles and carbon amount on algae growth. B.C. represents bicarbonate; A. indicates aerated and N.A. indicates non-aerated..... 116
Figure 5. 7. Emission spectra of the white and UV light inside the light box 117
Figure 5. 8. Light transfer from the 3L photobioreactor with and without wavelength shifting materials..... 118
Figure 5. 9. Measuring the light transmission of the reactor with coating either UV to blue shifting material or green to red shifting material..... 118
Figure 5. 10. Growth curves of control and coated reactors. Control1 is done without shifting material but using both UV and white light in order to see the UV light effect which causes cell death in a few days; Control2 is done without wavelength shifting materials and only with white light; UV to blue wavelength tuning is done with only Coumarin 1 material and both light sources on; green to red wavelength tuning is done with only Bestoil Orange 2G material and only white light on; and for the final one both Coumarin 1 and Bestoil Orange 2G materials used with both lights on..... 119
Figure 5. 11. Images of the experimental runs at the starting and final days: (a) Control 2, (b) UV to blue wavelength tuning, (c) green to red wavelength tuning (d) and both UV to blue and green to red wavelength tuning. 121
Figure 5. 12. Optimization of cell concentration of *D. salina* and the determination of Nile Red staining peak time. Each column symbolises the normalised value of every single concentration (100 (pure sample), 87.5, 75, 62.5, 50, 32.5, 25, 12.5 %) 123
Figure 5. 13. Optimization of Nile Red dye concentration for staining 75% concentrated *D. salina* samples. Nile Red staining readings were taken at diverse times 10, 15, 20, 25 and 30 minutes. The error bars symbolise the technical repeats (3 replicates) of four stained and four unstained readings. 124
Figure 5. 14. Standard addition Triolein concentration versus Nile Red fluorescence intensity calibration curve..... 126
Figure 5. 15. Dry weight vs OD concentration calibration curve of *D. salina* 126
Figure 5. 16. Fluorescence microscopy images (both bright field and coloured) of *D. salina* stained with Nile Red after growth under different light intensities using different wavelength shifting materials. A) *D. salina* cells grown under normal

condition without using any wavelength shifting material. B) *D. salina* cells grown under stress condition with more blue light using Coumarin shifting material. C) *D.salina* cells grown under more red light using Bestoil 2G wavelength shifting material. D) *D. salina* cells grown under more blue and red light using both Coumarin and Bestoil 2G wavelength shifting materials. 128

Figure 6. 1. Growth Curves of 1% CO_2 supplied control and coated reactors. The Control was measured without any wavelength shifting materials and only with white light; UV to blue wavelength tuning is measured with only Coumarin 1 material and both UV and white lights on; green to red wavelength tuning is measured with only Bestoil Orange 2G material and only white light on; and for the final one both Coumarin 1 and Bestoil Orange 2G materials were used with both lights on. 135
Figure 6. 2. Images of the experimental runs at the starting and final days: (a) Control, (b) UV to blue wavelength tuning, (c) green to red wavelength tuning (d) and both UV to blue and green to red wavelength tuning. 136
Figure 6. 3. Fluorescence microscopy images (both bright field and coloured) of 1% CO_2 supplied *Dunaliella salina* CCAP 19/30 stained with Nile Red after growth under different light intensities using different wavelength shifting materials. A) *D. salina* cells grown under normal condition without using any wavelength shifting material. B) *D. salina* cells grown under stress condition with more blue light using Coumarin shifting material. C) *D. salina* cells grown under more red light using Bestoil 2G wavelength shifting material. D) *D. salina* cells grown under more blue and red light using both Coumarin and Bestoil 2G wavelength shifting materials. 138
Figure 6. 4. Growth Curves of 5% CO_2 supplied control and coated reactors. Control is done without wavelength shifting materials and only with white light; UV to blue wavelength tuning is done with only Coumarin 1 material and both lights on; green to red wavelength tuning is done with only Bestoil Orange 2G material and only white light on; and for the final one both Coumarin 1 and Bestoil Orange 2G materials were used with both lights on. 140
Figure 6. 5. Images of the experimental runs at the starting and final days: (a) Control, (b) UV to blue wavelength tuning, (c) green to red wavelength tuning (d) and both UV to blue and green to red wavelength tuning. 141

Figure 6. 6. Fluorescence microscopy images (both bright field and coloured) of 5% CO_2 supplied *Dunaliella salina* CCAP 19/30 stained with Nile Red after growth under different light intensities using different wavelength shifting materials. A) *D. salina* cells grown under normal condition without using any wavelength shifting material. B) *D. salina* cells grown under stress condition with more blue light using Coumarin shifting material. C) *D.salina* cells grown under more red light using Bestoil 2G wavelength shifting material. D) *D. salina* cells grown under more blue and red light using both Coumarin and Bestoil 2G wavelength shifting materials. 144
Figure 6. 7. Growth Curves of 10 % CO_2 supplied control and coated reactors. Control is done without wavelength shifting materials and only with white light; UV to blue wavelength tuning is done with only Coumarin 1 material and both light on. 145
Figure 6. 8. Images of the experimental runs at the starting and final days: (a) Control, (b) UV to blue wavelength tuning. 146
Figure 6. 9. Fluorescence microscopy images (both bright field and coloured) of 10 % CO_2 supplied *Dunaliella salina* CCAP 19/30 stained with Nile Red after growth under different light intensities using different wavelength shifting materials. A) *D. salina* cells grown under normal condition without using any wavelength shifting material. B) *D. salina* cells grown under stress condition with more blue light using Coumarin shifting material. 148
Figure 6. 10. Growth Curves of 0.5% CO_2 supplied control and coated reactors. Control is done without wavelength shifting materials and only with white light; UV to blue wavelength tuning is done with only Coumarin 1 material and both light on. 149
Figure 6. 11. Images of the experimental runs at the starting and final days: (a) Control, (b) UV to blue wavelength tuning, ... 150
Figure 6. 12. Fluorescence microscopy images (both bright field and coloured) of 0.5 % CO_2 supplied *Dunaliella salina* CCAP 19/30 stained with Nile Red after growth under different light intensities using different wavelength shifting materials. A) *D. salina* cells grown under normal condition without using any wavelength shifting material. B) *D. salina* cells grown under stress condition with more blue light using Coumarin shifting material. 152

Figure 6. 13. *Dunaliella salina* growth with diverse percentages of CO_2 supply (0.5%, 1%, 5% and 10%). Control is done without wavelength shifting materials and only with white light; UV to blue wavelength tuning is done with only Coumarin 1 material and both lights on; green to red wavelength tuning is done with only Bestoil Orange 2G material and only white light on; and for the final one both Coumarin 1 and Bestoil Orange 2G materials were used with both light on. 153
Figure 6. 14. Accumulated lipid amount of different CO_2 supplied (0.5%, 1%, 5% and 10%) *Dunaliella salina* samples grown in 1.5M NaCl medium depending on the correlation with Nile Red Fluorescence Intensity. Each analysis for each experiment has 3 replicates of four stained and four unstained readings. 156

Figure 7. 1. Working principle and geometric shape of oscillator developed by Prof. Zimmerman 165

List of Tables

Table 1. 1. The major photosynthetic pigments of cyanobacteria and algae (Ben-Amotz et al., 2009, FAY, 1983, Chen and Blankenship, 2011, Stephenson et al., 2011) 24
Table 1. 2. Research projects on the effect of spectral conversion and light intensity on phototrophic species (algae unless otherwise stated)..... 31
Table 1. 3. Design properties of open and closed growth systems (Bangert, 2013, Duan and Shi, 2014, Pulz, 2001) 39

Table 2. 1. Solubility of Coumarin 1 and Rhodamine B in diverse 49
Table 2. 2. Calculated target masses and the actual measured masses of dyes and PMMA used to obtain the wavelength tuning film solutions to be used for spin coating 51
Table 2. 3. PDMS thin film production rates 53

Table 4. 1. *Dunaliella salina* concentrations used to prepare dry weight vs concentration curve 86
Table 4. 2. Dilution concentration of algal cell using fresh medium for Nile Red peak time determination 89
Table 4. 3. 96 Well plate layout for Nile Red fluorescence peak time determination. Note that the rows from R1 to R4 are the replicates of the sample, as well as row R5 to R8, too. 90
Table 4. 4. Procedure and settings used for the Gen5 2.05 software programme to measure lipid amount at different culture concentration..... 92
Table 4. 5. Preparation of different Nile Red concentrations from Nile Red stock ... 94
Table 4. 6. 96 Well plate layout for Nile Red peak time determination. Note that the rows from R1 to R4 are the replicates of the sample. 94
Table 4. 7. Amount of triolein and isopropanol used to obtain Nile Red lipid standard curve 95
Table 4. 8. 96 Well plate layout for Nile Red peak time determination. Note that the rows from R1 to R4 are the replicates of the sample 96

Table 5. 1Nile Red Fluorescence Intensity analysis of *D. salina* samples grown in 1.5M NaCl medium. Each Nile Red analysis for each experimental run has 3 replicates of four stained and four unstained readings. 125
Table 5. 2. Accumulated lipid amount of *D. salina* at normal and different stressed conditions. 127

Table 6. 1. Nile Red Fluorescence Intensity analysis and accumulated lipid amount of 1% CO_2 supplied *Dunaliella salina* samples grown in 1.5M NaCl medium. Each Nile Red analysis for each experimental run has 3 replicates of four stained and four unstained readings. 137
Table 6. 2. Nile Red Fluorescence Intensity analysis and accumulated lipid amount of 5% CO_2 supplied *Dunaliella salina* samples grown in 1.5M NaCl medium. Each Nile Red analysis for each experimental run has 3 replicates of four stained and four unstained readings. 142
Table 6. 3. Nile Red Fluorescence Intensity analysis and accumulated lipid amount of 10% CO_2 supplied *Dunaliella salina* samples grown in 1.5M NaCl medium. Each Nile Red analysis for each experimental run has 3 replicates of four stained and four unstained readings. 146
Table 6. 4. Nile Red Fluorescence Intensity analysis and accumulated lipid amount of 10% CO_2 supplied *Dunaliella salina* samples grown in 1.5M NaCl medium. Each Nile Red analysis for each experimental run has 3 replicates of four stained and four unstained readings. 151

CHAPTER 1:

LITERATURE REVIEW

1.1. Introduction

Industry has an important place in human life in that it produces the goods to make life easier for people. However, the amount of carbon dioxide emission from factories is significant and needs to be reduced because it is the most abundant anthropogenic greenhouse gas. Due to the fact that 183 tons of carbon dioxide is required to produce 100 tons of algal biomass (Chisti, 2007), growing microalgae, is one of the useful methods to minimize this problem. Microalgae utilise carbon dioxide as a feedstock and convert it to beneficial products such as agriculture and aquaculture foods (Pulz, 2001, Michels et al., 2014b) and high-value bioactives (Melis, 2002), complex oils, hydrocarbons and lipids (Guschina and Harwood, 2006) and with further process to biofuels (Chisti, 2010a, Chisti, 2010b, Stephenson et al., 2011, Batan et al., 2010). Using microalgae not only decreases carbon dioxide emissions but also preserves the productions derived from crops (Chisti, 2007). Algae growth is carried out under photosynthesis principles which requires light as an energy source (FAY, 1983), inorganic salts, water and carbon dioxide.

Large scale algal biomass production is done using either open raceway ponds or closed photobioreactors (Molina Grima et al., 1999). As will be in discussed detail in section 1.4, open pond systems are the most commonly used method; nonetheless, photobioreactors (PBR) are attracting the attention of the industry because they offer more control. Currently available PBRs may cause oxygen accumulation which causes photo-respiration, an undesired situation for algae growth since it inhibits algal biomass production. The solution to this problem is increasing the mass transfer and aeration of the system; hence, studies aiming to introduce bubbling (fine bubble or microbubble) technology into the PBRs are being performed by many researchers (Zimmerman et al., 2009, Ying, 2013, Zimmerman et al., 2011, Al-Mashhadani et al., 2015).

After eliminating the problem of oxygen accumulation and providing all the nutrients to grow the algae (including suitable level of CO_2), the only remaining parameter which may limit the photosynthesis rate is the light intensity. A major part of light absorption is performed by the chlorophyll pigments which can absorb blue and red

light at the peaks 450nm and 680 nm, respectively. As the sun is the light source for algal growth and it has a wide range of light emission wavelength, the light illumination using wavelength shifting materials will help to increase efficiency of growth. These wavelength shifting materials will convert the unused UV and green light to the usable blue and red light.

1.1.1. Objectives of the Project

The purpose of this research is developing photobioreactor (PBR) design by incorporating the wavelength shifting materials with an optimum amount of CO_2 supply in order to increase the algal biomass production. An optimized wavelength shifting material will be obtained by trying diverse coating techniques, by using a variety of dyes, solvents, polymers (matrix material to form robust structure on microscope slide) and PDMS (polymeric matrix to obtain smooth and robust films). Application of wavelength tuning materials will help to increase the amount of usable light, so algal growth will be shifted. On the other hand, bubbling from the bottom of the reactor will help to increase mass transfer and reduce O_2 accumulation and increase the mixing of the growth medium. Also different CO_2 concentrations will be tried to obtain an optimized CO_2 amount to grow *D. salina* faster. Moreover, the design of the PBR will be driven by considering the algae growth conditions, allowing more light penetration and reducing the reflection by using UV transparent materials. (Molina et al., 2001, Molina Grima et al., 2000).

1.2. What Are Microalgae?

After prokaryotic life began, blue- green algae (cyanobacteria) started to grow 3.5 million years ago. Algae, photosynthetic living organisms, are classified as macro algae and micro algae. Basically, algae can be categorized according to their coloured pigments such as green algae, red algae or brown algae (Chapman, 2013). In the literature, microalgae have been associated with fast growth typical doubling rates for

microalgae and cyanobacteria are 24 and 17 hours, respectively (Guschina and Harwood, 2006). This is a good feature producing biological products faster than other biological feedstocks such as crop, plants or energy plants for lignocellulosic materials (Hill et al., 2006).

Several studies have estimated that there are over 30,000 algae species and reported that algae can grow in many conditions like extreme salinity, extreme pH values, and wide temperature range (FAY, 1983). According to species, they can grow in desert, marine, fresh water, waste water or sewage (Oilgae, 2013). On the other hand, as with all living organisms, microalgae require appropriate growth conditions which are fulfilled with nutrients, light and CO_2.

Nutrients such as phosphorus (P) and nitrogen (N) are essential for algal growth. The growth medium should contain sufficient amounts of these inorganic chemicals. Chisti claimed that 1.1 million tons of phosphorus and 5.4 million tons of nitrogen are needed for the production of 82 million tons of algal biomass (Chisti, 2013). On the grounds of the sustainability of the algal production, these two essential nutrients must be fully recycled (Chisti, 2010b). Therefore, P and N can be gained back from algal biomass by anaerobic digestion of algal oil (Chisti, 2008). The last and most important input to the algal growth system must be CO_2 and as mentioned earlier, 183 tons of CO_2 is consumed while producing 100 tons of algal biomass (Chisti, 2007). Moreover, microalgae are a significant source for CO_2 storage as a consequence of rapid growth rates (Sayre, 2010). On the basis of previous information, microalgae are considered as environmentally friendly and help naturally to reduce greenhouse gases.

At the end of the photosynthesis reaction, diverse types of products are constructed depending upon the species of microalgae and the growth environment. These products can be listed as complex oils, hydrocarbons, lipids (Weyer et al., 2010), agricultural and aqua-cultural foods (Guzmán et al., 2010, Herrmann et al., 1997)and β-carotene as well as biofuels with further processing (Guschina and Harwood, 2006, Chisti, 2007, Borowitzka, 2013, Chisti, 2008, Mata et al., 2010). Moreover, the secondary red carotenoid astaxanthin, that has recently attracted notice as a nutraceutical food

because of its high antioxidant activity, is also used as a pigmentation addition agent in aquaculture (Ranjbar et al., 2008).

Microalgae have the ability to produce high amounts of lipid and this amount increases with decreasing initial nitrogen concentration (Karatay and Dönmez, 2011). Besides, some microalgae contain a huge quantity of oil (Mata et al., 2010) which could be possibly used directly as biofuels to produce electricity and heat, or altered to make bio-hydrogen and biogas by discrete biological conversion. Thus, microalgae can be potential sources for reducing petroleum use, and some researchers claim that third generation biofuels derived from algae will eventually replace petroleum. If the growth conditions are suitable, the growth rate of microalgae may reach to 1 day^{-1}, by way of contrast plants may reach to 0.1 day^{-1} or less (Chisti, 2010b).

Additionally, microalgae are used in carbon dioxide and nitrogen fixation (cyanobacteria only), bioremediation processes, wastewater and sewage treatments, cosmetic industry and pharmaceuticals (Chisti, 2007, Ranjbar et al., 2008, Karatay and Dönmez, 2011, Borowitzka, 2013). Even though the application areas of microalgae are wide ranging, harvesting is a costly procedure which needs further investigations. Filtration, sedimentation, centrifugation and flotation are the main harvesting methods (Oilgae, 2013).

1.2.1. Photosynthesis in Microalgae

Photosynthesis is a process which is described as the forming of organic compounds like sugar by the fixation of CO_2 (either free CO_2 ions or bicarbonate ions) through using an energy source, light, as shown in the equation below.

$$6CO_2 + 6H_2O \xrightarrow[\text{Light}]{} C_6H_{12}O_6 + 6O_2 \qquad (T = 20\text{-}30^{\circ}C)$$

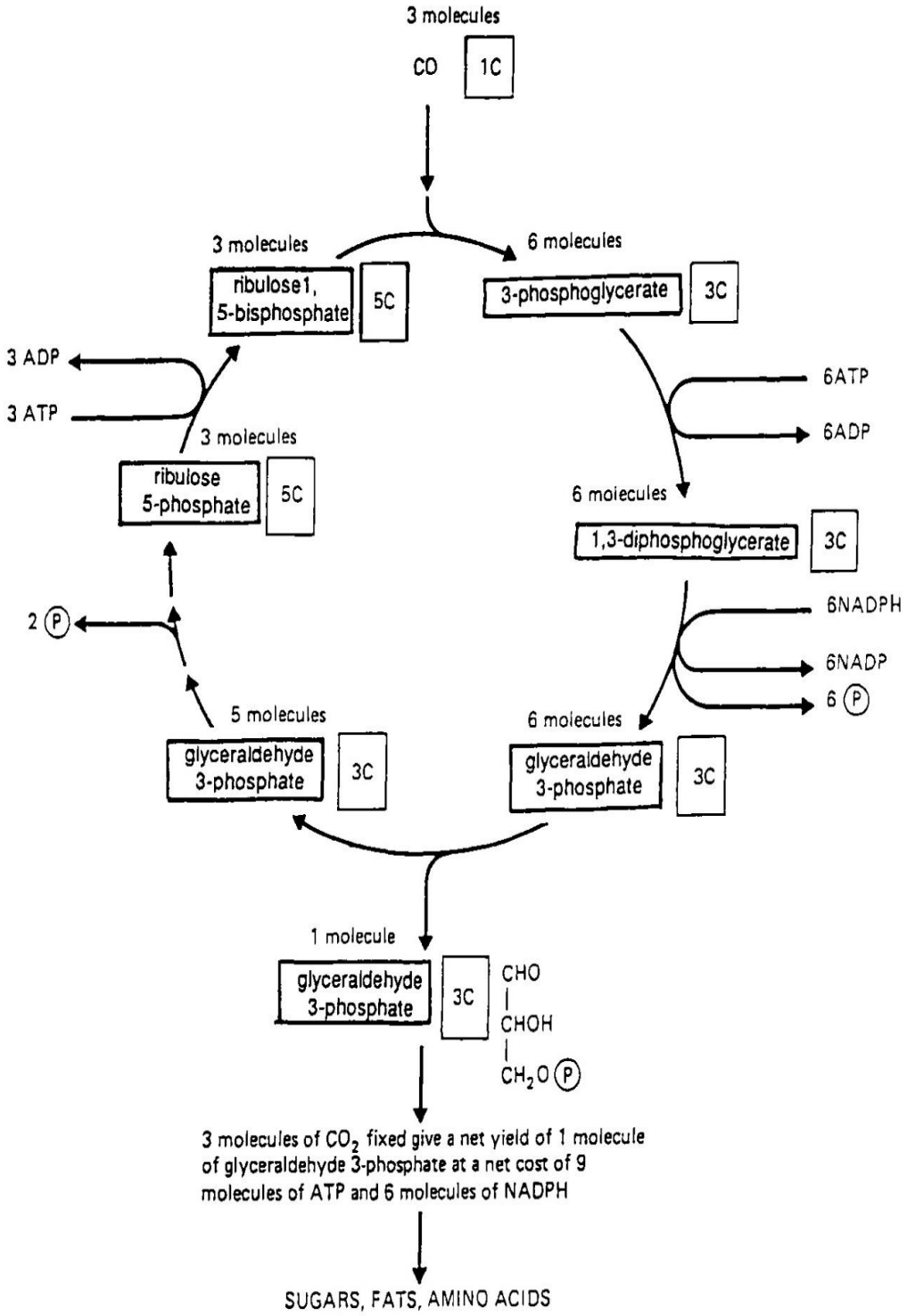

Figure 1. 1. Calvin cycle. Image is adapted from 'Photosynthesis' book written by. (Kohen et al., 1995)

After supplying all nutrients and a carbon source in the aqueous solution where microalgae are present, the driving force, light, of the photosynthesis will be provided by the sun (Melis, 2002). Then, this light energy will be converted to the chemical energy inside the cells (Figure 1.1) (FAY, 1983, Kohen et al., 1995). Photosynthesis is divided into two main parts; light-dependent and light-independent (Calvin cycle). In the first step of the Calvin cycle, CO_2 is attached to the ribulose-1, 5-biphosphate (RuBP) that is a 5 carbon sugar, by Rubisco enzyme so as to generate two molecules of 3-phosphoglycerate. Next, a series of sugar phosphates are formed by NADPH (nicotinamide adenine dinucleotide phosphate) which is an electron carrier. Energy (ATP) and reductant (NADPH) are produced during the light dependent reactions and water is split to produce electrons to reduce NADP and produce free O_2 as a by-product (FAY, 1983).

All cyanobacteria, as well as microalgae utilize, the same solar spectrum wavelength range between 400 nm and 700 nm which is referred to as the "visible spectrum" and also named as the "photosynthetically active radiation (PAR)" (Kirk, 1994, Blankenship, 2002, Chisti, 2010b, Xia et al., 2013). This harvested sunlight beams are used to drive the metabolic reactions during photosynthesis (Hu and Schulten, 1997). Table 1.1 illustrates the absorption wavelength ranges of photosynthetic pigments inside the phototrophic organisms. Among these pigments, chlorophyll and carotenoids are fundamental elements of light-harvesting complexes (LHCs) of photosynthetic cells. Photosynthetic light trapping progresses via these pigments which are present in microalgae and transfer it to the photosynthesis reaction systems. The colour of the incoming light ideally needs to overlap with the pigment absorption wavelength range that corresponds with the lowest excited state. (Ben-Amotz et al., 2009, Matthijs et al., 1996). Antenna pigments absorb and pass the photons through the photosynthetic reaction centres (PSII and PSI). The primary photochemical reactions proceed from relatively low-energy, long (red) wavelengths of light (680 nm PSII and 700 nm PSI). Thus, shorter energy, high energy (blue) wavelengths of photons absorbed by the antennae is re-emitted as heat and fluorescence. Therefore, the photosynthesis process cannot utilise the extra blue photons energy of light which

is about 75% larger than red photons. Thus, an additional 6.6% energy loss from incident solar energy occurs (Barber, 2009).

For the purpose of fast algal growth, the efficiency of photosynthesis should be high which can be obtained with overlap between photosynthetic pigments and solar irradiation (Wondraczek et al., 2013). The wavelength threshold can be exceeded by genetic engineering of algae. After discovering *chlorophyll d* and *f* (the most red-shifted chlorophyll), the spectral region was shifted to 750 which allowed 19% more photon flux access (Chen and Blankenship, 2011). A further application for enhancing light absorption may be the over-expression of photosystems (Stephenson et al., 2011) or truncating the light harvesting antenna size of chlorophylls (Melis, 2009).

The efficiency of photosynthesis depends on the algae species as the pigments and their tolerance capacity to the environment varies. Burris (1977) showed the differences of algae photosynthesis efficiency by making a study on 7 different algae species. Photorespiration, which decreases photosynthetic carbon fixation efficiency by 20% to 30% (Zhu et al., 2008), is one of the main reasons for low photosynthetic efficiency. When the oxygen concentration rises the photosynthesis rate decreases since the oxygen is competing with CO_2 fixation by Rubisco and this, Warburg's effect, is taken into consideration as photorespiration. Moreover, even though UV photons are only about 8% of the total sunlight, it is thought that the significant photosynthesis inhibition caused by solar radiation in natural ecosystems, is due to UV. Some studies shows that in solar radiation UV-B is almost as effective in inhibiting photosynthesis as UV-A where the ratio between UV-B and UV-A photons in natural radiation is only about 3:100 (Herrmann et al., 1997). Furthermore, photons harvested by protein chlorophyll (Chl)–carotenoid complexes, then transferred to the photosystem reaction centre, is important for the photosynthetic efficiency. If the amount of harvested photons is too low, etiolation symptoms occurs and photosynthesis cannot work efficiently. On the other side, excessive light produces more oxygen and causes photo inhibition (Darko et al., 2014).

Table 1. 1. The major photosynthetic pigments of cyanobacteria and algae (Ben-Amotz et al., 2009, FAY, 1983, Chen and Blankenship, 2011, Stephenson et al., 2011)

Group	**Class**	**Color**	**Absorption wavelengths (nm)**
Chlorophylls	Chlorophyll *a*	green	435, 670, 680, 700
	Chlorophyll *b*	green	450, 640
	Chlorophyll d and f	green	700-750 nm
Carotenoids	β- carotene	orange	431, 450-454, 478-480
	echinenone		455-459, 475
	zeaxanthin		430, 453, 479
	Canthaxanthin		466
	Xanthophyll	yellow	400 - 530
Phycobiliproteins	Allophycocyanin		650
	Phycocyanin	blue	610-625
	Phycoerythin	red	555-565

1.2.2. Limitations of Photosynthesis

More than 3800 zettajoules (1 zettajoule = 10^{21} joules) of solar energy are absorbed by Earth's atmosphere and surface annually. About 0.05% of this energy is captured in biomass each year through the process of photosynthesis (Sayre, 2010). In spite of photosynthesis developing on the plant about 3.5 billion years ago, it is still not very efficient at converting solar energy into chemical energy and the maximum efficiency of photosynthesis was reported as 8–15% (Stephenson et al., 2011, Goetz et al., 2011). A considerable amount of literature has been published on photosynthesis in microalgae. It is obvious that salinity, temperature, pH, light intensity and penetration, CO_2 amount and inorganic compounds like nitrogen, phosphorous and other trace elements play crucial roles during the growth of microalgae (Ben-Amotz and Avron, 1992, Knud-Hansen, 1998).

- **pH –** Depending on the species, microalgae can grow in an environment with a wide range of pH from 5 to 8 (Karatay and Dönmez, 2011, Ying et al., 2014). The pH value of the medium is related to the amount of CO_2 present. When CO_2 reacts with water molecules during the photosynthesis, carbonate ions (CO_3^{-2}), bicarbonate ions (HCO_3^-) and carbonic acids (H_2CO_3) are formed after a series of chain reactions. Thus, the protons released to the medium cause a pH decrease. Karatay et. al (2011) analysed the effect of discrete pH values (6-9) on the lipid production of cyanobacteria, and they concluded that maximum lipid production is obtained at pH 7.
- **Temperature –** As mentioned earlier, different species of algae can grow both in deserts or ice fields since they can adapt to temperatures between -7 and 75^oC (Oilgae, 2013). However, most of the species grow best between 20-30^oC. Thus, the temperature should be kept between this range and the temperature control inside the photobioreactors can be done using cooling jacket or heat exchangers (Tredici and Materassi, 1992). Also, the reduction of temperature at

night in outdoor cultures will cause increased respiration, which leads to increased algal biomass loss (Chisti, 2007).

- **Nutrients –** Algae need sufficient amount of nutrients (N, P, trace elements, iron, etc.) to survive. (Karatay and Dönmez, 2011, Chen and Blankenship, 2011).
- **Oxygen level –** As a result of photosynthesis, oxygen is generated and the excess of the free O_2 inhibits the algal growth (Molina et al., 2001). O_2 production rate inside a photobioreactor should be no more than 10g O_2 m^{-3} min^{-1} (Chisti, 2007, Chisti, 2008). As a solution to the issue of oxygen accumulation, aeration systems with microbubble production can be used inside photobioreactors (Zimmerman et al., 2011).
- **Carbon dioxide level –** CO_2 is a key reactant of photosynthesis; no reaction takes place in the absence of CO_2. A minimum of 1338 kJ of light energy is essential to form the two NADPH and three ATP molecules needed to fix one carbon atom that represents 466 kJ of chemical energy (Barber, 2009). Depending on the species, glucose, acetate, bicarbonates or CO_2 directly released from industry can be used as a source (Hard and Gilmour, 1996). Hence, the carbon dioxide should not be a limiting factor for algal growth if sourced from industry and this will also reduce production costs (Chisti, 2007, Chisti, 2013). Besides, the level of carbon dioxide should be considered carefully since more carbon dioxide means more oxygen generation which will inhibit the algal growth.
- **Available light, sunlight –** Light is a driving force for photosynthesis and it provides the energy requirement. Phototrophic organisms utilize only the PAR region of the sunlight which is between 400 and 700 (Kirk, 1994, Chen and Blankenship, 2011) and it is only 48.7% of the total solar system (Kruse et al., 2005) ; however, microalgae reflect the green light (500-650 nm) rather than absorbing. Also, in the literature, the relationship between algal growth and light intensity has been reported. Uyar et. al. (2007) claimed that inoculation for large scale production should be done in the morning, because a dark period after

inoculation will cause long lag time. Furthermore, light penetration through the reactor will be less if the density of the algal cells is too high (Zimmerman et al., 2011, Molina et al., 2001). Also, microalgae, generally, tend to produce saturated fatty acids in the shape of triacylglycerol (TAG) when the light intensity is high (Michels et al., 2014a).

1.2.3. *Dunaliella salina* as Algal Species

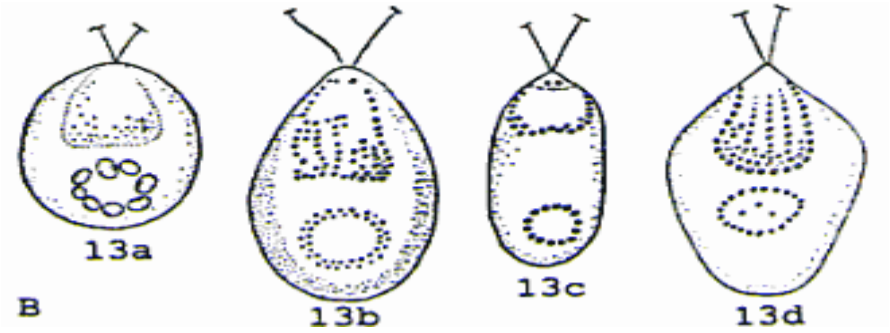

Figure 1. 2. **13a -** *D. salina* spp. *salina* fo. *salina*; **13b** - *D. salina* spp. *salina* fo. *magna*; **13c -** *D. salina* ssp. *salina* fo. *oblonga*; **13d -** *D. salina* spp. *salina* spp. *sibirica* (Ben-Amotz and Avron, 1992)

Dunaliella salina is a halotolerant, single-celled green microalga which has two flagella and various shapes such as oval, ellipsoidal, cup- or egg- shaped (Kleinegris et al., 2010, Kleinegris et al., 2011, Borowitzka et al., 1984). The flagella have a significant role by moving the cells in the medium and controlling the quantity of light that reaches the cells (Ben-Amotz and Avron, 1992, Ben-Amotz et al., 2009). Chlorophyll a and b, the main pigment s in *Dunaliella* cells, predominantly absorb light in the range 400-500 and 650-680.

The first *D. salina* species was discovered by Michel Felix Dunal in 1838 (Ben-Amotz et al., 2009), although, the "*D. salina*" name was given by Teodoresco in 1905 and, so far, twenty nine *D. salina* species have been described and some of them are illustrated

in Figure 1.2 (Borowitzka et al., 1984). *Dunaliella* species can survive at distinct ranges of temperature (10 -30 ^{o}C), pH (5.5 - 10) and NaCl concentrations from 0.5 to 5 M, and some species such as *D. salina* can be found in salt lakes (Ben-Amotz et al., 2009). As displayed in Figure 1.3, the colour of the algae can be either green or red owing to the response of some strains to different salinities. At high level of salinity *D. salina* produces β-carotene and this causes red colour (Helena et al., 2016). Furthermore, there is no definite cell wall around *D. salina* cells, and glycerol is generated to balance osmotic pressure and sustain enzyme activity in high salinity. Problem can be faced during the growth of *D. salina* when the salinity decreased to less than 15% NaCl (w:v), because cyanobacteria such as *Aphanothece halophytica, Spirulína sp* . and *Phormidium sp.,* some pennate diatoms and the dinoflagellate *Gymnodinium sp.* (Borowitzka et al., 1984) and protozoa (Hard and Gilmour, 1996) can grow in the medium. Another bottleneck for *D. salina* growth is UV radiation and *Dunaliella* avoids this problem by producing β-carotene which will shift the process to Xanthophyll cycle (stimulate energy dissipation inside the light harvesting antenna) (FAY, 1983, Ben-Amotz et al., 2009, White and Jahnke, 2002). β-carotene is also used in pharmaceutics as a precursor of vitamin A (Ben-Amotz and Avron, 1992, Stahl et al., 1993). Because of this ability of *D. salina*, bulk production of β-carotene was firstly suggested by Massyuk (Borowitzka et al., 1984) and then glycerol was suggested by Ben-Amotz (Ben-Amotz et al., 2009). Since 1978, Roche Research Institute of Marine Pharmacology (RRIMP) in Dee Why, Australia has been producing *D. salina* as a commercial source of ß-carotene. The aim of RRIMP was to isolate and culture marine microalgae and screen them to produce marketable chemical, antibiotics and pharmaceutically active compounds.

Additionally, *Dunaliella* species can be grown in a specific medium depending on the strain but nitrogen and phosphorus are fundamentals for each species. Nitrate is the best resource of N for *Dunaliella* since ammonium derivatives are less effective N sources at high concentrations (Ben-Amotz and Avron, 1992, FAY, 1983). Also, phosphate is the best as P source at concentrations between 0.02 and 0.025 g l^{-1} K_2HPO_4 (Borowitzka et al., 1984).

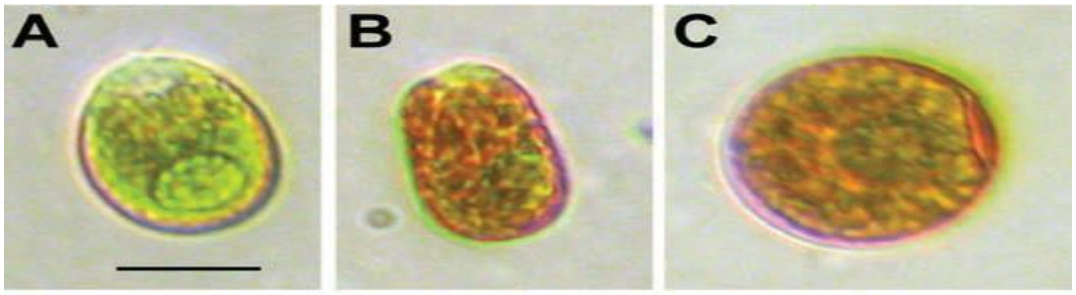

Figure 1. 3. Images of various *D.* salina species, isolated by Teodoresco, grown at different salinities; A – 1.5 M NaCl, B and C – 4.5 M NaCl (Ben-Amotz et al., 2009)

1.3. Utilising Solar Radiation

Photosynthesis requires light which can be provided either as artificial or natural. When both capital cost and labour cost are considered, using artificial light will cost too much (Molina Grima et al., 1999, Acién Fernández et al., 2013). In contrast, using natural source, sunlight, not only decreases the capital cost but also the labour cost since no manual control will be needed. Also, approximately 120000 TW solar energy, reaching the surface of the Earth, is a sustainable resource exceeding predicted human energy demands by >3 orders of magnitude. The sun has a wide spectral irradiance range from UV to radio wavelengths. The peak in Figure 1.4 represents the visible light emitted from the sun. As mentioned earlier, algae can utilize only some of this visible part which is also called as photosynthetically active radiation (PAR) (Kirk, 1994, Chen and Blankenship, 2011), whilst UV light radiation causes damage to the cells (Herrmann et al., 1997, White and Jahnke, 2002). Approximately 43% of solar irradiance is visible light, 49% is near-infrared and 7% is UV light, which consist of UV – C (<280 nm), UV – B (280-320 nm) and UV – A (320-400 nm) which is 95% of UV irradiance released by sun (Ben-Amotz et al., 2009, White and Jahnke, 2002, Holzinger and Lütz, 2006) and filtered by the ozone up to 310 nm (Hagfeldt et al., 2010). Additionally, only 48% of the solar radiation is absorbed by the atmosphere. Some green algae like Micrasterias can adapt its metabolism for the UV light by forming mucilage sheaths and internal UV absorbing compounds. On the contrary,

crucial and irreversible damages occur on the cell like as lesions in DNA (Holzinger and Lütz, 2006, White and Jahnke, 2002), when photosynthetic living organism are exposed to the UV light radiation.

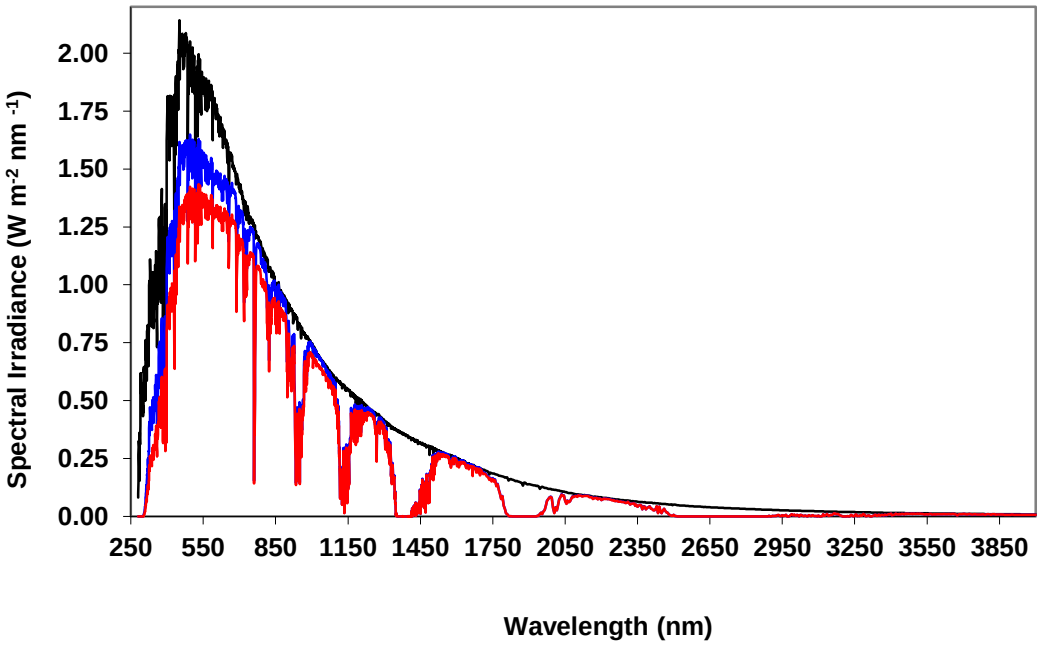

Figure 1. 4. Direct Normal Spectral Irradiance on 37° Tilted Sun-Facing Surface (ASTM, 2012)

While using the sun as light source for algal growth, utilization of light must be considered. In order to enhance the utilization, unused wavelengths could be converted to the used ones which can be achieved by wavelength tuning materials.

1.3.1. Wavelength Tuning Films

Table 1. 2. Research projects on the effect of spectral conversion and light intensity on phototrophic species (algae unless otherwise stated)

Authors	**Phototrophic species**	**Material / Equipments**	**Results**
(Wondraczek et al., 2013)	*Haematococcus pluvialis*	$Sr_{0.4}Ca_{0.59}Eu_{0.01}S$ Conversion from green to red light	>20% spectral conversion 36 % increase in cell generation
(Xia et al., 2013)	*Spinacia oleracea* (spinach)	$Ca_{0.4}Sr_{0.6}S:Eu^{2+}$	enhancement of CO_2 consumption by >25 %
(Mohsenpour et al., 2012, Mohsenpour and Willoughby, 2013)	*Chlorella vulgaris*	- Lumogen F dyes - Xenon arc lamp radiation	increased biomass productivity of *C. vulgaris* up to 20 %
(Delavari Amrei et al., 2014)	*Chlorella sp. (PTCC 6010)*	Uvitex OB	an increase in the biomass productivity rate of 10 %
(Ranjbar et al., 2008)	*Haematococcus pluvialis*	White fluorescent light intensity from 21.5 to 94.3 µmol m^{-2} s^{-1}	Increased astaxanthin accumulation by 32%
(Miyake and Kawamura, 1987)	*Rhodobacter sphaeroides 8703* (Photosynthtic bacterium)	xeon lamp (50Wm^{-2}) & xenon lamp-based solar simulator (75 Wm^{-2}) 20,000 lux at 35°C	→Hydrogen evolution rate 262 µl/h/mg (dry weight) at 20,000 lux → Hydrogen evolution rate 151 µl/h/mg (dry weight) at 10,000 lux (Almost 74% increased efficiency)
(Mao et al., 1986)		10,000 lux illumination at 30°C	

(Uyar et al., 2007)	*Rhodobacter sphaeroides* (Photosynthtic bacterium)	Rhodamine B solution and $CuSO_4$ solution to filter the wavelength >760 nm and <630nm, respectively	→ Enhancing the light intensity by 180 W/m^2 to produce hydrogen → Increased hydrogen production by 39% under infrared light (750-950 nm)
(Blair et al., 2014)	*Chlorella vulgaris*	Green, red and blue LED	Improved growth rate and biomass productivity compared to the green and red colour.
(Chin-Hang et al., 2012)	*Chlorella sp.*	Red and blue LED	Higher lipid content with blue LED
(Vadiveloo et al., 2015)	*Nannochloropsis sp.*	Red, green, pink, blue LED	Higher growth rates in pink, red LED compared to blue and green ones.
(Gaytán-Luna et al., 2016)	*Chlamydomonas reinhardtii*	White and red light	improved dry cell weight with red light (14.78% dcw) compared to white light (4.4% dcw)
(Wang et al., 2010)	*Schistosoma japonica* (parasitic worm)	White and blue light	Blue light decreases the egg formation time (6days) by half compared to white light

Green microalgae contain chlorophyll a and chlorophyll b which predominantly absorb light at the range 400-500 (blue light region) and 620-680 (red light region). There is no absorption between 500 and 620 which corresponds to green, yellow and orange light. Conversion of this unutilized light to absorbed wavelengths using wavelength tuning materials will raise the amount of useful solar irradiance reaching the microalgae cells (Lee and Palsson, 1994, Matthijs et al., 1996, Kohen et al., 1995, Koku et al., 2002, Wondraczek et al., 2013). Several experiments on spectral conversion and increasing light intensity have been done so far starting from early 1970s, and their effects on phototrophic species have been investigated (see Table 1.2). While producing wavelength tuning materials, some criteria must be under consideration such as; (1) emission wavelength range which will overlap with algae cell's absorbance wavelength; (2) quantum efficiency of the material; (3) reflection and refraction indexes of the material; (4) cost of production; (5) decomposition time of substances (Hovel et al., 1979, Van Sark et al., 2005, Klampaftis et al., 2009, Trosch et al., 2003, Prokop et al., 1984).

Solar radiation absorption can be defined using Beer-Lambert law that explains the attenuation of light due to the features of the material where light is penetrating. The following equation indicates the Beer - Lambert law;

$$\boldsymbol{A = \alpha\, c.t}$$

where **A→** absorbance (dimensionless), α**→** absorption coefficient **c→** concentration **t→** thickness of material (Fox, 2010).

As illustrated in Figure 1.5, when the light interacts with a material, it can travel in different pathways (Rowan et al., 2008, Klampaftis et al., 2009, Delavari Amrei et al., 2014). After being absorbed by the material, it can be re-emitted directly from the material interface. Otherwise, based on the Snell's law, which claims that luminous intensity of a reflecting surface has direct correlation to the cosine of the angle θ between the observer's lines to the surface normal, the incident light may reflect if the angle θ is bigger than the critical angle of the material. The reflection angle will be the

same as the incident angle (like a mirror effect). If the angle θ is smaller than the critical angle, then the ray will be refracted (Ohanian, 1989, Kirk, 1994, Hovel et al., 1979).

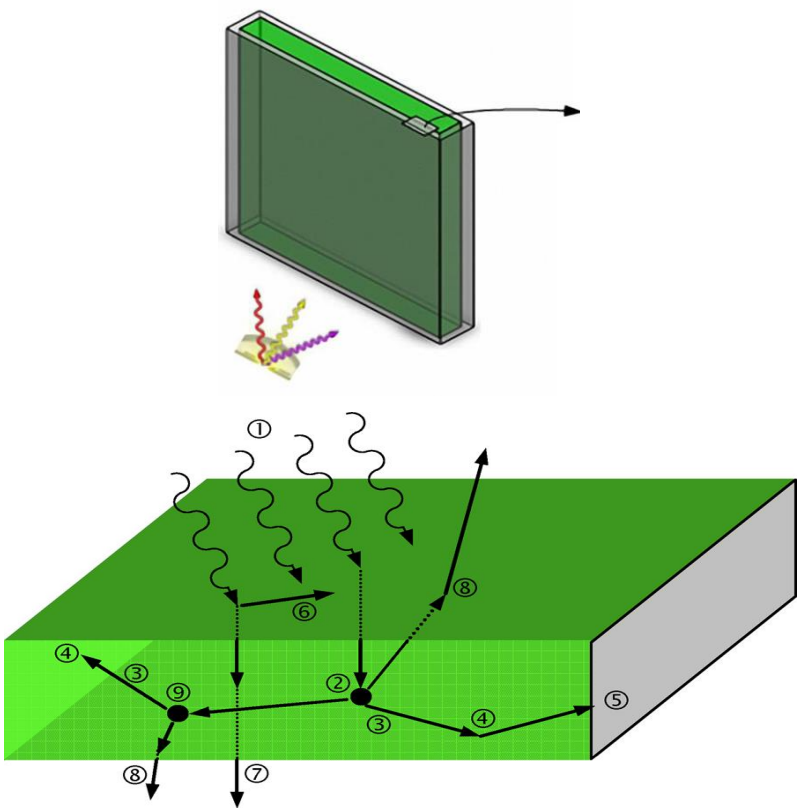

Figure 1. 5. Pathways of (1) incident photons (2) re-emitted directly with higher quantum yield (3); reflected through back to edge (4) and may exit through the sides (5). Without entering the material, it may reflect from surface (6). Transmit directly through another surface (7). Escape regarding Brewster angle (8) or absorbed by the host matrix (9) (Rowan et al., 2008, Mohsenpour et al., 2012)

A good wavelength tuning material will absorb a high amount of unused wavelengths of light as well as emitting a high amount at the desired wavelengths overlapped with chlorophyll absorption bands. Anti-reflective materials are necessary so as to decrease the reflection from the surfaces of the materials and so increase the absorbed light amount. In his study, Fink (2009) found that transmitted light for anti-reflecting applied material is 81% of incident light; whereas, it is 29% for non-anti-reflecting material.

The wavelength tuning materials, can be deposited using different coating methods like spray coating, dip coating, flow coating, laminar coating, roll coating, printing, spin coating, and sol-gel coating. Each of them has pros and cons but spin coating is the one which provides a good quality, smooth and reproducible thin-films; thus this method will be used in the current project. Another method that will be used in the project is sol-gel method or pre-baking which is crucial for the production of anti-reflective and multilayer coatings (Qingna et al., 2007, Borsetto et al., 1996, Koc et al., 2005). For both techniques, the films are heated after each coating at temperature range 70-110^{o}C; thus the thickness of the films reduces.

Additionally, wavelength shifting material production requires a transparent polymer, e.g. PMMA (Poly(methylmethacrylate)), polystyrene and PDMS (Poly(dimethylsiloxane)) can be used as matrix material which will lock the dye inside and give robustness to the wavelength shifting material. Furthermore, wavelength shifting material, i.e. quantum dots or fluorophores are needed to absorb and re-emit light with high quantum efficiency.

1.3.1.1. Quantum Dots

Quantum dots are nano-sized semiconductor particles which show the quantum mechanical properties which examine the attitudes of materials and light at atomic sizes. Common types of quantum dots include core-type quantum dots (CdSe/CdS), core-shell quantum dots (core -CdSe and shell-ZnS) and alloyed quantum dots (CdS_xSe_{1-x} / ZnS) (Sigma Aldrich). These nano particles are used in a variety of applications like solar cells, LEDs, transistors, biosensors and cell targeting fluorescence. The size of the quantum dots range between 2-10 nm, and depending on the diameter, it can emit discrete colour of light (Fox, 2010, Lee et al., 2002) . If the dots are small, then blue light is emitted, but if the dot is large then red light is emitted. Also, quantum dots are very robust; thus are attractive to use in producing wavelength tuning material. Nevertheless, they are very expensive so it will not be economical while working at large scales for industry.

1.3.1.2. Organic Fluorophores

Another material used for wavelength tuning material is fluorophores which are cheaper than quantum dots. There are two crucial features of fluorophores: (1) the fluorescence lifetime which is identified by the average time spent by a molecule in the exited state before returning to ground state; (2) quantum yield that is described as the ratio of number of photons emitted to the number of photons absorbed (Lakowicz, 2006). Fluorophores are organic luminescent chemicals which absorb light at a certain wavelength band and re-emit it at a longer wavelength band based on Stokes shift (see Section 1.3.2) and Pauli Exclusion Principle (Fox, 2010). These luminescent organic dyes are commonly used in biological application for cell targeting and analysing instruments as well as used in lasers, textile dyeing, OLEDs solar panels and cosmetics. Currently, a wide range of organic dyes is available commercially; however, all of them are not suitable to use in this project. The reason for using the fluorescent dyes is to increase the availability of useful light; hence, the fluorophores which convert UV to blue light and green to red light are essential for this project. Additionally, the organic fluorophores chosen should be cheap and have chemical stability. Examples of organic dyes that have the ability to convert UV light to blue light are Coumarin derivatives and 1,2-,Diphenylacetylene which will be used in this project. Nile red, Texas red, Rhodamine derivatives (see Appendix 1) Bestoil Red 5B and Bestoil Orange 2G are the ones which absorb green light and emit red light (Prokop et al., 1984). Bestoil red and Bestoil orange dyes will be used in this project.

1.3.2. Working Principle of Wavelength Tuning Films

Luminescence which is an emission of light from a substance, generally occurs with two main mechanisms; electroluminescence (emission occurs by running an electrical current through the material) and photoluminescence (re-emission of light after absorption) (Fox, 2010).

Fluorophores emit using photoluminescence mechanism which is first observed by Sir George Gabriel Stokes in 19th century (Lakowicz, 2006). Based on the Stokes experiment which depends on the conversion of energy, Figure 1.6 is drawn. Figure 1.6 illustrated the sequence of luminescence process of a photon. A photon is absorbed at ground state (S_0) and then atom reaches to the excited state (S_2). Then the atoms in the excited states relax to lower energy level of S_1 which is called as interval conversion and occurs within 10^{-12} s or less. Then the atoms return back to ground state with a lower energy but longer wavelength. The absorbed photon has higher energy yet the emitted one has lower; thus, there is energy lost due to energy transfer to the kinetic energy. This energy difference is called as Stokes shift (Fox, 2010, Hovel et al., 1979).

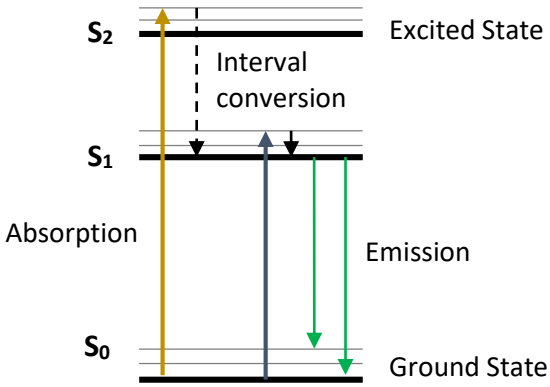

Figure 1. 6. The schematic representation of Stokes Shift; a photon is absorbed and atom jumps to exited state (S_2), and then relaxes to intermediate (S_1) before returning ground state (S_0) (Lakowicz, 2006)

Stokes made the experiments before the advent of quantum theory, so after the quantum theory had been explained, Pauli Exclusion Principle has also been used to define photoluminescence. This principle states that two half-integer spin (fermions) cannot occupy the same quantum state at the same time. Thus the absorbed photons decay down to intermediate level (S_1) before emission (Fox, 2010, Prokop et al., 1984)

1. 4. Algae Growth Systems

1.4.1. A Brief Overview of Algae Growth Systems

For large scale algae production, CO_2 can be captured from the industries where it is emitted in large volume while producing their materials. Large scale algal growth systems require some fundamentals such as mass transfer, circulation of CO_2 and O_2 gases, steady temperature (generally about 20-30^oC), supply of nutrients and last but the most important one for this project, light (Molina Grima et al., 1999, Molina Grima et al., 2003, Ben-Amotz et al., 2009). Light penetration through the reactor depends upon the algae concentration, dimensions (height, radius, width, etc.) and the material that algae and reactor are made of as well as anti-reflective coating (Molina Grima et al., 2000, Nakada et al., 1998). Additionally, the cultivation of microalgae needs to be cost-effective in order to use it commercially for sustainable algal biomass generation. For this purpose, it is essential to decrease the growth time (lag phase) and increase biomass generation which can be achieved by using a fast growing seed culture as the inoculum (Ben-Amotz et al., 2009). Currently used algal growth systems are either open raceway ponds or photobioreactors (Molina Grima et al., 1999, Sánchez Mirón et al., 1999, Tredici and Materassi, 1992).

Open raceway ponds are the most common commercially used systems since they are easy to operate and design, yet their contamination probability is higher than in photobioreactors. On the contrary, photobioreactors are assumed to be expensive because of the requirement for 24 h continuous artificial light illumination but this can be solved using transparent bioreactors and sunlight (Hard and Gilmour, 1996). Potentially, wavelength shifting materials will further improve light availability as mentioned in the previous section. Also, biomass accumulation in photobioreactors is more than open ponds. Numerous studies have compared both growth systems and the differences and similarities of design parameters as reported are represented in Table 1.3. Compared to the open ponds, photobioreactors have a low area/volume ratio. Water and CO_2 losses are almost zero whereas they are high for raceways (Pulz, 2001).

Table 1. 3. Design properties of open and closed growth systems (Bangert, 2013, Duan and Shi, 2014, Pulz, 2001)

Feature	Open system	Closed system
area-to- volume ratio	large (4-10 times higher than closed counterpart)	small
algal species	restricted	flexible
main criteria for species selection	growth competition	shear-resistance
population density	low	high
harvesting efficiency	low	high
cultivation period	limited	extended
contamination	possible	unlikely
water loss through evaporation	possible	prevented
light utilization efficiency	poor/fair	fair/excellent
gas transfer	poor	fair/high
temperature control	none	excellent
most costly parameters	mixing	oxygen control, temperature control
capital cost	small	high

1.4.2. Open Raceway Ponds

Open system algal ponds typically cover an area about 0.5-200 hectares with depth 0.2-0.3 metres and have been used for large scale algal cultivation since 1950s (Duan

and Shi, 2014). Open ponds are composed of closed-loop recirculation channels and mixing inside the ponds is obtained by a paddlewheel (Chisti, 2007). Open pond systems include circular ponds, raceway ponds, inclined trapezoidal ponds, high rate algal ponds (HRAP) and rectangular "mixing board" ponds (Tredici and Materassi, 1992, Craggs et al., 2012), most current commercial ponds are raceways, which are easy and cheap to build up and operate. Although, 98% of commercial algae cultivation is done in open ponds, it has drawbacks; decline of algal generation during the night due to respiration and the most important bottlenecks are contamination and cadmium (Cd) uptake, a toxic heavy metal. Rebhun and Ben-Amotz reported that chemicals (manganese (Mn) and sodium (Na)) in the *Dunaliella* growth medium have an effect on Cd uptake. Mn has an antagonist effect for Cd uptake (Rebhun and Ben-Amotz, 1988) and NaCl at a concentration above 1M, reduces the Cd uptake to a minimum value of 0.1 pg Cd (mg alga)$^{-1}$ (Rebhun and Ben-Amotz, 1986).

1.4.3. Closed Photobioreactors

Another growth system, photobioreactors, gives a chance to solve the issues related with the open ponds. Photobioreactors (PBR) can be used both inside the lab or outdoors for large scale cultivation (Duan and Shi, 2014). The crucial problem of open pond algae cultivation, contamination, is overcome using closed system photobioreactor since the researcher has more control over the system. However, the system is sophisticated because of the requirements for monitoring and adjustments of pH, temperature, gas inlet and outlet (Chisti, 2007, Pulz, 2001). As shown in Figure 1.7, there are 4 fundamental kinds of photobioreactors; flat plate, tubular, air-lift and bubble column (Duan and Shi, 2014, Pulz, 2001, Acién Fernández et al., 2013). Light availability for the microalgae inside the culture base on the length of the light path in the PBR, the photon flux density (PFD) on the PBR surface, and the light attenuation caused by the self-shading effect of the cells. Therefore, biomass concentration an important factor for optimizing the productivity (Michels et al., 2014a).

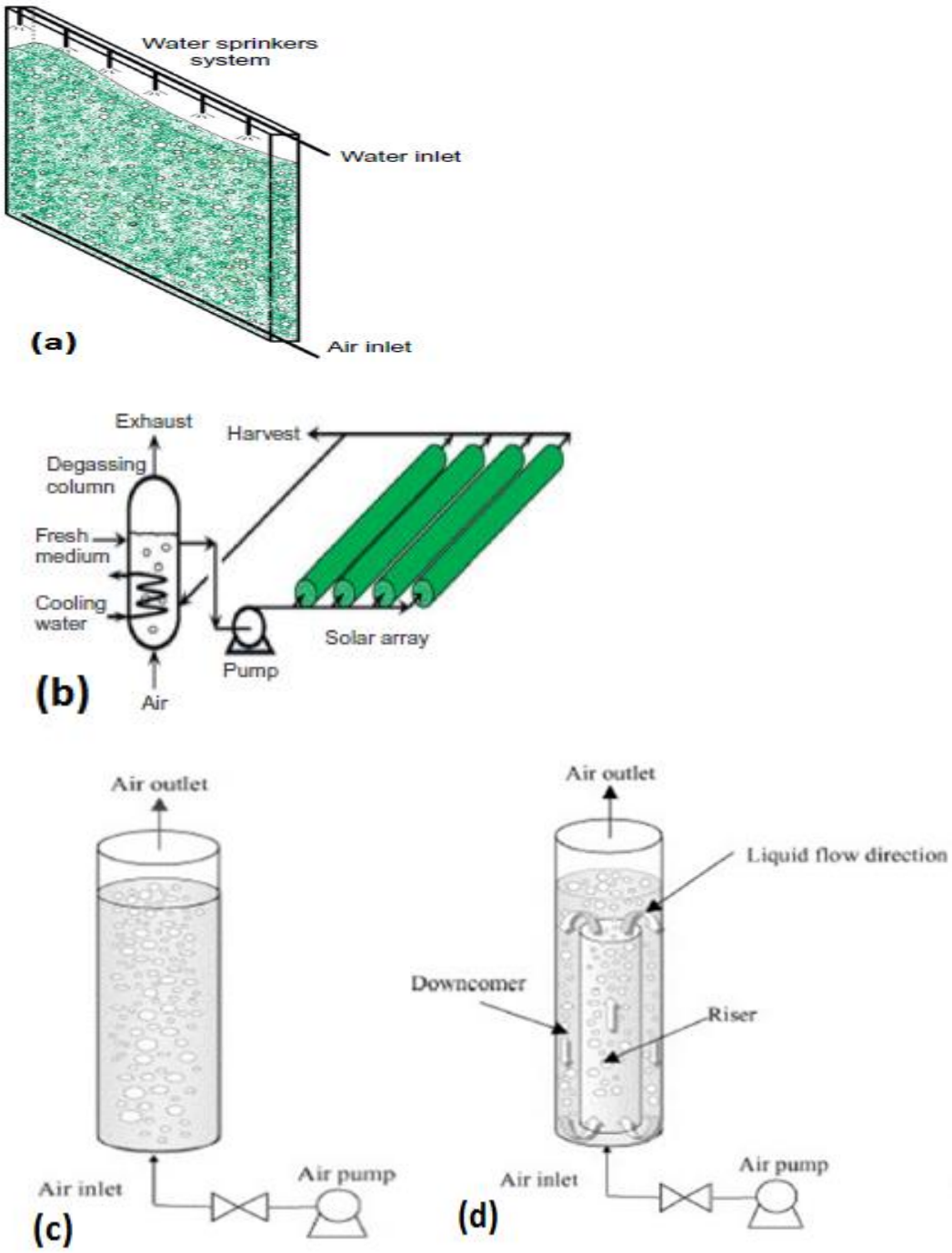

Figure 1. 7. Several photobioreactors for algae growth; (a) flat plate, (b) tubular, (c) bubble column and (d) air-lift (ALB) (Duan and Shi, 2014)

A flat-plate photobioreactor is composed of multiple flat sections which are made from plastic and the height and width of the plates can be up to 1.5m and 0.1m, respectively

(Wang et al., 2012). Kitajima et al, (1998) examined the effect of depth on hydrogen production and concluded hydrogen production has an inverse relationship with depth. As can be seen from Figure 1.7, area to volume ratio, also, is very high in this type reactor, hence the light penetration is high and that means a large amount of algal production. The fluid flow inside the reactor is supplied by using either a pump or airlift mechanism (Acién Fernández et al., 2013, Duan and Shi, 2014).

Secondly, tubular photobioreactor types are commonly used for algal biomass generation. This reactor is designed to maximize the solar ray penetration with horizontal oriented tubes which will increase the surface area where light can pass through. Tubes are made from either glass or plastic with diameter up to 0.1m (Chisti, 2007, Molina et al., 2001). This reactor type has been used in Spain, Hawaii and Germany in pharmaceutical and food industries (Chisti, 2007). However, the presence of too many gas bubbles in the solar tubes will interfere with light absorption and reduce the flow of culture broth in the tubes. Also, pH of the medium increases because of consumption of carbon dioxide while the medium moves along a photobioreactor tube (Chisti, 2008).

Next type is bubble column photobioreactors which are made from plastic or glass with dimensions up to; 0.2 m radius and 4m height. If the column height exceeds 4 m, then the O_2 accumulation may increase and a CO_2 gradient might exist (Xu et al., 2009). Temperature control is ensured with heat exchangers. This photobioreactor type is favoured because of its good mixing features. That mixing feature not only strips the O_2 accumulation but also reduces the nitrous oxide (N_2O), greenhouse gas, generation during dark period (Batan et al., 2010), whilst ensuring a good CO_2 supply.

Last type, and the type used in this project is the airlift photobioreactor (ALB). It is a kind of bubble column reactor. However, ALB has an inner baffle which prevents mixing of the supplied CO_2 and the generated O_2 and allows better mass transfer as well as mixing which will be explained in detail in the following sections (Duan and Shi, 2014). Flow pathway of the light part in the down-comer is nearly laminar, the light/dark cycle in the airlift photobioreactor is more regular than that in the bubble column. Therefore, oriented liquid circulation and regular light/dark cycle in the airlift

photobioreactor can give a better opportunity for cells to be illuminated by the average light intensity. Also, a portion of the cells inside the bubble column may stay in the dark zone for a long time and others may stay longer in the light zone, which may create stress on cells and cause morphological changes (Ranjbar et al., 2008).

1.4.4. Airlift Loop Photobioreactors as Proposed Reactor

Airlift loop photobioreactors consist of a CO_2/air riser and down-comer as demonstrated in Figure 1.7 (d) (Duan and Shi, 2014). ALB reactors supply better mixing and mass transfer due to bubble induced flow mechanism. Due to these properties, it is easy to overcome the drawbacks of algae production like slow CO_2 arrival to all cells, dissolved O_2 accumulation, algae cells that stick on the walls and dark zones (Zimmerman et al., 2011). ALB design requires more investigation into these problems and also light penetration issue. It is crucial to know how to operate an ALB under natural sunlight, and the wavelengths which overlap with chlorophylls, the photosynthetic pigments (Uyar et al., 2007).

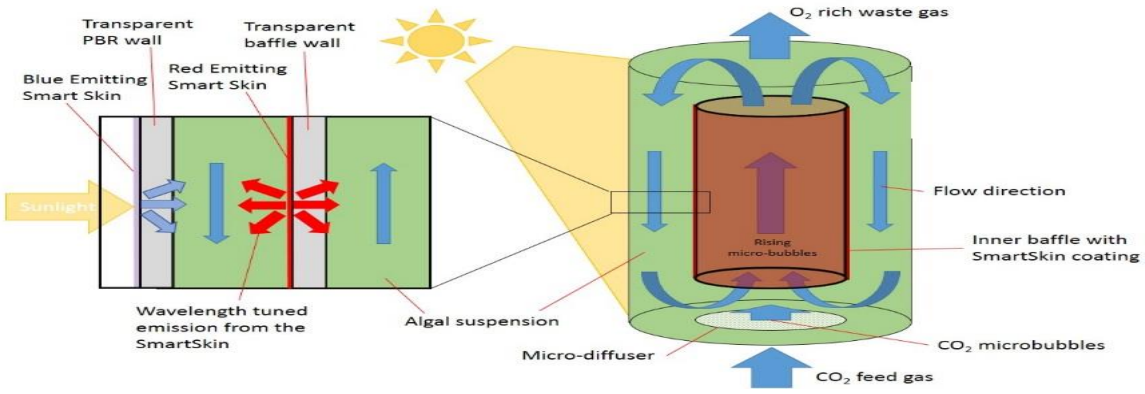

Figure 1. 8. Representative image of ALB associated with wavelength shifting material and bubbling technology proposed by Dr. Alan Dunbar.

A design for an ALB has been proposed by Dr. Alan Dunbar (Chemical and Biological department, University of Sheffield) for this project as shown in Figure 1.8, but the design was improved by me as the project progressed. In all cases the main efforts were to maximize surface-to-volume ratio, in order to give more efficient light source,

for efficient light delivery to the culture, and to increase mass transfer of gases (Lee and Palsson, 1994). The precondition of the design is a transparent material to build the photobioreactor. Then, another requirement is light conversion of UV to blue light and green to red light for more light energy. Based on the design, CO_2 will be supplied at the bottom of the reactor with a fine bubble sparger, and then the flow will be upward. Accumulated O_2 absorbed into the bubbles will be circulated with fine bubbles from the sparger. As discussed earlier in the limitations part, dissolved O_2 level has an inhibitory effect on growth rate. Additionally, CO_2 although desirable for photosynthesis, will lead to higher growth in turn will lead to high cell concentrations. These cells may attach to the reactor wall and cause a decline in the light penetration through the medium that yields dark zones in the reactor (Figure 1.9) (Chisti, 2007). All these issues can be resolved by microbubbles due to their high surface area properties. Owing to the high mixing feature of microbubbles, algae cells in the dark zone and attached to the reactor walls will be circulated by bubbles. Thus, they will reach more CO_2 and light. Residence time of the bubble rises with decreasing bubble size, as a result of this, time for mass and momentum transfer increases too (Zimmerman et al., 2009).

Controlling distribution of light will allow the control of the process performances so the physical light-limited regime will be eliminated (Pruvost et al., 2015). Therefore, the reactor will be coated with two different wavelength shifting materials; one outside the reactor walls and another one inside the reactor. Incident light will pass through the first wavelength shifting material and the light will be converted, a high amount of beneficial blue light will be absorbed by chlorophyll pigment and unused green light will be converted at the second wavelength shifting material and will be reflected back to enhance the algal growth.

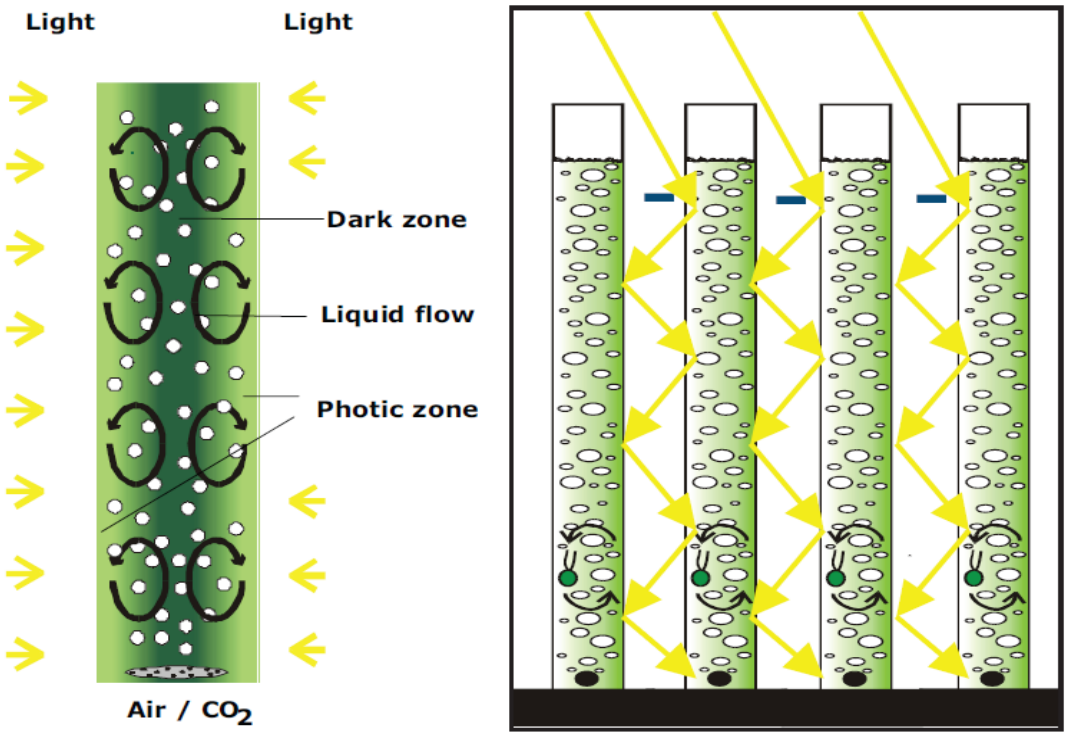

Figure 1. 9. Illustration of light and dark zones inside the photobioreactor as a result of high cell concentration (Ben-Amotz et al., 2009).

All in all, as stated in the aim of the project, the airlift photobioreactor which will be used in this thesis will be designed depending on the limitations mentioned above sections and enhancement of *D. salina* will be obtained.

CHAPTER 2. FABRICATION OF WAVELENGTH TUNING MATERIALS

2.1. Introduction

As explained in Chapter 1, literature review, microalgae are photosynthetic living organisms and they require special (appropriate temperature, pH, salinity, etc.) conditions to grow better. Section 1.1.2 describes the fundamental parameters and limitations of the photosynthesis clearly. After supplying all the required nutrients to the growth system, the only remaining driving force for photosynthesis will be providing the light necessary. Since the use of artificial light will increase the capital and process cost of the algae growth, it is desirable to utilize a more sustainable energy source, such as sunlight. The light wavelength range of the sun is mentioned in the Section 1.3. (Utilising solar radiation), and unfortunately only a small portion of this wide range are used during photosynthesis. In order to increase the utilization of the available light source, it is possible to shift photons from the unused light ranges (UV and green light band) to used ranges (blue and red light band) by fabricating and using good wavelength tuning materials.

This chapter will include the materials and methods for how the wavelength shifting materials are produced and results and discussion part of the fabricated materials. And depending on these results, choosing the appropriate wavelength shifting materials for the *Dunaliella salina* growth.

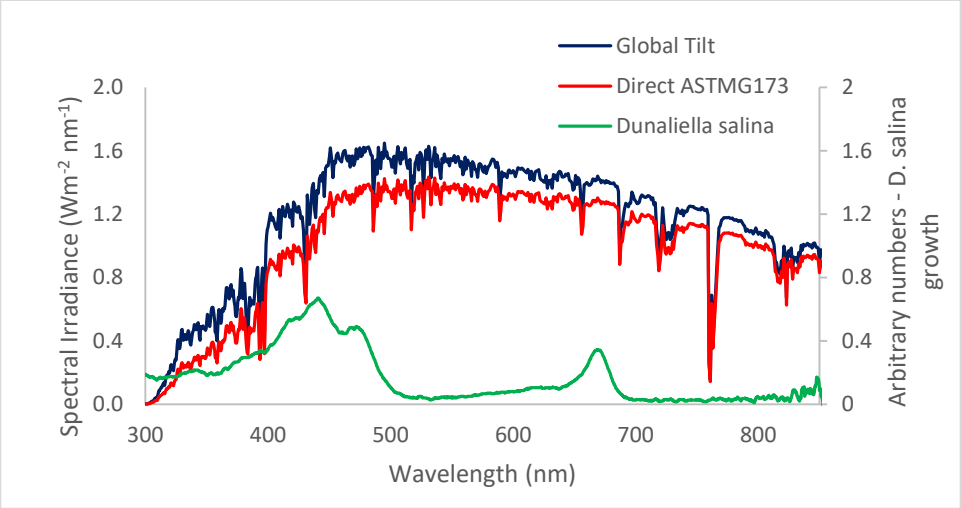

Figure 2. 1. Direct and global spectral irradiance on 37° tilted sun-facing surface (ASTM, 2012) and absorbance spectrum of chlorophylls inside *D. salina*.

2.2. Materials and Methods

2.2.1. Fabrication of Wavelength Tuning Materials

The first step of the project is to generate the wavelength tuning material in order to convert harmful and unused UV light (100-400 nm) into blue light (400-500nm) using a blue emitting organic dye (see Figure 2.1 modified and repeated figure for easy reading). Two different UV to blue converting dyes have been identified and tested. Other wavelength tuning materials will convert the unused green light (500-577 nm) to more useful red light (620-680 nm). Another important point of this wavelength tuning material generation is selection of a suitable matrix material so as to get a robust shifting material. The matrix material must be UV transparent since UV light is needed to be converted. Furthermore, the host (matrix) material needs to show high transmittance and low scattering especially in the region of the absorbed light. The host material can be glass, Perspex, PMMA, polystyrene, PDMS (poly(dimethylsiloxane)) or quartz (expensive). The selection of organic dyes was done based on previous research by MSc student David Hosking and 4th year MEng student Connor Smyth and Krys Bangert (Bangert, 2013, Smyth, 2014) (PhD student, Molecular Biology and Biotechnology). David Hosking used Coumarin 1 (blue emitting) and Rhodamine B (red emitting) as fluorophores and PMMA as polymer matrix. He reported the solubility of these chemicals in different solvents (See Table 2.1) (Hosking, April, 2013). Additionally, Connor Smyth made experiments with Coumarin 1 and 1,2-Diphenylacetylene as blue emitting organic dye and Bestoil Red 5B and Bestoil Orange 2G as red emitting fluorophores and PMMA and polystyrene as polymer matrixes (Smyth, 2014).

On the basis of previous studies and their absorption and emission bandwidths (see Appendix 2 and3), organic dyes were chosen as Coumarin 1, 1,2-Diphenylacetylene, Bestoil Red 5B and Bestoil Orange 2G; polymer matrixes were PMMA and polystyrene and PDMS (poly(dimethylsiloxane)); solvents were THF (tetrahydrofuran), toluene, chloroform and chlorobenzene (See Appendix 4 for complete materials list).

Table 2. 1. Solubility of Coumarin 1 and Rhodamine B in diverse

Solvent	**Rhodamine B**	**Coumarin 1**	**PMMA (Polymethylmethacrylate)**
Chloroform	Yes	No	Yes
Chlorobenzene	Yes	Partially	Yes
Toluene	Yes	Yes	Yes
THF (Tetrahydrofuran)	Yes	Partially	Yes

Wavelength tuning films were produced using both spin coating on microscope slides and curing PDMS which will be explained in sections 2.2.1.1 and 2.2.1.2. Using PDMS for spin coating might not give a good result as dye/PMMA mixture because of the high viscosity of PDMS. Therefore, curing it into a mould was an appropriate method.

Figure 2. 2. Spin coating apparatus – Laurell Technologies Corporation used for the coating the microscope slides with prepared dye/solvent solutions.

2.2.1.1. Dye Coating

Dye/ solvent mixtures with different ratios were prepared before making the wavelength tuning coatings. THF was the solvent used since it is known this solvent can dissolve the organic dyes as proved in the previous studies. The concentration of organic dye in the solvent (mg/ml) for Coumarin 1 and 1,2-Diphenylacetylene was varied. Concentrations of 1, 0.1, 0.05, 0.01 and 0.001 mg/ml were used. Additionally, the concentration of organic dye in the solvent (mg/ml) for Bestoil Red 5B and Bestoil Orange 2G are as follows; 0.1, 0.05, 0.03, 0.01 and 0.001mg/ml. For all organic dyes, 1:1 mg/ml dye to solvent concentration was kept as stock solution. In order to prepare these concentrations, 20 mg of each organic dye was weighed and poured into 20 ml vials, and then 20 ml of THF was added to each of the vials and shaken to dissolve the organic dyes. After shaking the stock solutions to mostly dissolve dye, vials were left 24h in order to ensure complete dissolution. After all dye particles were dissolved, solutions were diluted to the concentrations given above. These solutions were used for all applications to produce the wavelength shifting films.

n the next step, a polymer matrix, PMMA, was added to the chosen dye solutions which are 0.01 mg/ml and 0.03 mg/ml for UV absorbed dyes (Coumarin 1 and 1,2-Diphenylacetylene) and green light absorbing dyes (Bestoil Red 5B and Bestoil Orange 2G), respectively. These concentrations gave the highest absorption amount after analysis (see Results and Discussion, Section 2.3), therefore, they were selected for further experiments. The proportions for coating solutions were based on dye to PMMA and the ratio were obtained as indicated in Table 2.2.

The initial experiment conducted used Coumarin 1 since the Coumarin 1 was the best fluorescent dye in the studies- reported previously (Hosking, April, 2013, Bangert, 2013). Coumarin 1 produced from 95% solvent and 5% solid percentages by weight were used and found to be the most successful mixture. Preparation of the wavelength tuning films in the Hosking's report can be explained as; firstly, solid mixture (g/g) was obtained with Coumarin 1 and PMMA at different percentages 5%, 10%, 20% and 30%, and then dissolved in the solvent, toluene (Hosking, April, 2013).

Table 2. 2. Calculated target masses and the actual measured masses of dyes and PMMA used to obtain the wavelength tuning film solutions to be used for spin coating

	Dye amount (mg)	Calculated PMMA amount (mg)	Actual weighed PMMA amount (mg)	Dye / PMMA ratio
0.01 mg dye/ml solvent UV absorbed dye in THF	0.15	4.85	4.9	1: 32.33
		14.85	14.9	1: 100
		29.85	30	1: 200
		299.85	299.8	1: 2000
0.03 mg/ml Green light absorbed dyes	0.6	7.5	7.56	1: 12.5
		10	10.28	1: 16.7
		15	15.1	1: 25
		20	20.7	1: 33.33

The next step was to coat a substrate with the blend solution prepared by using a spin coater (See Figure 2.2). Glass microscope slides were used as the substrate; therefore, the microscope slides were cleaned. The glass slides were rinsed with toluene inside an ultrasonic bath for 20 minutes and then dried with compressed air. Then, each slide was put into the spin coater one at a time and the spin rate was set to 1000 rpm for 60 seconds with an acceleration rate of 15 rpm/second. According to the spin coater working mechanism (Koc et al., 2005), film thickness reduces due to centrifugal effects in the first 10 seconds and then through evaporation during the remaining time. Moreover, concentration of the starting mixture and spin rate affects the thickness of the material.

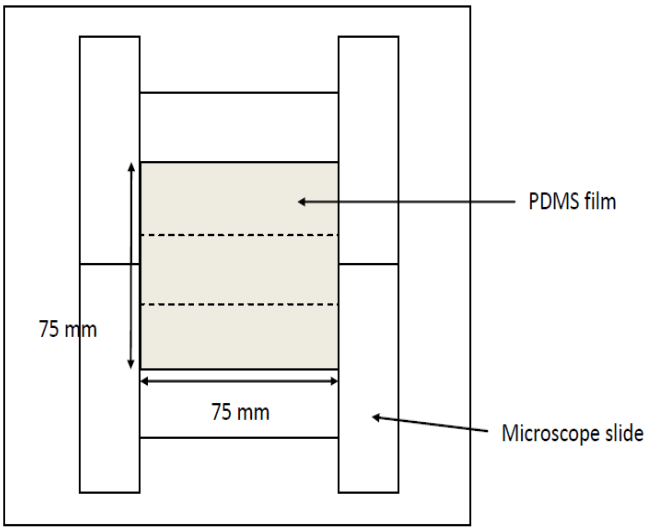

Figure 2. 3. Construsted PDMS mould used to cure the PDMS/dye mixtures. The base of the mould is a thick clear glass and the edges of the mould is made using microscope slides. The slides were stuck to the base glass using Parafilm paraffin (melted inside the oven).

2.2.1.2. Dye- PDMS Thin Films

PDMS (SYLGARD(R) 184 silicone elastomer - supplied from Dow Corning) is supplied as two constituents which are the base polymer and a curing agent (silicone resin solution). These constituents are mixed with a fix base/curing agent ratio (10/1) by weight. As reported by Lee et al.(2003), THF, toluene, chloroform and chlorobenzene can be used to dissolve with PDMS. Thus, previously prepared organic dye / THF solutions as well as newly obtained solution by mixing Bestoil Orange 2G with chloroform or chlorobenzene (ratios are 1 and 0.5) are utilized to get PDMS thin films.

Table 2. 3. PDMS thin film production rates

Organic dye	Dye/Solvent (mg/ml)	Dye/Solvent mixture amount (g)	PDMS amount (g)	Fluorophore (dye solution) / PDMS solution ratio (g/g)
Coumarin 1 + THF	0.1	0.8014	0.7996	10/10
	0.5	0.7005	0.7009	10/10
	1	3.0027	3.0363	10/10
	1	1.0352	0.5114	20/10
	1	1.5252	0.4908	30/10
Bestoil Red 5B + THF	1	2.24	2.28	10/10
	1.5	0.8514	0.8513	10/10
	1.5	1.5103	1.0112	15/10
	1.5	0.776	1.5073	10/20
Bestoil Orange 2G +THF	0.5	0.71	0.7082	10/10
	1	3.5104	3.5064	10/10
	1	3.255	2.17	15/10
	1	0.8014	1.6088	10/20
Bestoil Orange 2G + Chloroform	0.5	0.7426	0.7320	10/10
	1	0.7382	0.7215	10/10
Bestoil Orange 2G + Chlorobenzene	0.5	0.5218	0.5179	10/10
	1	0.8663	0.8658	10/10

A mould in which to cure the PDMS into a flat sheet was designed and constructed before all else (See Figure 3.1), then 6.5g of the PDMS base was put into a beaker and 0.65g of curing agent was added to obtain raw PDMS solution some of which was spread to make a thin film (without any fluorophores) as a control sample. Additionally, fluorophore mixtures were added to PDMS solution with different weight ratios as indicated in Table 2.3. Before spreading in the mould each solution was mixed rigorously to obtain a very smooth mixture and, any large bubbles were burst using a small spatula. Then, it was poured onto the mould and any remaining bubbles were burst. Next, the mould was put into an oven for 24h at 80^{o}C. After 24h, PDMS film was peeled off from mould ready for analysis with UV/VIS spectrometer.

2.2.1.3. Absorbance Measurements

After fabricating the wavelength tuning films, they were characterized by measuring their absorption wavelengths using an Ocean Optics spectrometer which can measure wavelengths between 200 nm and 850 nm (Figure 2.4). Data was analysed and recorded using the associated Ocean Optics SpectraSuite software. The spectrometer software mainly uses the equation below to calculate the absorption of photons. This equation is expressed as;

$$\mathbf{A} = \log_{10} \frac{I}{I_o}$$

where **A**→ absorbance (dimensionless), **I**→ transmitted radiation intensity (counts) and $\mathbf{I_o}$ → incident radiation intensity (counts) (Ohanian, 1989, Van Sark et al., 2005) , and the SpectraSuite software gives the direct solution of above equation.

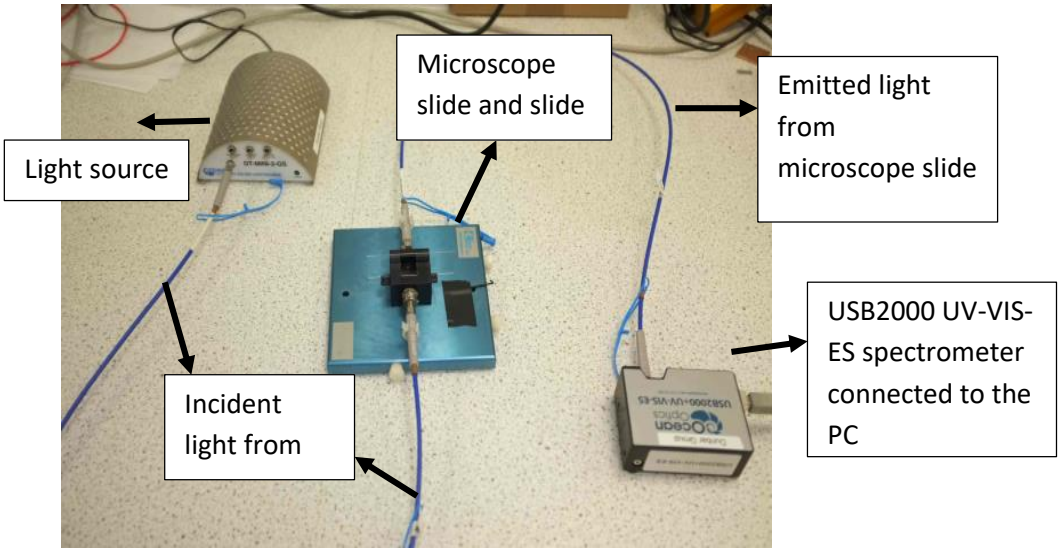

Figure 2. 4. Spectral test instruments Ocean Optics used for the absorption measurements of the produced wavelength shifting materials.

Dye / PMMA mixtures were analysed for absorption; Ocean Optics spectrometer was turned on (light sources deuterium lamp and halogen bulb) to warm up for half an hour, then the Ocean Optics SpectraSuite software was opened and parameters were set as integration time,15; scans to average, 4; Boxcar width, 4. 1 ml of reference solvent, THF, was poured into the quartz cuvette (Hellma Analytics 111-QS) and reference was saved for Lambert equation. And then, 1 ml of mixture was poured into a quartz cuvette and put to the cuvette holder and data recorded and then exported as an Excel file. In order to measure the absorption of coated microscope slides and PDMS films, the cuvette holder was modified as in Figure 2.4 such that it can conveniently hold thin films. Then, the analysis was done as previously but this time an uncoated microscope slide and raw PDMS were used as the reference samples.

2.2.1.4. Emission Measurements

The emission measurements were done using a high sensitive FluoroMax 4 (Horiba Group) instrument. All these kind of spectrometers are mainly built up with a light source, sample holder and a detector. The working principle of these instruments is basically defined as; incident photons delivered by the light source firstly impinge

upon the monochromator and then it is transmitted through the slits which limits the light transmission so as to control the resolution. The slit width management allows to decrease the noise in the absorption/ emission spectrum of the materials. After slits, the light passes through the sample and then the absorption / emission counting is transferred to the software in order to calculate and draw the absorption / emission spectrum (see Figure 2.5).

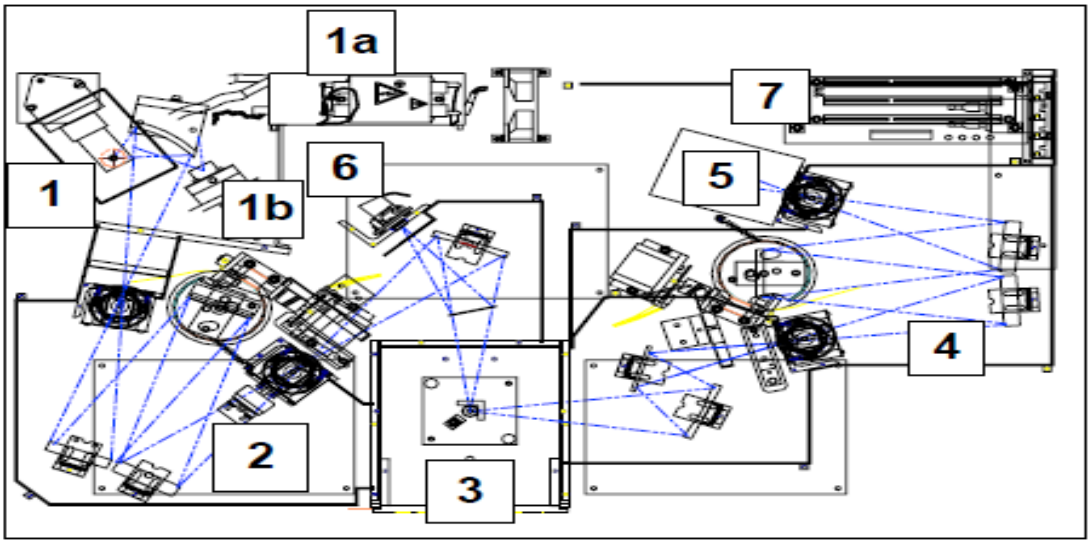

Figure 2. 5. Optical layout of FluoroMax 4 machine where; 1- Xenon lamp, 1a- Xenon lamp power supply, 1b – Xenon flash lamp, 2- Excitation monochromator, 3- Sample holder, 4- Emission monochromator, 5- Signal detector, 6- Reference detector and 7- Instrument controller. (Image is adapted from user manual of FluoroMax 4).

In order to measure the emission of the samples, firstly, the machine was turned on and left for 30 mins to warm up the lamps, then set the parameters were set as: For Coumarin: slit widths, 4; integration time, 1; excitation wavelength, 350nm; and emission wavelengths 365-650nm. For Bestoil Orange 2G and Bestoil Red 5B: slit widths, 10; integration time, 1; excitation wavelength, 510nm; and emission wavelengths 550-850nm. The parameters are different for each type of dye since their absorption range are different and these parameters gave the best smooth graphs.

Moreover, slit width differs for each sample and if the width is narrow, it gives better resolution and accurate results but lets in less light. Slit widths were adjusted to 4 for Coumarin, 10 for Bestoil Orange 2G and Bestoil Red 5B, because the emissivity of samples is different.

Then the following were chosen within the instrument software settings; reference detector (R1c), signal detector (S1c) and PL corrected for variations (S1c/R1c). There are 2 important considerations for emission measurements; the sample must be put into the camber with a 30^{o} angle so as to eliminate reflection, and the emission wavelength must start at a wavelength 20-30 nm longer than the given absorption peak wavelength, otherwise the emission peak will not be accurate.

2.3. Results and Discussion

2.3.1. Wavelength Tuning Material Analysis

An appropriate wavelength tuning material is defined by its absorption and emission properties. A wavelength tuning material should absorb light at wavelengths that microalgae, *Dunaliella salina*, does not absorb, and re-emit light as intensely as possible at wavelengths that *Dunaliella salina* absorbs. Thus, Coumarin 1 and 1,2-Diphenylacetylene should ideally absorb UV light and re-emit blue light; whereas, Bestoil Red 5B and Bestoil Orange 2G should absorb green light and re-emit red light.

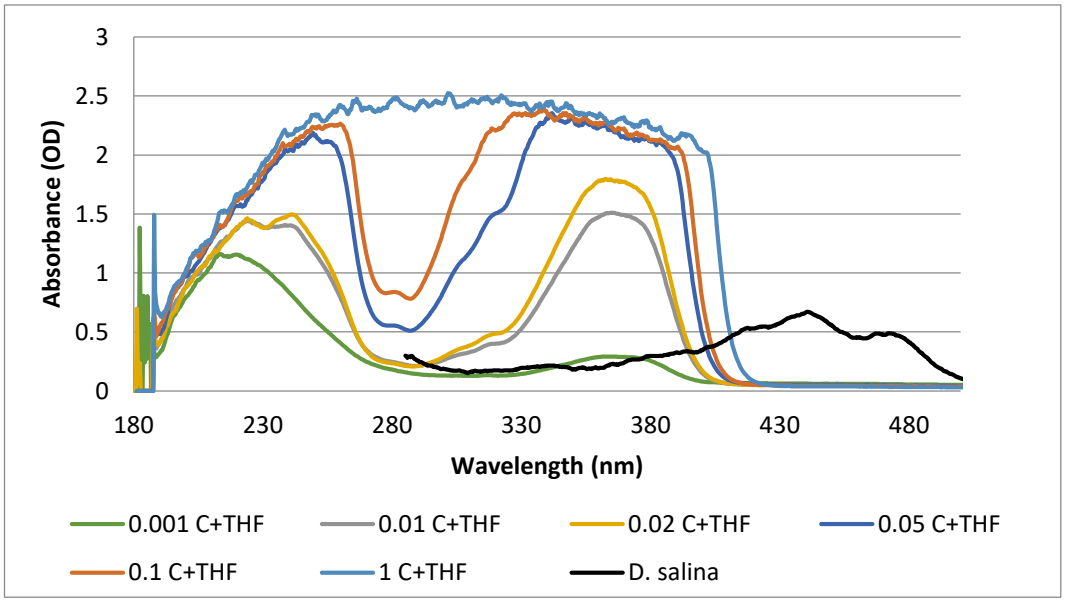

Figure 2. 6. Absorption spectra of Coumarin1 solutions at different Coumarin 1(C) /THF ratios

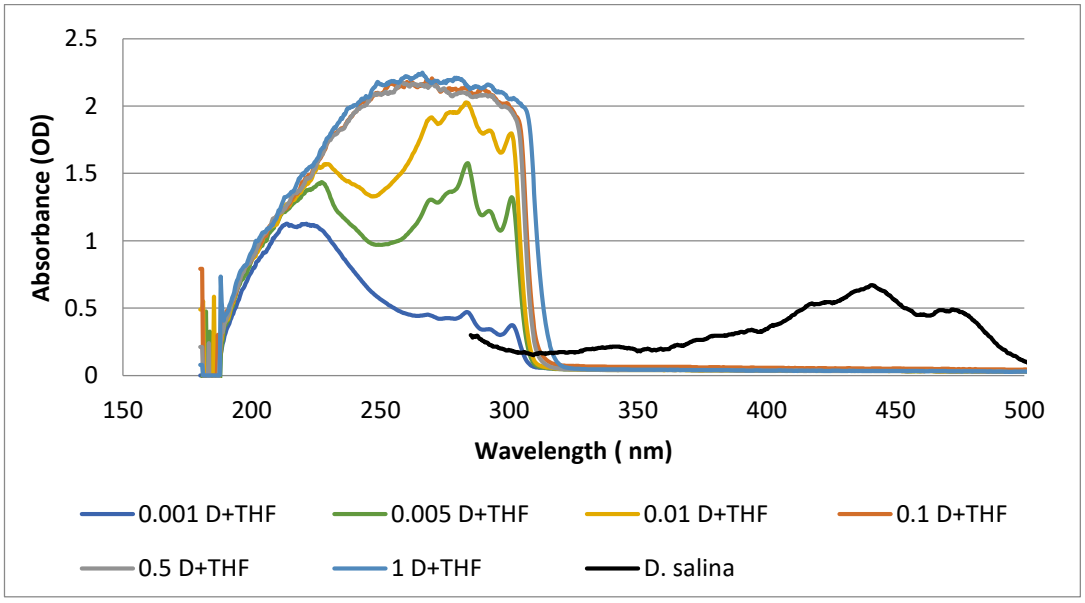

Figure 2. 7. Absorption spectra of 1,2-Diphenylacetylene solutions at diverse 1,2-Diphenylacetylene (D) / THF ratios

2.3.1.1. UV Light to Blue Light Conversion Analysis

The UV- A region is important for wavelength tuning material, because only this wavelength band of the sun reaches to the atmosphere surface and this will be absorbed by shifting material as discussed earlier in Literature Review. Experiments began with mixing organic dye with an appropriate solvent. Thereby, Coumarin 1 and 1,2-Diphenylacetylene were individually mixed with THF at different concentrations. The analysis indicates that Coumarin 1 has a good absorption pattern (Figure 2.6) compared to 1,2-Diphenylacetylene (Figure 2.7) since it absorbs UV light between 300-400 nm which is the wavelength band of UV ray reaches to the earth as shown in Section 2.1. THF was used as reference for each analysis. As demonstrated by Figure 2.6, the absorbance of the 1 C+THF is very broad and there is no dip at 280 nm which is due to scattering. Furthermore, there are two peaks for all samples; one is real absorption spectrum of Coumarin 1 dye and the other one, most probably, occurred because of reflection which fooled the spectrometer. Moreover, the absorption band of Coumarin 1 ranges between 300 and 400 nm. After 400nm, visible spectrum starts, the Coumarin/THF mixtures mostly absorb UV light. On the other hand, there is no absorption over 310nm for 1,2-Diphenylacetylene that means it absorbs only UV – C and UV – B region not UV – A region.

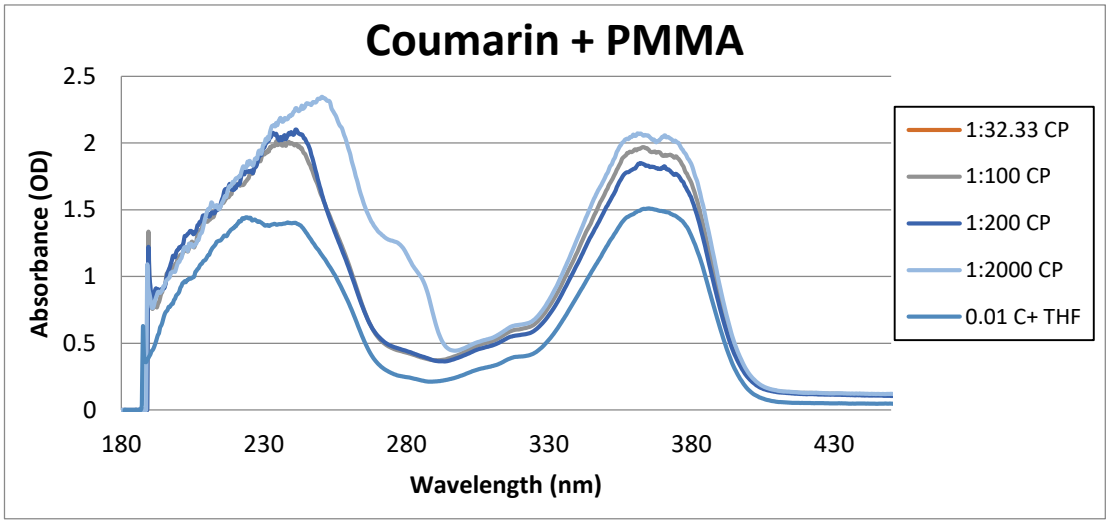

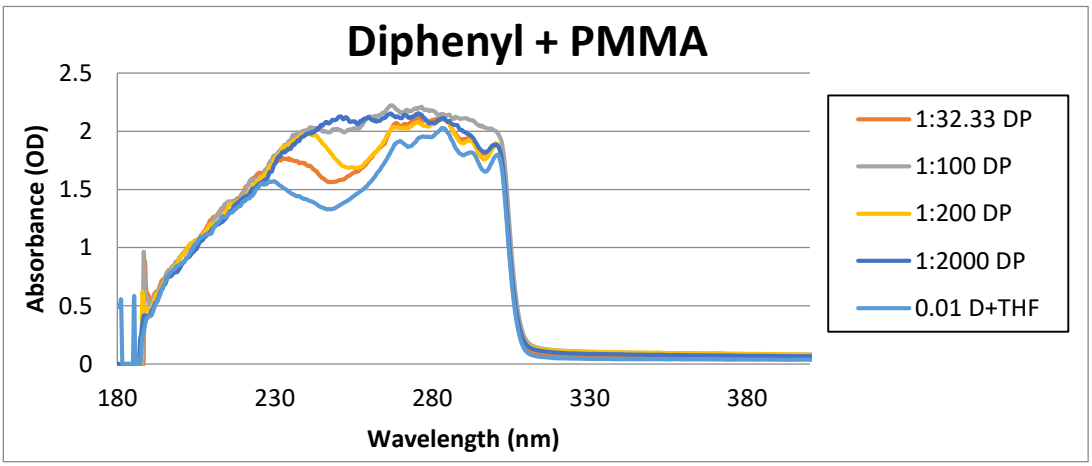

Figure 2. 8. Absorption patterns of Coumarin 1(C) /PMMA (P) and 1,2-Diphenylacetylene (D)/PMMA (P) mixtures at discrete rates.

The next experiment demonstrates the absorption patterns of new solutions of UV absorbed fluorophores and PMMA. For this purpose, one of the organic dye/ THF solution concentrations which show better absorption results among others was chosen for each blue emitting dyes as 0.01 for both Coumarin 1 and 1,2-Diphenylacetylene (from Figure 2.6 and 2.7). Then, PMMA was added to these solutions at various ratios in order to see if the polymer matrix is changing the absorption amount. The analysis results of these liquid solutions are given in Figure 2.8. The absorption pattern of 1,2-Diphenylacetylene does not vary with changing PMMA amount, no absorption beyond 310 nm. As mentioned previously in Section 1.3, solar irradiance below 310 nm is

filtered by atmosphere (Hagfeldt et al., 2010). It is clearly shown in Figure 2.6 and 2.7, 1,2-Diphenylacetylene is not a convenient fluorophore for this project since it cannot absorb UV light after 310nm which is UV-A bandpass of the spectrum reaches to the atmosphere surface. Contrary, Coumarin 1 gives an absorption peak about 370 nm. It absorbs UV – A light and absorption finishes just before *Dunaliella salina* absorption starts. *D. salina* absorption data was measured by disrupting the algae by adding ethanol to the algal suspension in water and measuring the absorbance by Dr. Alan Dunbar from the Chemical and Biological Engineering department of University of Sheffield.

Since Coumarin 1 gave the best absorption results, coatings of these mixtures were deposited onto microscope slide using spin coating. However, there was no measurable absorption, even if there was a coating present. This is due to low amount of Coumarin 1 in the solution which resulted in no absorption feature. Therefore, more concentrated Coumarin 1/ PMMA mixtures are needed to ensure the strong absorbance.

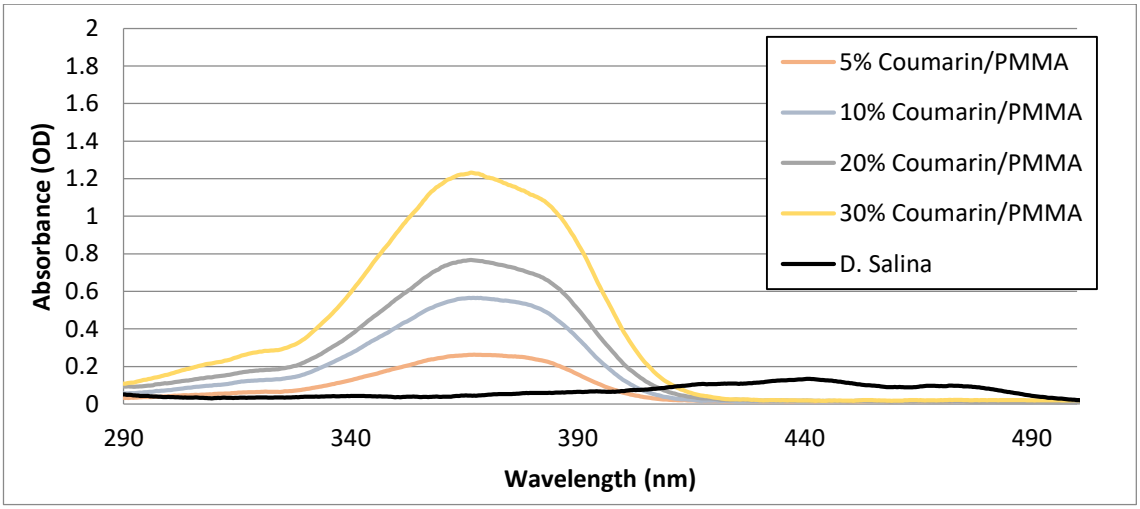

Figure 2. 9. Absorption result of coating (film) of Coumarin 1 - toluene - PMMA mixture with different Coumarin 1/PMMA percentages

Since the initial coatings of Coumarin 1 mixtures were not successful, deposition of a previously successful mixture was performed and Figure 2.9 indicates that these were successful coatings since it is not absorbing the light that is absorbed by algae. There is a small overlap with *Dunaliella* and Coumarin shifting material's absorption wavelengths but it is not extensive, so it is probably negligible. After, comparison of

the different percentages, 20% Coumarin 1 /PMMA (20% means the Coumarin 1 amount inside the PMMA) coating was chosen to be used in algae growth experiments because OD amount is higher than others and overlap amount is less than 30% one.

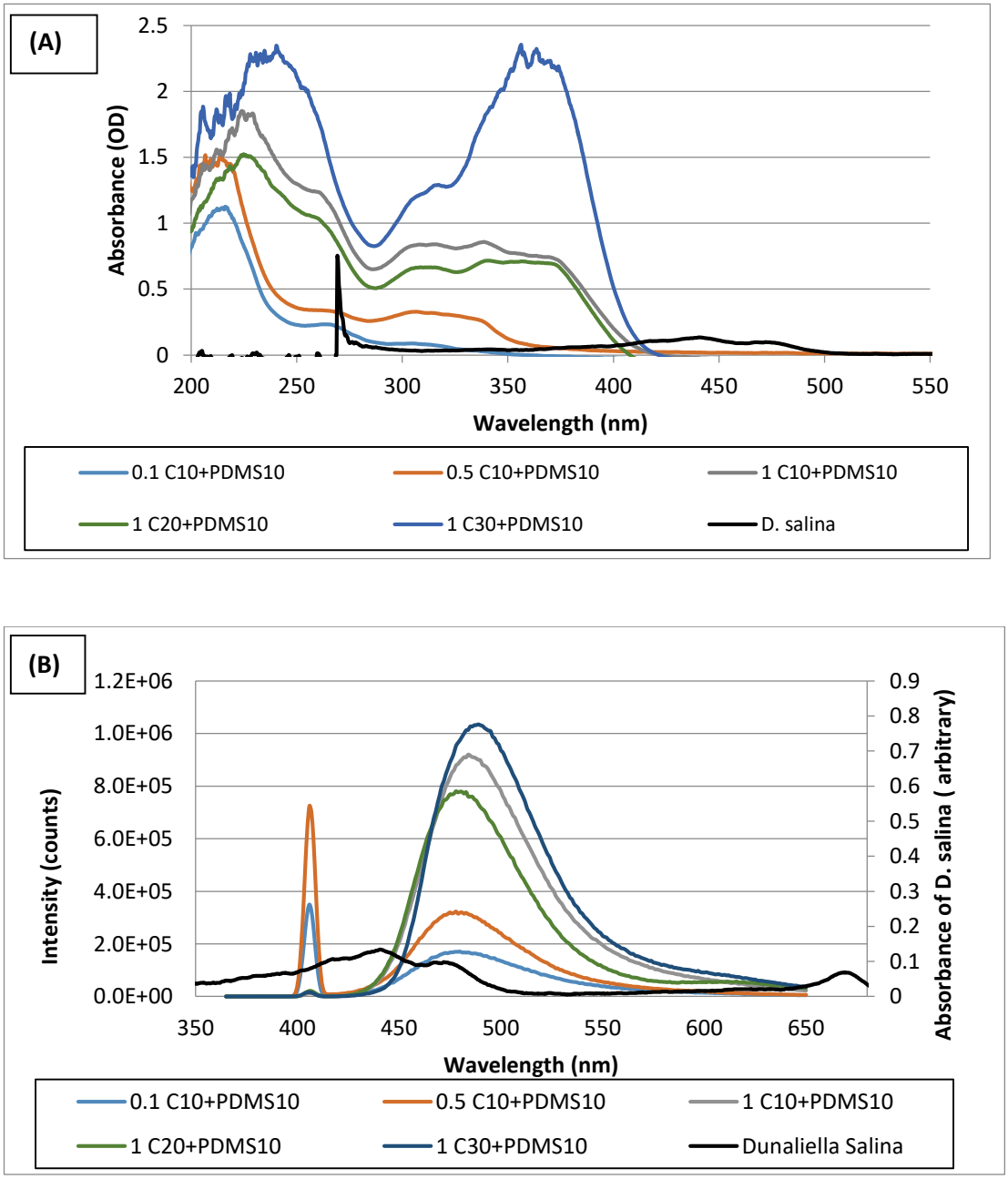

Figure 2. 10. **(A)** Absorption and **(B)** emission spectra of different Coumarin/PDMS mixtures. C represents Coumarin 1; and initial concentrations (0.1, 0.5, and 1) represent Coumarin 1/THF ratios.

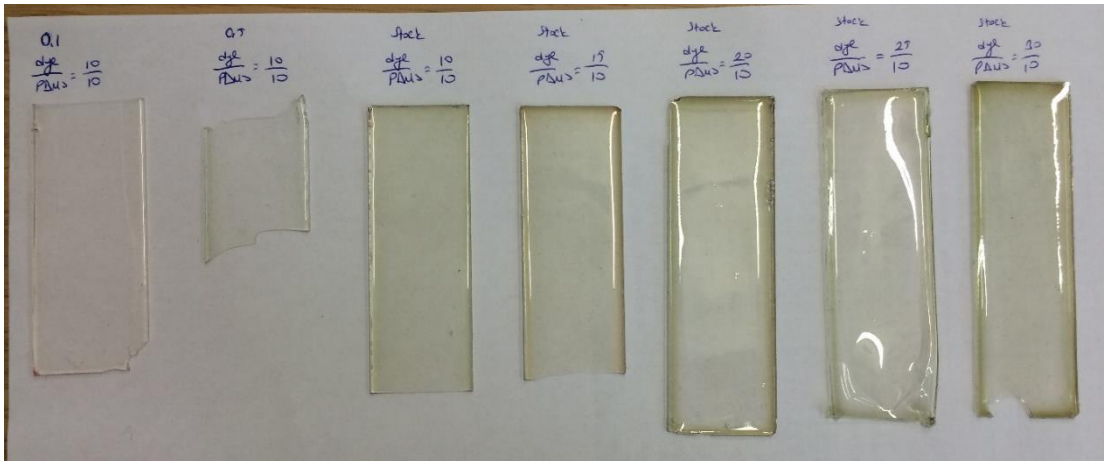

Figure 2. 11. Fabricated Coumarin 1/ PDMS shifting materials at different mixture percentages

Final experiment regarding UV to blue light emission was done by mixing Coumarin 1 and PDMS at various concentrations. Figure 2.10 gives both absorption and emission wavelengths of these wavelength tuning materials; emission wavelength overlaps with *D. salina* absorption wavelength. The overlap is good but it is not covering fully the absorption of algae. Optimization of both absorption and emission curves shows that the best PDMS shifting material to be used in algae growth will be a dye: PDMS blend mixed in a ratio 10:10 ratio. Also, emission peak is about 450 nm which is almost the middle of *D, salina* absorption band. Figure 2.11 illustrates the physical images of the produced Coumarin/ PDMS materials and at lower concentration (dye to solvent) materials become thinner and this causes difficulties while peeling off the shifting film from the mould.

2.3.1.2. Green Light to Red Light Conversion Analysis

The same experiments done in Section 2.3.1.1 were done for both Bestoil Red 5B and Bestoil Orange 2G, but the organic dye/ solvent ratios were different (Figure 2.12). It is obvious that Bestoil Red 5B has an absorption with a slightly shorter range (455 – 570 nm) compared to Bestoil Orange 2G (440 – 570 nm). For both fluorophores, when the concentration decreases below 0.01, no absorption is observed which might be due

to the limitation of the equipment. Whereas, increasing the concentration above 0.05 organic dye/THF does not allow for easy measurement of the absorption properties of the solution since the dye amount is not sufficient to detect. Therefore, the fluorophore/ solvent ratio should be between 0.01 and 0.05 for red emitting organic dyes (Bestoil Red 5B and Bestoil Orange 2G). On the basis of this deduction, 0.03 fluorophore/ THF ratio was selected to be mixed with polymer, PMMA.

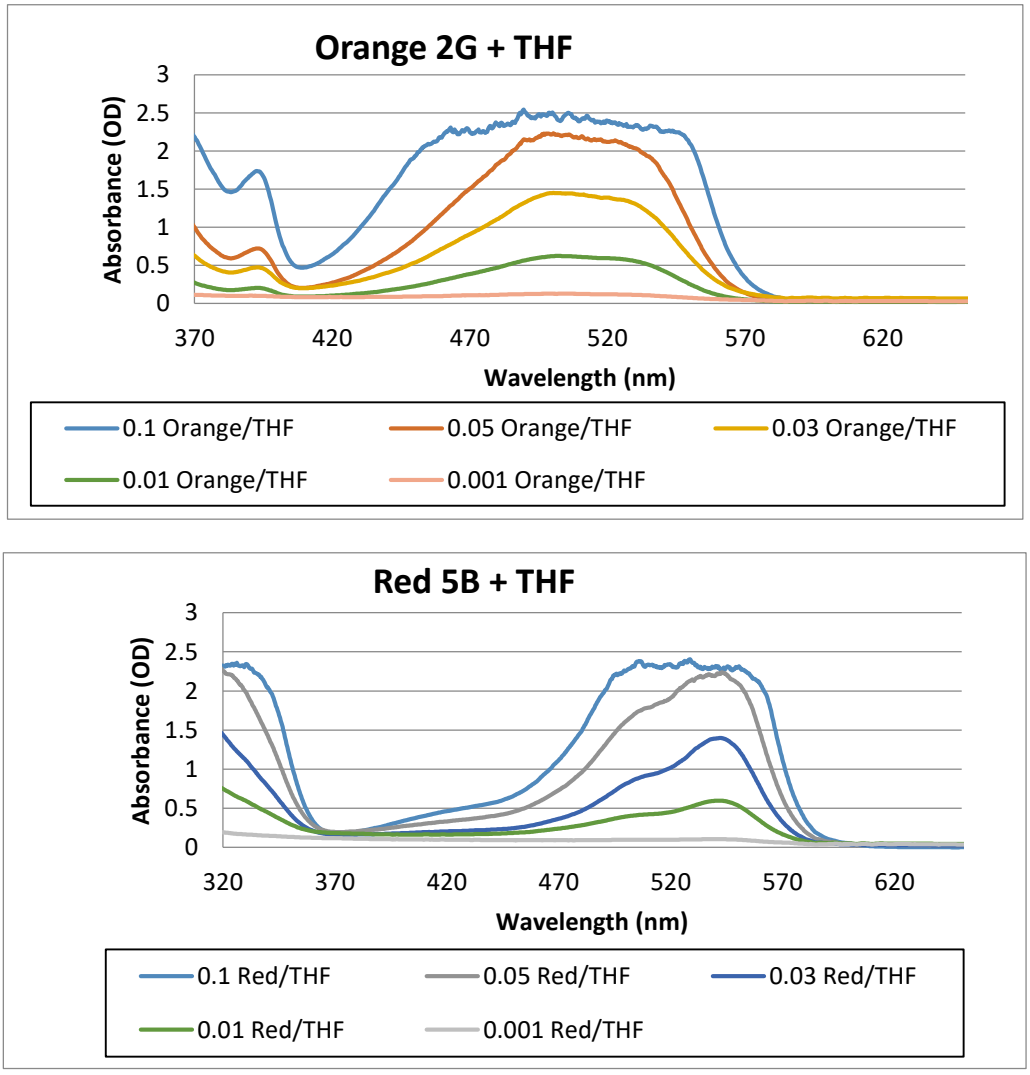

Figure 2. 12. Absorption graphs of Bestoil Orange 2G and Bestoil Red 5B mixtures with THF as solution

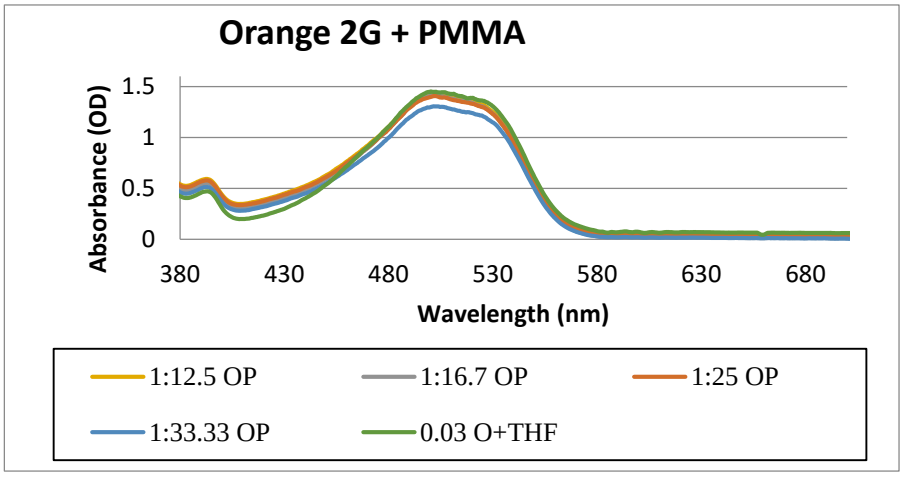

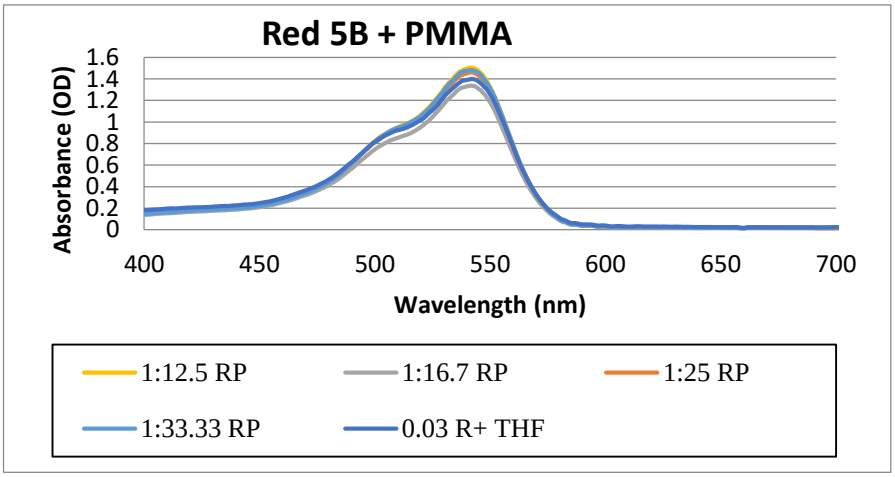

Figure 2. 13. Absorption curves of PMMA (P) mixtures with Bestoil Orange 2G (O) and Bestoil Red 5B (R) as solution

As performed for UV to blue light conversion fluorophores, adding PMMA at various organic dye/PMMA ratios was applied for these fluorophores as well. Figure 2.13 represents the absorption analysis of these studies. There is notably no difference between the various PMMA amounts since PMMA is not absorbing light. Although, the coating and the colour of the dyes can be seen by eye, without using microscope, there was no absorption peak for coated microscope slides. Most probably the films are very thin to measure the absorbance spectra. The reason for this can be the viscosity of the solution or amount of the organic dyes inside the solution. If the viscosity is lower, then the thickness of the coating will be very low; and this will yield very low absorption possibly below the instrument detection limit. On another view, when the

concentration of the organic dye is not sufficient, no incident light will be detected by the wavelength tuning materials since PMMA is a highly transparent material.

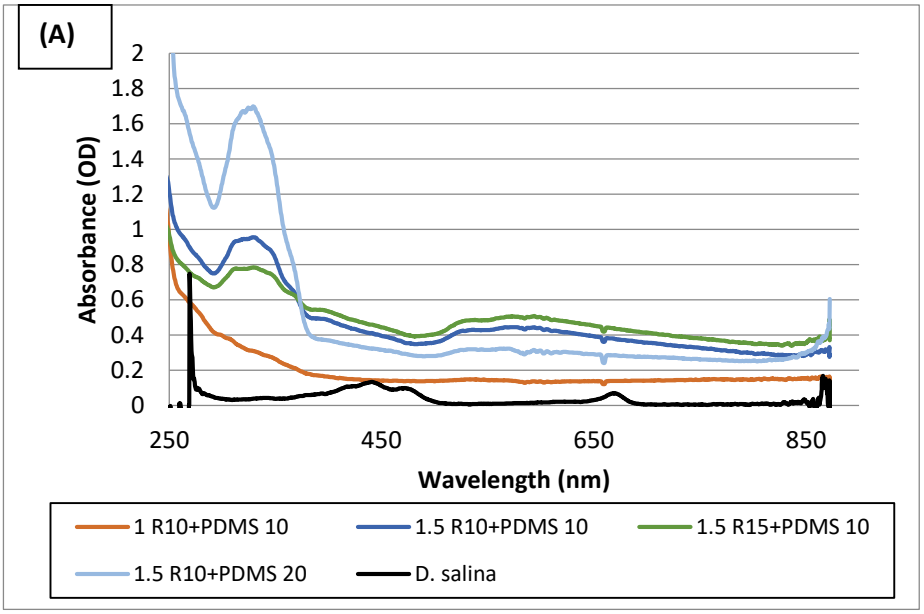

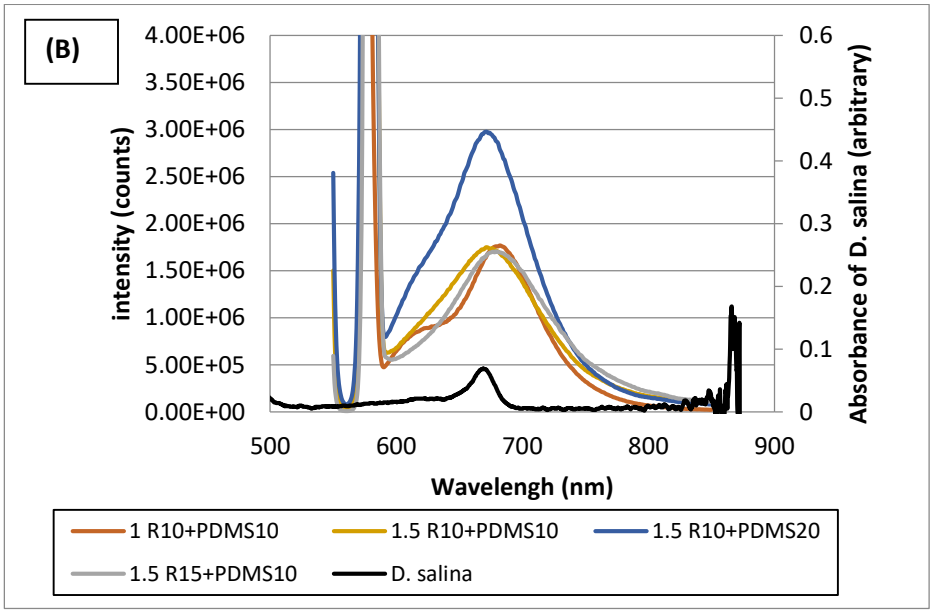

Figure 2. 14. **(A)** Absorption and **(B)** emission pattern of Bestoil Red 5B (R) mixtures with PDMS. Initial concentrations (1 and 1.5) represent Bestoil Red 5B/THF ratios.

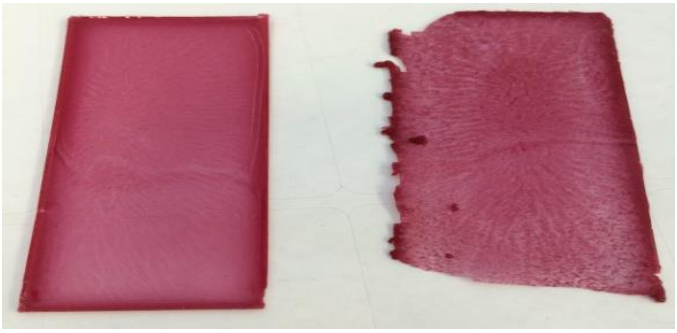

Figure 2. 15. Mixture sample of Bestoil Red 5B with PDMS

Since spin coating experiments for Bestoil Red 5B and Bestoil Orange 2G were not successful as expected (no absorption spectra was obtained), red emitting tuning material was fabricated by combining the fluorophore/THF mixture with PDMS. Different combinations were examined for both Bestoil Red 5B (Figure 2.14) and Bestoil Orange 2G (Figure 2.16). Unfortunately, Bestoil Red 5B has no ability to mix with PDMS well; therefore, no strong absorption peak is obtained for this fluorophore as can be seen from Figure 2.14. The absorption peak is between 300-400 nm but it is not the desired region. Also, it seems there is some absorption (500-700 nm) but the curve is broad with no strong peak existing; this is the result of dye molecules poorly-dissolved dye particles inside the PDMS mixture. These particles are caused by agglomeration (Figure 2.15) which results in scattering and reflection. Since there is no absolute absorption, the emission is lower compared to Bestoil Orange 2G (Figure 2.16). Actually, there are small emission peaks that might be related with PDMS itself, not organic dye.

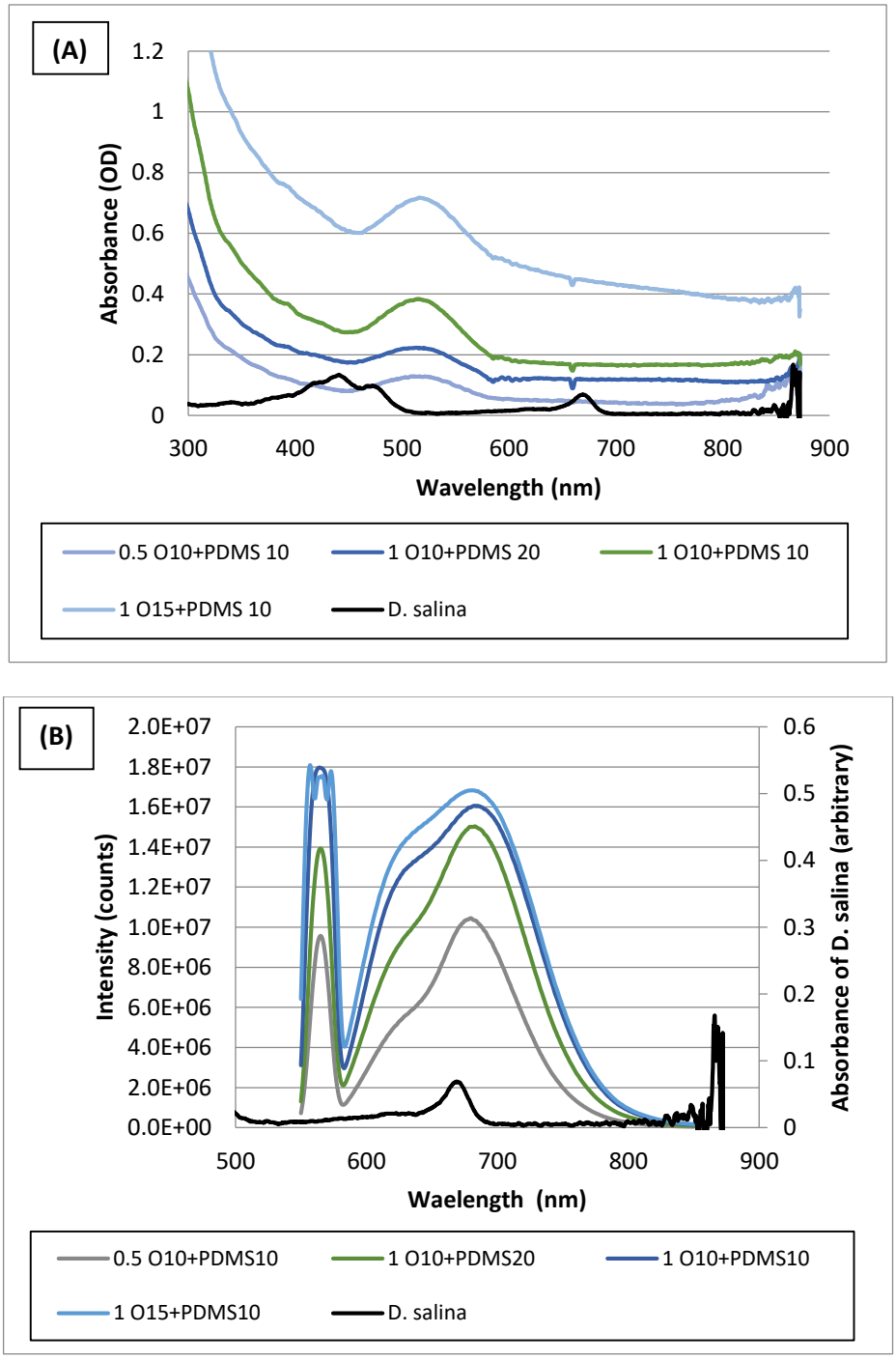

Figure 2. 16. **(A)** Absorption and **(B)** emission pattern of Bestoil Orange 2G (O) mixtures with PDMS. Initial concentrations (0.5 and 1) represent Bestoil Orange 2G/THF ratios.

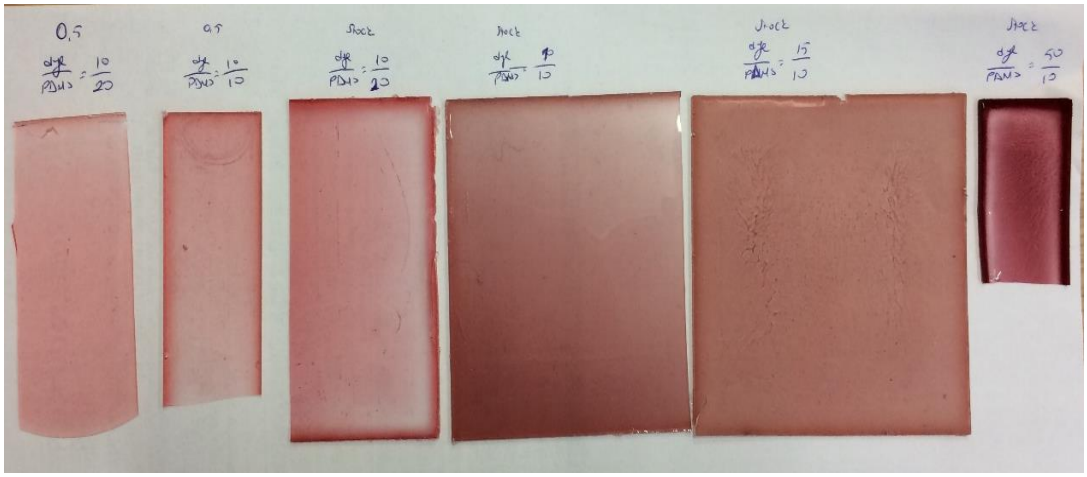

Figure 2. 17. Fabricated Bestoil Orange 2G (O) / PDMS shifting materials at different mixture percentages

In contrast to Bestoil Red 5B, Bestoil Orange 2G showed better results when mixed with PDMS, it is less aggregated, see Figure 2.15 and 2.17 for physical comparison. Notwithstanding it is small, there is a visible absorption peak for all samples. The absorption OD of the samples is not very high, but this is not a big problem since the emission is high. The reason for this small peak is some agglomeration of Bestoil Orange 2G/THF solution among the PDMS base. Moreover, as shown in Figure 2.16, the absorption band of the samples partially overlaps with *D. salina* absorption wavelengths. If the dye absorbs some useful light in the 380-480 nm range, this will cause a slower growth of *D. salina*, so it needs to be solved by changing concentrations or solvent or using another fluorophore. On the other hand, if this shifting material is located to an inner baffle, the incoming useful light will be absorbed by algae first so the overlap may not be neglected. Conversely, the emission bandwidth directly overlaps with *D. salina* absorption bandwidth at red region. As a result of this, stock (1) Bestoil Orange 2G (10) / THF + PDMS (10) mixture will be used for algae growth tests.

Furthermore, experiments were implemented with other solvents in order see the effect of solvents on PDMS (boiling point 200^{o}C) curing. After curing procedure, it was observed that the thin films were not uniform for both Bestoil Orange 2G – chlorobenzene and chloroform mixtures. Also, Figure 2.18 and 2.19 proves that these

mixtures result in lots of scattering which raises the curves. It is clear that adding chlorobenzene (boiling point 131°C) and chloroform (boiling point 61.2°C) make the aggregation worse. This might be because the chlorobenzene and chloroform may evaporate before PDMS was cured.

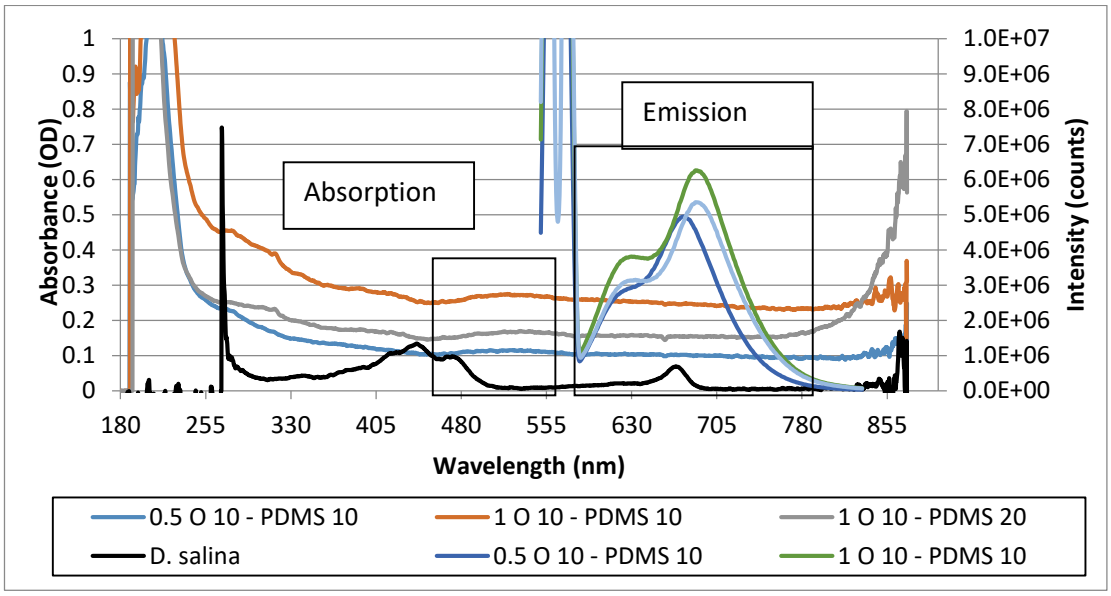

Figure 2. 18. Absorption/ emission graph of Bestoil Orange 2G (O) /Chlorobenzene mixed with PDMS. Initial concentrations (0.5 and 1) represent Bestoil Orange 2G (O) /Chlorobenzene ratios.

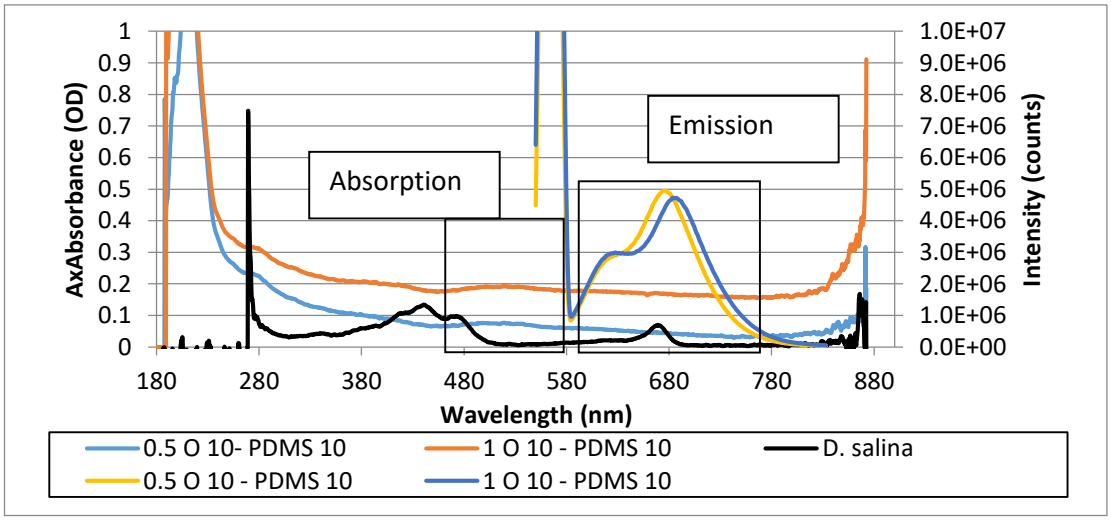

Figure 2. 19. Absorption/ emission graph of Bestoil Orange 2G (O)/ Chloroform mixed with PDMS. Initial concentrations (0.5 and 1) represent Bestoil Orange 2G(O) /Chloroform ratios.

2.4. Conclusion

In summary, this chapter includes the explanation of how wavelength tuning films were fabricated. The effect of different solvents, dye and host materials and their concentrations on the absorption/ emission features of the material were examined.

Fluorescent organic dyes are promising as wavelength tuning material owing to their high quantum efficiency and because they easily dissolve in many solvents and can be embedded in a polymeric matrix. Therefore, four different dyes, 1,2-Diphenylacetylene, Coumarin 1, Bestoil Orange 2G and Bestoil Red 5B were used in this study. Depending on the spectral analysis of UV to blue light shifting dyes, it is clear that Coumarin 1 fits the needs of the project very well by absorbing UV light between 300-400 nm and re-emitting in the interval 400-550 nm where *D. salina* can absorb. On the other hand, 1,2-Diphenylacetylene is not suitable for the project because it only absorbs light below 320 nm which is largely filtered by atmosphere and therefore not present in the solar spectrum. The case for the green to red shifting dyes is a little bit different. Both Bestoil Red 5B and Orange 2G have very similar absorption and emission wavelength band, however the Orange 2G better serves the project because it mixes with PDMS better to produce wavelength tuning film. It absorbs green light and emits red light at wavelengths ranging from 620nm to 780 nm.

All the polymers used in the experiment (PMMA, polystyrene and PDMS) work very well as host materials. Especially, PMMA and polystyrene showed good attributions for the spin coating experiments. They mix very well with the dye and the solvent and application on the glass support is easy. On the other side, PDMS has a good feature as a host material as it is easily applied to the reactor. The spin coating process for small sizes is easy, however, it would be hard to apply this method on bigger sized reactors. Although the spectral analysis pattern of both films produced by spin coating and the PDMS curing methods are almost same as each other, PDMS curing is chosen for the further experiment when the large scale algae production is taken into consideration. Making only one mould for the PMDS cure was sufficient because use it repeatedly. After the curing process is completed, the material can be peeled off from the mould and attached to the reactor easily due to its elastic and sticky properties.

CHAPTER 3. DESIGNING PHOTOBIOREACTOR FOR *DUNALIELLA SALINA* GROWTH

3.1. Photobioreactor Design

While designing the photobioreactor, it is important to consider the light transmittance properties of the raw material. Therefore, the most appropriate material for the purpose is either glass or Perspex where both have the feature of the transmitting the light. As explained in the literature review part, Chapter 1, the thickness and the angle of the incident light is important for better emission and less reflection. It is important to get almost perpendicular incident light so as to minimize the reflection of the light. When the geometrical shapes considered it is easy to get a perpendicular light impingement to the flat surface compared to the round ones. When the general photobioreactor designs are take account of, they are mainly made in either round or the flat shape. In order to eliminate the reflection during the *Dunaliella salina* growth with the illumination of light from a flat light box, it is decided to use the flat bioreactor for the further experiments.

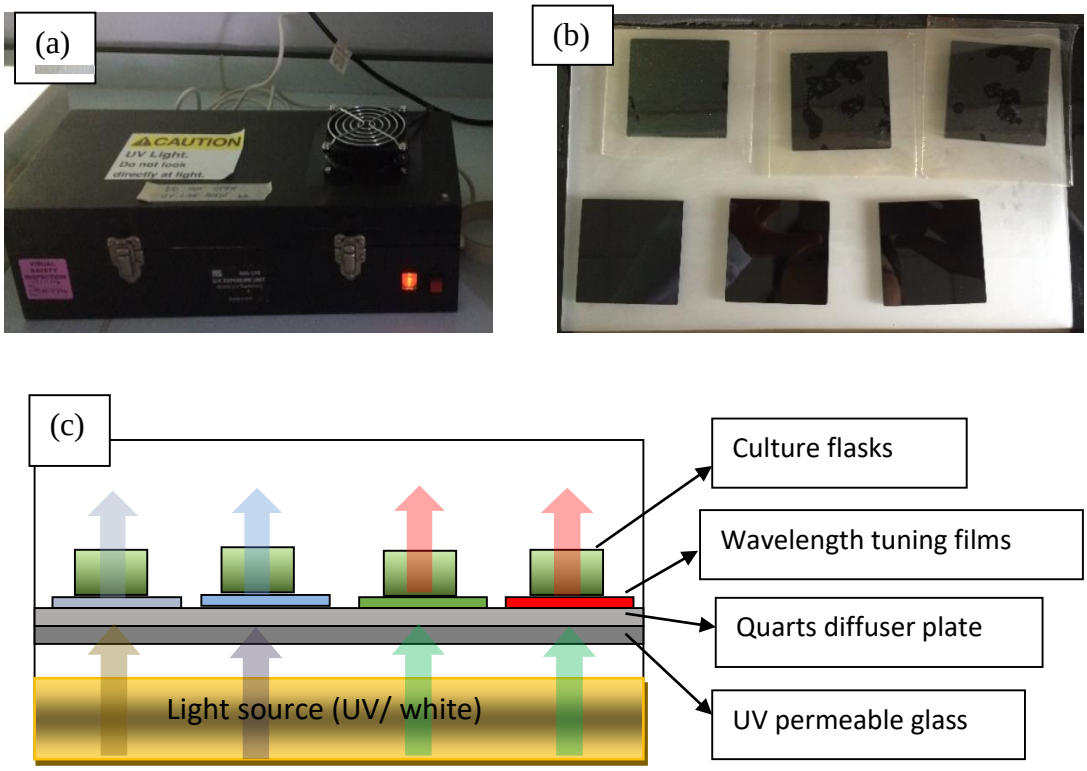

Figure 3. 1. Algae growth systems **(a)** UV light box, **(b)** visible light filter to cut the light 400nm over and **(c)** scheme of UV light box

3.4.1. Small scale reactor and its coating process

Dunaliella salina growth is divided into three sizes; small size with either 250 ml flasks (round shape) as preliminary experiments but not shown here, 50 ml cell culture flasks (flat shape) as small scale and 3L photobioreactor as large scale. The small scale growth flasks are designed to use inside modified UV light box (transilluminator) (Modified RS-555-279 UV Exposure Unit) (Figure 3.1 (a)) with different light exposure orientation with wavelength tuning material coating. The custom modified UV light box (Figure 3.17 (a)) includes a fused high transparency quartz diffuser (Instrument Glass – Optical white crown spectacle B270 Glass) with dimensions 250mm x 150mm x t1.15mm; 1 UV light (Philips F8T5/BL Fluorescent Bulb); and 1 white light (F8W/35 Fluorescent Bulb). For some experiments, algal growth was performed separately under UV light only or white light only; thus, 2 UV or 2 white light bulbs were used accordingly. The UV lights used in the box are Philips TL8W/10 tubes and white lights are 8W – T5 cool white (see Figure 3.2 and Figure 3.3 for light intensities). UV and white bulbs were used for UV to blue light conversion with Coumarin shifting material and green to red light conversion with Bestoil Orange 2G shifting material, respectively. The temperature of the box was measured with a thermo couple (Farnell – Part no: TK-612) at several intervals.

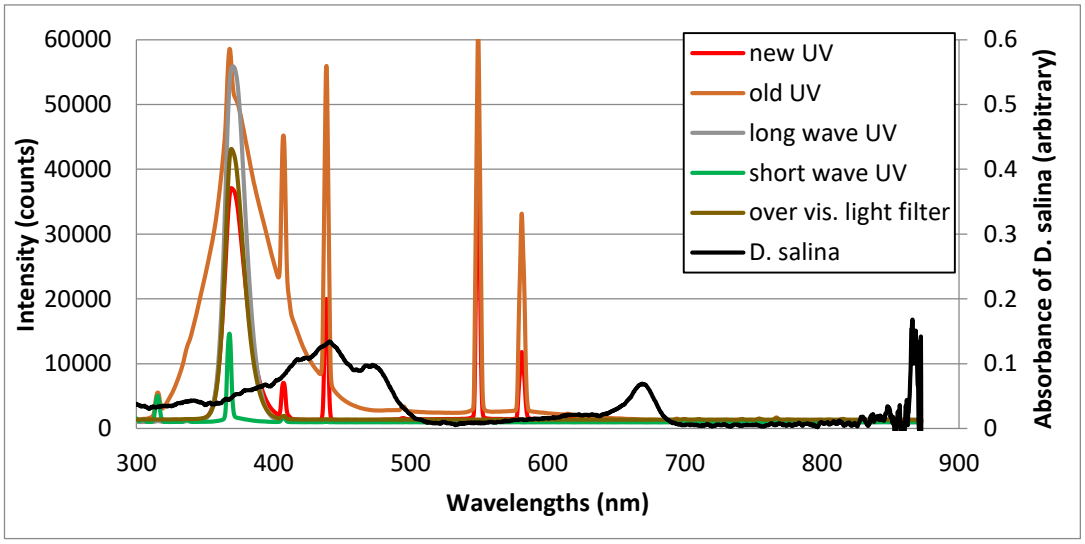

Figure 3. 2. Intensities of UV lights inside UV light box (old and new replacements) and black box (long wave and short wave) and absorbance of *D. salina*

As can be noticed from Figure 3.2, UV light inside the UV light box emits light at wavelengths over 400 nm which is in the visible light band. Therefore, a visible light filter was needed in order to cut the emission over 400nm (Figure 3.1 (b)); so a 320 nm bandpass colour glass filter was supplied from Optical Filters (see Appendix 5 for transmission curve of filter).

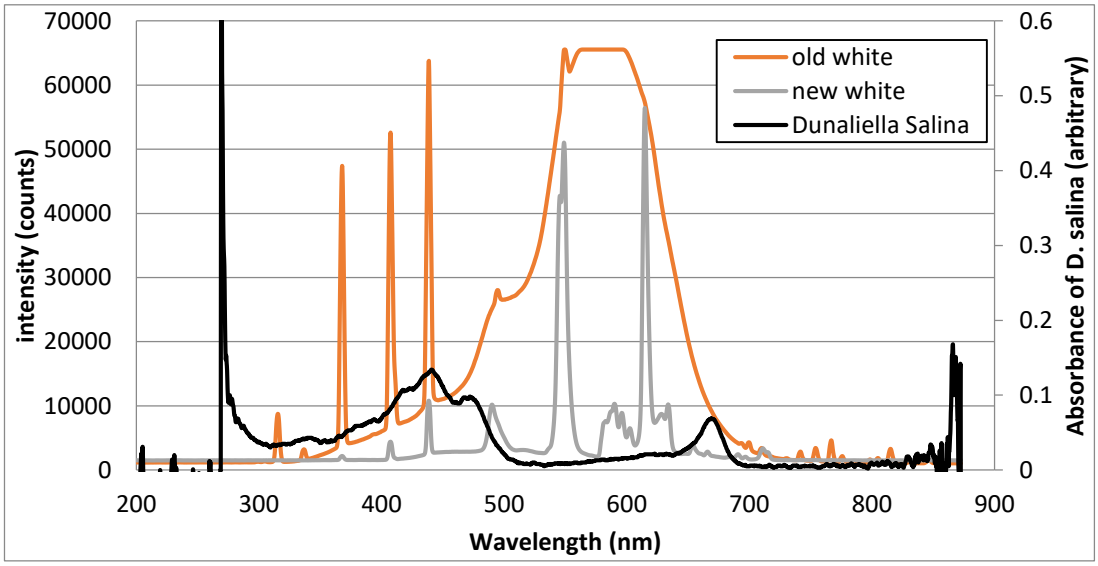

Figure 3. 3. Intensities of white lights in UV light box (old and new replacements) and H-floor growth room and absorbance of *D. salina*

The growth chamber, transilluminator, is designed for using the culture flasks (VWR (CAT no; 737-2311), made from polystyrene). The working principle of the UV light box is given in the Figure 3.1 (c); light (UV and/or white light) is located to the bottom of the box and there is UV permeable glass on top of light tubes. And just over this glass, there is a quartz diffuser plate which is used to obtained better light distribution. After passing the quartz diffuser, the incident light hits to the wavelength material and re-emitted through the small culture reactors. These culture reactors are covered with aluminium foil except underside where light penetrated and located inside the UV light box as shown in Figure 3. 4 (b).

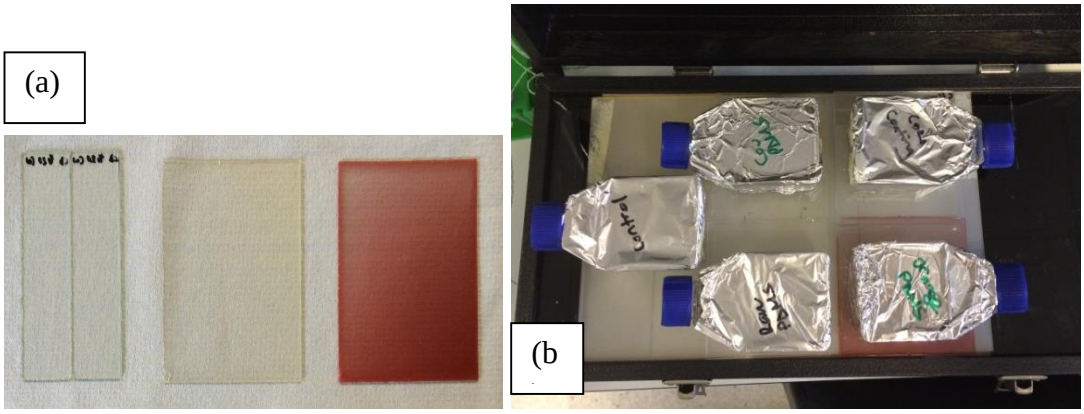

Figure 3. 4. **(a)** The wavelength tuning materials and their arrangement inside; **(b)** the UV light box (transilluminator)

3.4.2. Fine bubble addition to the small culture reactors

The second part of the project deals with fine-bubble injection of CO_2 rich gases into the growth system. The proposed set-up can be seen in Appendix 6. The growth system incorporating fine-bubbles (Figure 3.5 (a)) was composed of a prototype sparger with 5mm diameter (or air stones), a gas pump (5W, output stream is 7.2 L/min, supplier HAILEA), white light on the bench.

First, 5mm holes were drilled in the side of the flasks to pass the connecting pipework into the flasks; 3 mm holes were also drilled in the lids to allow the gas to leave the flasks. Meantime, the pipes and sparger/ air stone (Figure 3.5 (b)) were put into an autoclave for sterilization. Next, the sparger / air stones were inserted into the flasks.

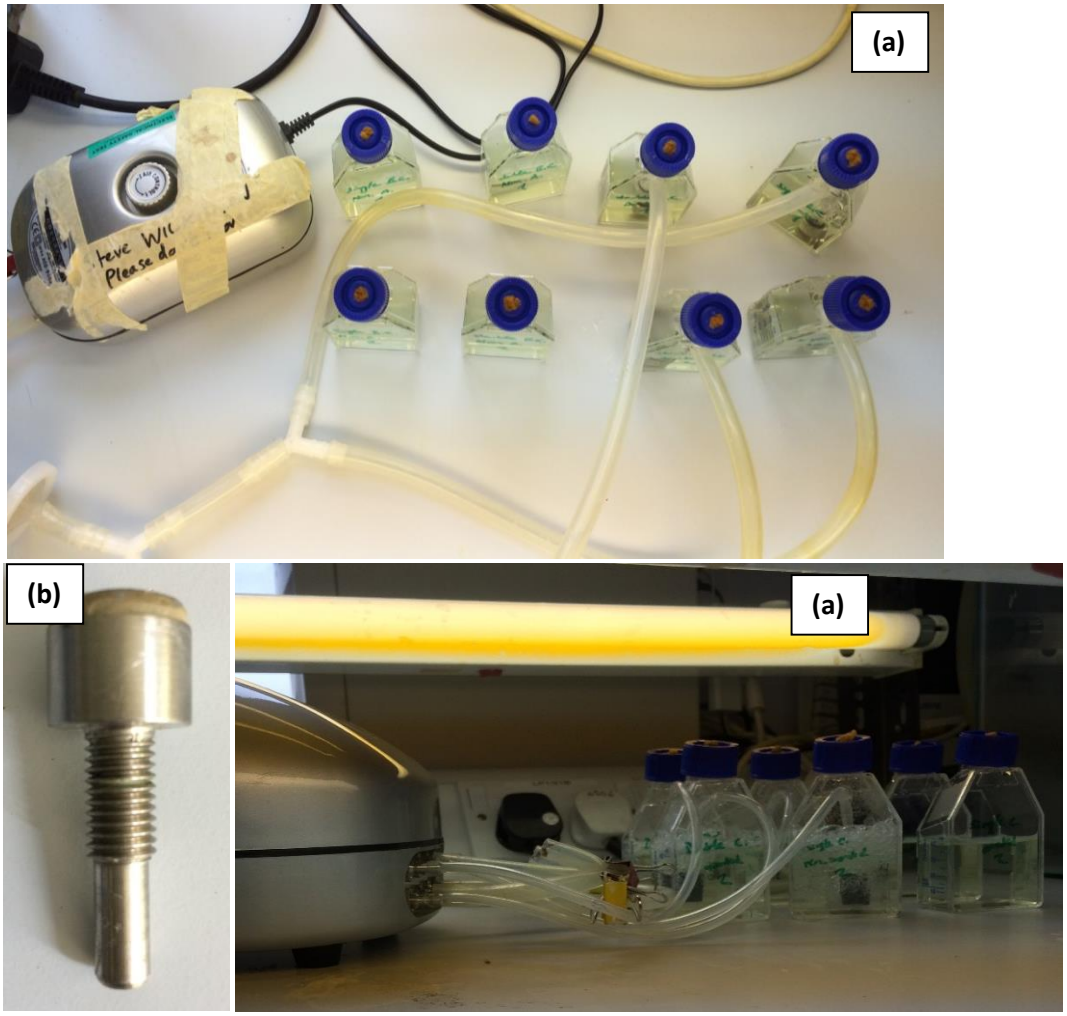

Figure 3. 5. Introducing microbubble technology to algal growth system **(a)** growth set-up and **(b)** sparger used in the experiment

3.4.3. 3L flat plate photobioreactor

In this study, 3 litres flat plate airlift photobioreactor is used to grow *Dunaliella salina*. The main design of the photobioreactor, Figure 3.6, is taken from previous PhD student Krys Bangert (Bangert, 2013) and some modifications are done in order to prevent algae accumulations in some dead zones. Additional Perspex were put to the bottom of the reactor where the dead zones occur due to no circulation.

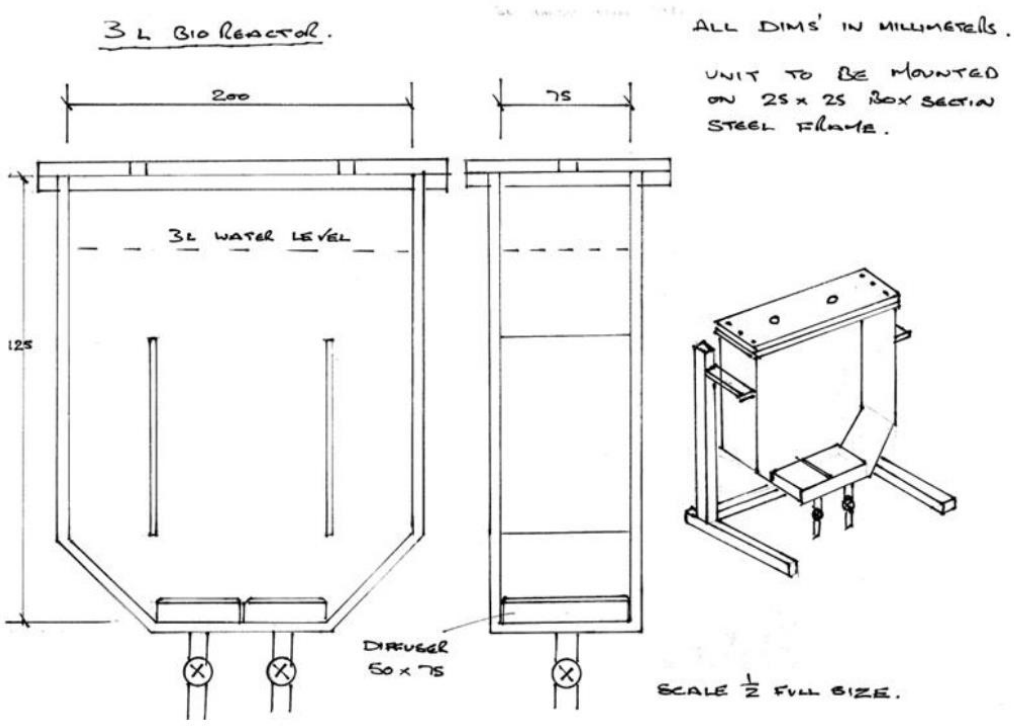

Figure 3. 6. Technical drawing of 3L flat plate photo-bioreactor design. (Bangert, 2013)

There are two airlift photobioreactors with the same design, and these bioreactors were built by the technician Mike Omeara and subsequently modified by technicians Andy Patrick and Cliff Burton of Chemical and Biological Engineering Department workshop at The University of Sheffield. The photobioreactor was made from Perspex Altuglas. The two spargers at the bottom of the reactor were produced by Material Science and Engineering Department's technician of The University of Sheffield by enclosing a 50µm pore sized ceramic microporous material with a stainless steel (316 type). These spargers were attached to ETG ball valves which were connected to gas cylinder/ air pump in order to supply gases inside the reactor so as to obtain a good medium circulation and minimize the cell build up on the reactor walls and also to reduce the accumulation of dissolved O_2. Triangular Perspex wedges were added on either side of both the spargers; thus, the problem of growth algae accumulation in these regions because of poor gas circulation was solved. The reactor lid that is sealed

with a 1mm thick nitrile rubber was closed properly using 18 screws and there is an outlet on this lid which is used to take culture sample every 24 hours.

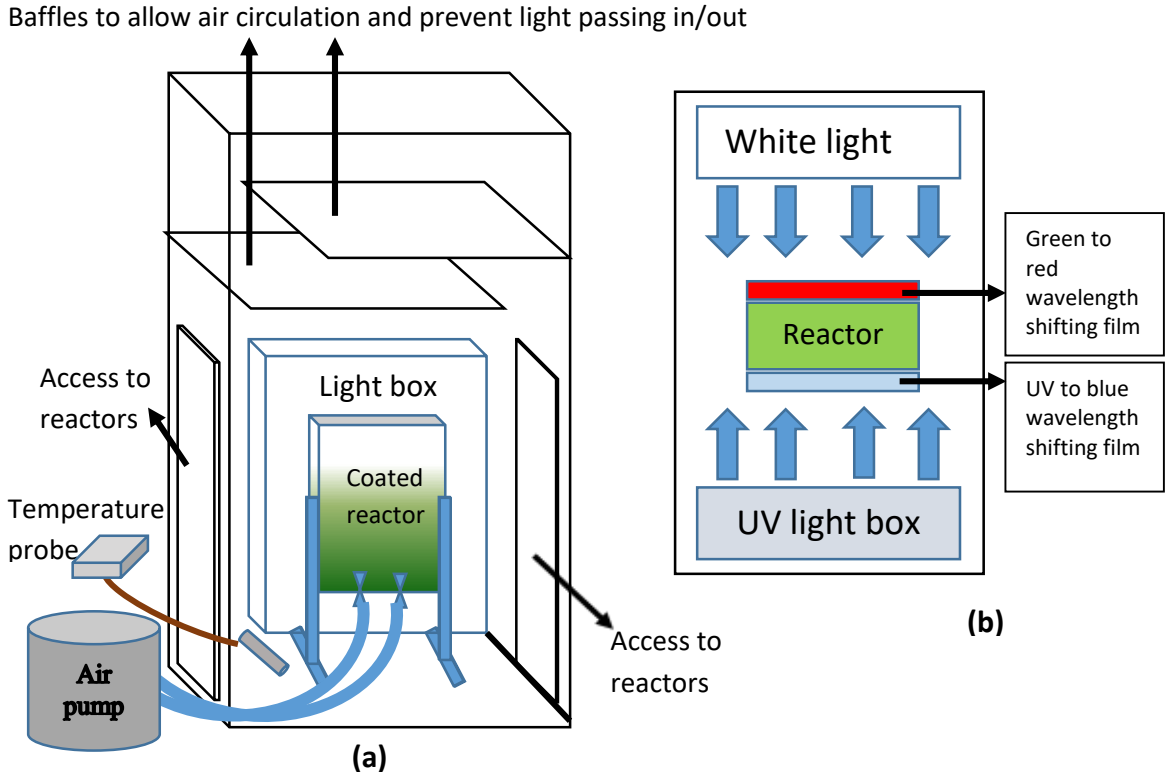

Figure 3. 7. Scheme of experimental set-up for *Dunaliella salina* growth **(a)** Design of the growth chamber showing the dark enclosure, baffles to allow air circulation. Note the front is shown as transparent and only one light box is shown for clarity. **(b)** Plan view of the reactor and light source positioning within growth chamber. For control experiments no wavelength shifting material was present.

A black box is designed and built by me using Correx corrugated plastic sheets. This box has dimensions as 120cm x 80cm x 50cm for height x wide x depth, respectively. There are two small doors on the both side of the box to be able to put the photobioreactor inside/outside of the box while taking sample each day. The box is completely closed system to prevent daylight to come in or harmful UV light to come out; however, there are two baffles above the reactor as seen in Figure 3.7. These baffles help to circulate air inside the chamber and decrease of the ambient temperature

increase due to light boxes. Two A2 size light boxes were put inside the box for each UV (2 tubes of Philips 15W 18" 450mm Fly killer – TPX15-18) and white light (2 tubes of GCL Fluorescent cool white, T8-15W 450mm) illumination, see Figure 3.8 for the emission spectrum of these light boxes. For the UV light box, there is a UV transparent and grounded low iron glass with dimensions 460mmX635mmX3mm as heightXwideXdepth, respectively, for better UV light distribution. A temperature probe is added to record ambient temperature inside the chamber for 24 hours. The photobioreactor valves are attached to the rotameter to control the inlet gas flowrate at 150cc/min. Each side of the photobioreactor is coated with fabricated dye/PDMS tuning films.

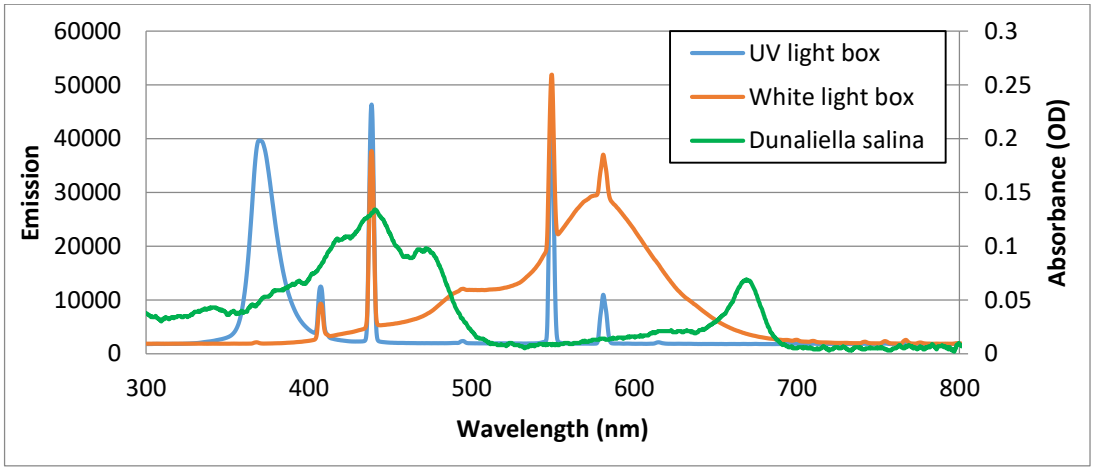

Figure 3. 8. Emission spectra of the white and UV light inside the light box

3.2. Conclusion

All in all, this chapter includes the explanation of design of small scale and 3L photobioreactor and the experimental set-up. The fundamental parameters to design the photobioreactor were to maximize surface-to-volume ratio in order to supply more useful light, to distribute the incident light more abundantly to the culture, and to increase the mass transfer of gases effectively (Lee and Palsson, 1994, Lee et al., 2014). When the light distribution inside the reactor is good, the total light utilization will be maximized by minimizing the photoinhibition and also self-shading.

Gas transfer is another essential problem in photobioreactor design due to carbon dioxide needs to be supplied and accumulated oxygen should be removed. Sparging the system from the bottom will improve total utilized light like as: (1) presence of air bubbles will increase light penetration depth, and (2) increasing the bubbles' movement will prompt some degree of mixing tangential to the flow direction

On the basis of the small scale reactor design trials, flat surface was considered preferable geometrical shape for better light penetration. The temperature issue is a main problem for the reactor design as will be discussed in the algae growth chapter. Also, amount of the inlet gas flowrate and the light intensity for the illumination is important and effective parameters on the growth.

CHAPTER 4. MATERIALS AND METHODS FOR DUNALIELLA SALINA GROWTH

4.1. *Dunaliella salina* Medium

The chosen algae strain is *Dunaliella salina* CCAP 19/30 supplied from Culture Collection of Algae and Protozoa (CCAP), Oban, UK. A suitable growth medium for *Dunaliella* was developed by Hard and Gilmour (1996), and is prepared as follows;

2.4 M $MgSO_4.7H_2O$	133.1 g in 225 ml
2.0 M $MgCl_2.6H_2O$	91.5 g in 225 ml
1.0 M $CaCl_2.2H_2O$	33.1 g in 225 ml
4.0 M $NaNO_3$	34.0 g in 100 ml
0.5 M Na_2SO_4	63.9 g in 900 ml
0.1 M NaH_2PO_4	3 g in 250 ml
2.0 M KCl	74.6 g in 500 ml
1.0 M HEPES pH 7.6	59.6 g in 250 ml
1.5 mM FeEDTA pH 7.6	0.0551 g in 100 ml

Supplements (Trace elements)

185 mM H_3BO_3	4.576 g	
7 mM $MnCl_2.4H_2O$	0.5541 g	
0.8 mM $ZnCl_2$	0.0436 g	All in a total of 400 ml
0.02 mM $CoCl_2$	4 ml of 2mM	
0.0002 mM $CuCl_2$	0.4 ml of 0.2 mM	

$CoCl_2.6H_2O$ (2mM)	0.1071 g in 225 ml
$CuCl_2.2H_2O$ (0.2 mM)	0.0307 g in 900ml

All stock solution chemicals were dissolved in distilled water and stored in Duran bottles at room temperature. *Dunaliella* medium was prepared in a 1 L Duran bottle as shown in the following table. First, the required amount of NaCl was dissolved into a 1L flask containing approximately 850 ml of distilled water, and then all components except $NaHCO_3$ were added to the flask. After that, pH was adjusted to 7.5 by adding NaOH or HCl; volume was made up to 1L and finally $NaHCO_3$ was added as a carbon source. Then, the medium was put into an autoclave to sterilize it.

Stock Solution	**Concentration wanted (mM)**	**Volume of stock for 1 liter (ml)**
Solid NaCl	e.g. 1.5 M	87.75 g
2 M KCl	10	5
2 M $MgCl_2$	20	10
1 M $CaCl_2$	10	10
2.4 M $MgSO_4$	24	10
4 M $NaNO_3$	5	1.25
0.5 M Na_2SO_4	24	48
100 mM NaH_2PO_4	0.1	1
1.5 mM FeEDTA	0.0015	1
Trace elements	1 ml $litre^{-1}$	1
1 M HEPES pH 7.6	20	20
$NaHCO_3$ (solid)	1 g $litre^{-1}$	1 g

4.2. pH measurements

An FE-20, Metler Toledo pH meter was used in order to measure the pH of the reactors. Since the ideal pH of the *Dunaliella* medium is about 7.5, calibration of the instrument was done at two points i.e. pH 7 and pH 10. Each day, 1.5 ml of the sample was taken from the reactor and transferred to a 15ml Falcon tube. After the pH probe was put inside the tube and the meter display showed a constant number, and the reading was taken. The probe was washed and cleaned before and after each measurement.

4.3. CELL DENSITY MEASUREMENT

4.3.1. Spectrophotometer

Analysis of the algal growth was done by measuring optical density (OD) using a UV-Vis Unicam Helios Alpha spectrophotometer where the integration time was set to 1 second and the wavelength is set at 595nm. Samples were taken every 24h during each algae growth experiment starting from zero hours. For the small scale cell culture flasks, each of them was shaken before taking samples to eliminate uneven algae suspension; on the other hand, for the large scale algae growth, samples were directly taken from bottom of the 3L airlift photobioreactor. Each time 1 ml of sample was transferred to a 1ml plastic cuvette (634-0675 Polystyrene, VWR). 1ml of distilled water was used as the blank before measuring optical density of the sample, since the original *Dunaliella* media and the distilled water has the same OD reading as reference solvent.

4.3.2. Dry weight calculations versus OD concentration

In order to understand how much biomass was produced in each algae growth experiments, it is essential to make the correlation between dry weight of the unstressed algae growth and all other stressed growth conditions. Therefore, *D. salina* cell dry weight was measured depending on the process explained in the study of Storms et al. (2014) after some modifications. Firstly, it is important to have a well grown (optically dense) *D. salina* culture with OD_{595} = 1. A set of dilutions were prepared based on Table 4.1 with a final volume of each dilution as 30ml. The dilution of the culture was done using fresh *D. salina* medium by adding the algal suspension and medium inside 50 ml Falcon tubes as shown in Table 4.1. After that, 1 ml sample from each tube was taken and OD at 595 nm was measured, then the sample was returned to the tube after measurement.

Table 4. 1. *Dunaliella salina* concentrations used to prepare dry weight vs concentration curve

Tube Number	Concentration (%)	Culture (ml)	Media (ml)
12	0.0	0.0	30.0
11	8.3	2.5	27.5
10	16.6	5.0	25.0
9	33.3	10.0	20.0
8	41.6	12.5	17.5
7	50.0	15.0	15.0
6	58.3	17.5	12.5
5	66.6	20.0	10.0
4	75.0	22.5	7.5
3	83.3	25.0	5.0
2	91.6	27.5	2.5
1	100.0	30.0	0.0

All Falcon tubes were centrifuged at 3000 *g,* then the supernatants were discarded. Next, the pellets at the bottom of the tubes were resuspended (Tube 12 has no pellet, but it was treated as though it has) in 5 ml of distilled water and transferred into 15 ml Falcon tubes. Then, all tubes were centrifuged at 3000 *g* and the supernatants were discarded again. Then, the pellets were resuspended in 1 ml of distilled water and transferred to pre-weighed (on a fine balance) 1.5 ml Eppendorf (microcentrifuge) tubes. The tops of another set of fresh Eppendorf tubes were removed, and a hole was put in each extra top to dry the samples in freeze dryer, and then the Eppendorfs containing the samples were sealed using these tops with holes. As next step, the Eppendorf tubes were frozen overnight at -80^{o}C and then freeze dried (lyophilised) for 24 to 48 hours until samples were completely dried. After 2 days, tubes were taken from the freeze dryer, the extra tops with holes were removed and weighed on fine balance. Finally, dry weight of each tube was calculated and the concentration curve was plotted using Excel (Figure 4.1). Afterwards, the OD value of the optimum cell concentration was converted into the dry weight value, mg ml^{-1}, as shown in the Excel sheet equation as y = 0.3089x (taken from Figure 5.1).

Where y= Dry weight (mg/ml) and x = OD595

Then, the percentage of neutral lipid was calculated by dividing the concentration of neutral lipid by the value of the cell dry weight and multiplying by 100.

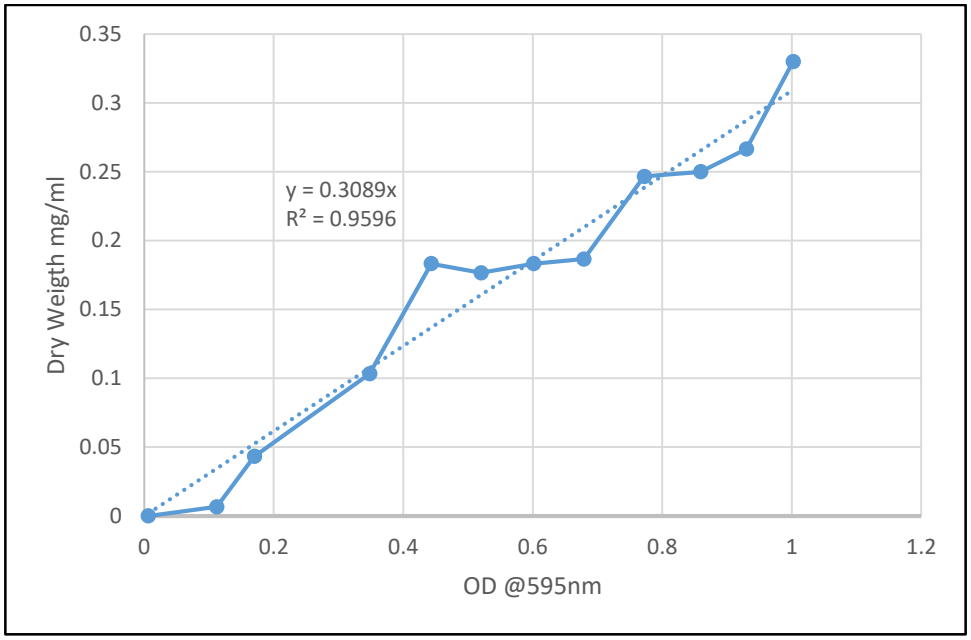

Figure 4. 1. Dry weight vs OD concentration calibration curve of *Dunaliella salina*

4.4. LIPID DETERMINATION

4.4.1. Nile Red fluorescence for neutral lipid quantification

The amount of intracellular neutral lipid in *D. salina* growth cultures was determined after each experimental set-up using the Nile Red dye to detect lipid droplets inside the cell. The analysis protocol was prepared combining some literature studies made by Alonzo and Mayzaud (1999), Bertozzini et al. (2011), Chen et al. (2009), Cooksey et al. (1987), Elsey et al. (2007), Gardner et al (2011), Gardner et al (2012), Pick and Rachutin-Zalogin (2012). *Dunaliella salina* cultures were grown until their stationary

phase which is about 15-30 days depending on CO_2 supply to the system. At the end of each experimental run, at least 10 ml culture sample was aseptically removed from the photobioreactor and transferred to a 15 ml Falcon tube.

Table 4. 2. Dilution concentration of algal cell using fresh medium for Nile Red peak time determination

Percentage	100	87.5	75	62.5	50	37.5	25	12.5	Total (µl)
Culture (µl)	1000	875	750	625	500	375	250	125	4.5
Medium (µl)	0	125	250	375	500	625	750	875	3.5

4.4.1.1. Optimization of cell concentration and peak fluorescence time for Nile Red analysis

It is essential to decide the optimum peak fluorescence time and cell concentration using unstressed well grown algal cells so as to continue and analyse the lipid content of *D. salina* cells grown under stressed conditions. Therefore, the steps below are followed in order to determine the appropriate cell concentration.

- A well grown *D. salina* culture (approximately OD_{595} = 1) was taken from a subcultured flask and transferred into 15 ml Falcon tube. Again distilled water, dH_2O, was used as reference solvent.
- The culture sample was centrifuged for 5 min at 3000 *g*. Then the supernatant was discarded and the required amount of fresh medium added to the pellet in order to make the OD 1 at 595nm. Then the pellet was mixed rigorously and the pellet was resuspended again inside the tube.
- A series of 8 dilutions (see Table 4.2) of algal culture were then made in 1 ml from this adjusted culture using dH_2O, at 12.5, 25, 37.5, 50, 62.5, 75, 87.5 and 100% in 1.5ml Eppendorf tubes.

- The diluted samples were then transferred to 8 channels of one of the multi-channel pipette reservoir (Thermo Scientific). Next the cultures were transferred to the 96 well flat bottom clear plate (Grenier Bio-One Cellstar 655 185) from row E to H as shown in Table 4.3. Each cell of the plate has 200µl culture.

Table 4. 3. 96 Well plate layout for Nile Red fluorescence peak time determination. Note that the rows from R1 to R4 are the replicates of the sample, as well as row R5 to R8, too.

Dilution from 1(A) @ OD595 (%): mg/ml		100	87.5	75	62.5	50	37.5	25	12.5	Empty Wells			
		1	2	3	4	5	6	7	8	9	10	11	12
A	R1	stain1	stain5	stain9	stain13	stain17	stain21	stain25	stain29	BLK	BLK	BLK	BLK
B	R2	stain2	stain6	stain10	stain14	stain18	stain22	stain26	stain30	BLK	BLK	BLK	BLK
C	R3	stain3	stain7	stain11	stain15	stain19	stain23	stain27	stain31	BLK	BLK	BLK	BLK
D	R4	stain4	Stain8	Stain12	stain16	stain20	stain24	stain28	stain32	BLK	BLK	BLK	BLK
E	R5	unsta1	unsta5	unsta9	unsta13	unsta17	unsta21	unsta25	unsta29	BLK	BLK	BLK	BLK
F	R6	unsta2	unsta6	unsta10	unsta14	unsta18	unsta22	unsta26	unsta30	BLK	BLK	BLK	BLK
G	R7	unsta3	unsta7	unsta11	unsta15	unsta19	unsta23	unsta27	unsta31	BLK	BLK	BLK	BLK
H	R8	unsta4	unsta8	unsta12	unsta16	unsta20	unsta24	unsta28	unsta32	BLK	BLK	BLK	BLK

- These eight tubes were then centrifuged at 3000 *g* for 10 minutes in a bench top centrifuge, the supernatant discarded, and the pellets resuspended in 20µl of dH_2O.
- Two 1.5 ml Eppendorf tubes were then prepared for each of the 8 culture concentrations, one for stained, one for unstained cells. 10 µl of the resuspended algal pellets was the transferred to each if the stained and unstained, labelled tubes.
- Next, 50 µl of dimethyl sulfoxide (DMSO) was then transferred to each Eppendorf tube.
- Then, 930 µl dH_2O was added to tubes labelled stained and 940 µl dH_2O to all unstained labelled tubes.
- Then the stained tubes were prepared by adding 20 µl of Nile-red fluorescent dye (which contains 15.9µg/ml Nile Red stock solution dissolved in DMSO) was added to each stained tubes then the timer started. Next, the stained samples were transferred to the another multi-channel reservoir and the 4*200µl samples were put inside the 96 well plate cell from row A to D for each concentration, see Table 4.3.
- Then the 96 well plate was placed inside the chamber of the plate reader instrument (Biotek flx800) with the lid removed. The software, Gen5 2.05, was used to make readings of the samples. The reading was taken every 5 minutes interval for total of 30 minutes. The Peak Finder setting parameters for the software programme were identified by Krys Bangert in his PhD thesis (Bangert, 2013) and the details of these settings are given in Table 4.4.
- The results of the readings were exported to Excel and the unstained fluorescence values subtracted from the stained values in order to remove any chlorophyll auto-fluorescence Average fluorescence values for the 4 technical replicates at each cellular concentration were obtained, allowing for optimum cell concentration, and thus optical density, and peak fluorescence time to be established.

Table 4. 4. Procedure and settings used for the Gen5 2.05 software programme to measure lipid amount at different culture concentration

Procedure Details	
Plate Type	96 WELL PLATE
Read	Fluorescence Endpoint
	Full Plate
	Filter Set 1
	Excitation: 485/20, Emission: 580/50
	Optics: Top, Gain: 60
	Read Speed: Normal

4.4.1.2. Optimum Nile Red concentration determination

The second stage optimization of the Nile Red analysis was finding the right concentration of Nile Red to be used. The optimization procedure was applied using the combination of previous work done by Alonzo and Mayzaud (1999), Bertozzini et al.(2011), Chen et al (2009), Cooksey et al.(1987), Elsey et al.(2007) , Gardner et al (2011), Gardner et al. (2012) and Pick and Rachutin-Zalogin (2012). Using the stock solution (1 mg/ml) which was kept in the -80^{o}C to reduce the evaporation, 6 new Nile Red samples were prepared at different concentrations (0.05, 0.1, 0.2, 0.3, 0.4, and 0.6 µmol /ml) Nile Red concentrations were prepared by dissolving in DMSO as indicated in Table 4.5.

On the basis of the previous analysis procedure (Section 5.4.1.1), the optimized *Dunaliella* concentration was chosen at OD 595nm. The well grown *Dunaliella* culture (at least 10ml) was taken aseptically and centrifuged for 5min at 3000 *g* and the supernatant was discarded. Then fresh medium was added in order to adjust the culture to that concentration of OD 595 nm against dH_2O. Then, the adjusted culture was divided into 6 different Eppendorf tubes and then centrifuged at 3000*g* for 10 minutes in a bench top centrifuge, the supernatant discarded, and the pellets resuspended in 20µl of dH_2O. Then the same procedure as explained in Section 5.4.1.1 was applied to all unstained and stained labelled tubes. The only difference, this time, 10 µl of the 6 different Nile Red concentrations were added to each of the tubes labelled as stained.

200 µl of the samples were placed in a 96 Well plate as described in Table 4.6. Then, the plate was located in the reader with the lid off and the software Gen5 2.05 was run for 30 minutes with 5 minutes intervals. And the readings were recorded using the same settings as described in Section 5.4.1.1. Then, the results were exported to the Excel file and the average and the standard deviation of the four replicates (stained and unstained) were calculated. The values of unstained cells were subtracted from the stained ones so as to avoid the chlorophyll auto-fluorescence. The net fluorescence results were normalised and the optimum Nile Red concentration was chosen along with best algal cell concentration and best peak fluorescence time.

Table 4. 5. Preparation of different Nile Red concentrations from Nile Red stock

Nile Red (µmol ml^{-1})	Primary Stock 1mg ml^{-1} (µl)	DMSO (µl)
0.05	16	984
0.1	32	968
0.2	64	936
0.3	100	900
0.4	128	872
0.6	192	808

Table 4. 6. 96 Well plate layout for Nile Red peak time determination. Note that the rows from R1 to R4 are the replicates of the sample.

NR Conc (µmol ml^{-1})			**0.05**	**0.1**	**0.2**	**0.3**	**0.4**	**0.6**						
			1	**2**	**3**	**4**	**5**	**6**	**7**	**8**	**9**	**10**	**11**	**12**
Nile Red Stained Cells	**R1**	**A**	200	200	200	200	200	200	0	0	0	0	0	0
	R2	**B**	200	200	200	200	200	200	0	0	0	0	0	0
	R3	**C**	200	200	200	200	200	200	0	0	0	0	0	0
	R4	**D**	200	200	200	200	200	200	0	0	0	0	0	0
Unstained cells	**R1**	**E**	200	200	200	200	200	200	0	0	0	0	0	0
	R2	**F**	200	200	200	200	200	200	0	0	0	0	0	0
	R3	**G**	200	200	200	200	200	200	0	0	0	0	0	0
	R4	**H**	200	200	200	200	200	200	0	0	0	0	0	0

4.4.2. TRIOLEIN CALIBRATION CURVE

Triolein is a lipid standard often used in the food industry and values are expressed as triolein equivalent lipid levels. A concentration calibration curve for standard Nile Red fluorescence was carried out using triolein on the basis of work by Bertozzini et al. (2011). A 10 mg ml^{-1} triolein lipid standard stock was made by adding 50 mg of triolein (Sigma T7140) to 5ml isopropanol and dissolved. Then 1ml aliquots were transferred to 5 x 1.5 ml Eppendorf tubes labelled 1 to 5 in order to be used in the experiments later as stock.

Eight algal samples were prepared under the conditions optimized in Section 5.4.1.1 and taken through the procedure explained in Section 5.4.1.1 up to the addition of 50 µl DMSO. At this stage, 910 µl dH_2O was added to the tubes labelled stained and 920 µl dH_2O to all the unstained tubes. Then triolein and isopropanol (total volume 20 µl) were added to each stained and unstained tube as shown in Table 4.7 to give concentrations of 0.2, 0.16, 0.12, 0.08, 0.06, 0.04, 0.02, 0 mg ml^{-1}.

Table 4. 7. Amount of triolein and isopropanol used to obtain Nile Red lipid standard curve

Conc Tiolein (mg/ml)	**0.2**	**0.16**	**0.12**	**0.08**	**0.06**	**0.04**	**0.02**	**0**
Triolein (µl)	20	16	12	8	6	4	2	0
Isopropanol (µl)	0	4	8	12	14	16	18	20

In the next step, 10 µl of optimum Nile-red fluorescent dye concentration obtained in Section 5.4.1.2 was then added to each tube labelled stained. The method was then

continued as described in Section 5.4.1.1. Then 1ml of each stained and unstained sample were transferred to the multi-channel reservoir, and then 200 µl aliquots of each sample were poured into 96 well plate as shown in Table 4.8.

Table 4. 8. 96 Well plate layout for Nile Red peak time determination. Note that the rows from R1 to R4 are the replicates of the sample

Conc. of Triolein (mg/ml)			0.2	0.16	0.12	0.08	0.06	0.04	0.02	0	Empty Wells			
			1	2	3	4	5	6	7	8	9	10	11	12
Stained cells	A	R1	200	200	200	200	200	200	200	200	0	0	0	0
	B	R2	200	200	200	200	200	200	200	200	0	0	0	0
	C	R3	200	200	200	200	200	200	200	200	0	0	0	0
	D	R4	200	200	200	200	200	200	200	200	0	0	0	0
Unstained cells	E	R5	200	200	200	200	200	200	200	200	0	0	0	0
	F	R6	200	200	200	200	200	200	200	200	0	0	0	0
	G	R7	200	200	200	200	200	200	200	200	0	0	0	0
	H	R8	200	200	200	200	200	200	200	200	0	0	0	0

Then, the 96 well plate was located in the reader with the lid off and the software Gen5 2.05 was run for 30 minutes with data collected at 5 minutes intervals. And the readings were recorded using the same settings as described in Table 4.4. Then, the results were exported to the Excel file and the average and the standard deviation of the four replicates (stained and unstained) were calculated. The values of unstained cells were subtracted from the stained ones so as to avoid the cellular background fluorescence. The relationship between Nile Red fluorescence intensity and concentration of triolein mixture was exemplified by plotting the calibration curve, Figure 4.2. Afterward, each

fluorescence intensity amount obtained under different stressed conditions was converted into the concentration of lipid depending upon Excel sheet equation;

$x = y / 34162$

Where x is the concentration of Triolein in mg /ml and y is the Nile Red Fluorescence Intensity.

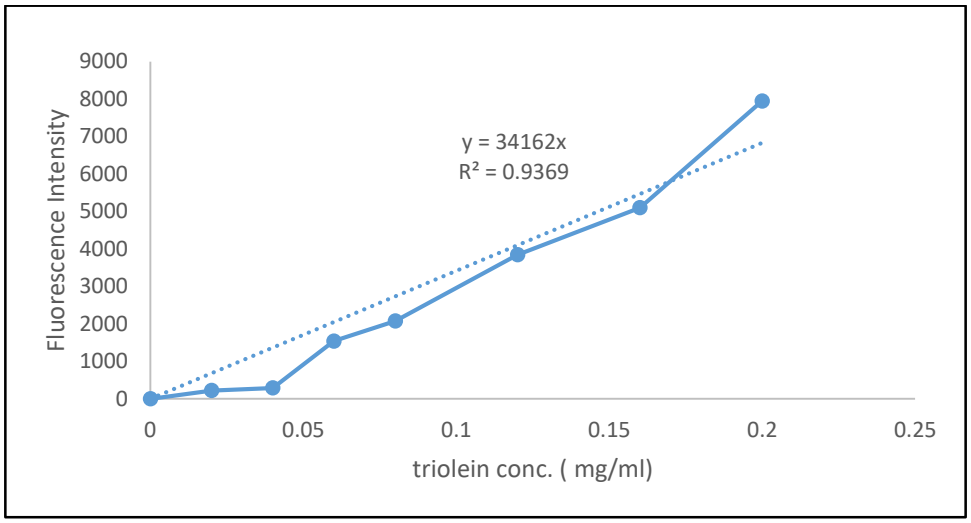

Figure 4. 2. Standard addition Triolein concentration versus Nile Red fluorescence intensity calibration curve

4.5. FLUORESCENT LIGHT MICROSCOPE IMAGING

Another way of observing the neutral lipid bodies which look like oil droplets is using a light microscopes after staining the cell with Nile Red fluorescent dye. Thus, the shapes and sizes of the lipid bodies of *D. salina* under different stressed conditions were examined using the Fluorescence Microscope, Zeiss Axiovert 200M, (Carl Zeiss Microlmaging, Inc.) consist of an Exfo X-cite 120 excitation light source, band pass filters (Carl Zeiss Microlmaging, Inc. and Chroma Technology Corp.), an α plan=Fluor 100x/1.45 NA, plan-pochromat 63x/1.40 oil immersion lens and a digital CCD camera (Orca ER, Hamamatsu). 2 light channels; Green Channel (GFP, and

NeonGreen) and Red Channel (RFP, HcRed, mCherry, mKate, mRuby) which have excitation wavelength as 525 nm and 700 nm, respectively, were used inside the microscope. The procedure for this screening analysis were modified from the study done by Cooksey et al. (1987).

Dunaliella salina cultures were grown until stationary phase which is about 14 – 30 days depending on the amount of CO_2 supplied to the system. At the end of this time 5ml of culture was taken aseptically from photobioreactor and added to a 15 ml Falcon tube. Then, the sample was adjusted to an absorbance of OD 0.7 at 595nm, which is also the optimum cell concentration obtained in Nile Red analysis in Section 4.4.1.1, using fresh medium. One ml was then taken and added to a 1.5 ml Eppendorf tube and then; 8µl of Grams Iodine (purchased from Camlab Chemicals) was added to the sample and shaken to kill the cells and stop motility. Ten µl of 100 µl ml^{-1} Nile Red in 100% DMSO (the concentration of Nile red is 0.2 µl ml^{-1}, which was obtained in Section 5.4.1.2) was added and mixed by inversion. A timer was then started to check the progress of the dye penetration. 10 µl of the stained sample was then added to a clean slide and a coverslip was added gently. The edges of the slide were then sealed with nail varnish to avoid the possibility of evaporation. Once the varnish had dried, the slide was placed in the microscope, a single drop of mineral oil was placed on the cover slip and the image was brought in to focus using excitation light only. Three sets of photographs were taken for each cell of interest, one for bright field, one for red light and one for green light. All imaging was taken using a 60x oil immersing lens and a digital CCD camera as 0.5µm Z-stacks. The images were merged using software programme, Openlab (Improvision) and further scaling process done using Photoshop (Adobe). The capturing setting parameters were arranged as;

- Bright Field → 30 millisecond exposure time and gain is 0.
- Red Colour → 20 millisecond exposure time and gain is 0.
- Green Colour → 100 millisecond exposure time and gain is 0.

4.6. CULTURE CONDITIONS AND MAINTENANCE

4.6.1. CULTURE MAINTENANCE

Subculturing of *D. salina* was performed at regular intervals, typically every 10-14 days and they were kept in growth room (Figure 4.3) in Molecular and Biology Department as described in Section 4.6.2. Each time, pre-autoclaved 250ml conical flasks were inoculated by adding 10 ml of an actively growing culture, which had been established for approximately 10 days, to 100 ml of *D. salina* growth medium. Both processes were carried out using aseptic techniques. The containers were flamed with a Bunsen burner before and after transfer, and all transfer pipette tips used were pre-sterilised by autoclaving. The flasks were shaken manually before taking samples.

Figure 4. 3. MBB H-Floor Growth room is used to keep subcultures and sample flasks after each experimental run

4.6.2. MBB H-FLOOR GROWTH ROOM

Stock algal cultures were stored and incubated in 250 ml conical flasks (with foam bungs), under controlled environmental conditions (Figure 4.3). The MBB H-Floor growth room was maintained at a constant 25°C and had three different lighting intensities available depending on the tier of shelf used. The samples used in this project were kept at the bottom shelf to keep light intensity at an appropriate level, see Figure 4.4 for the relative light intensity next to the flask in H-floor growth room (25 µmol m^{-2} s^{-1}).

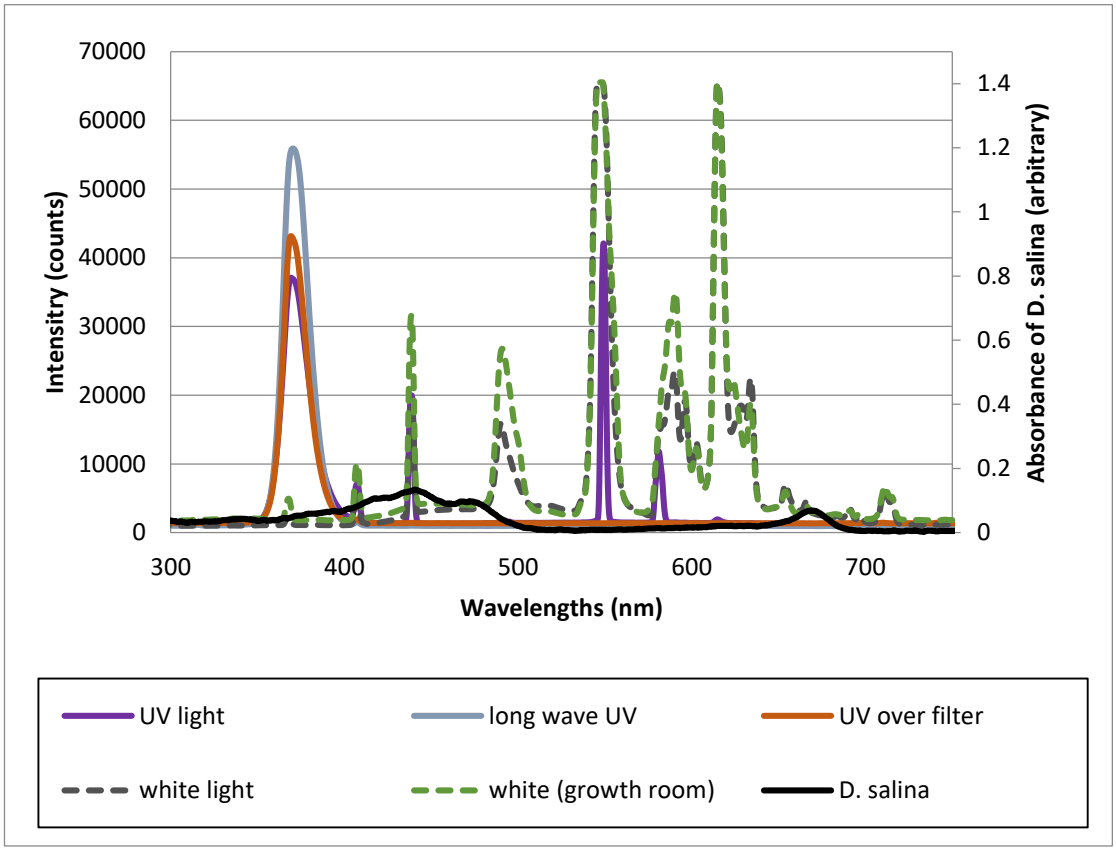

Figure 4. 4. Intensities of lights in UV light box (old and new replacements) and H-floor growth room and absorbance of *D. salina*

4.7. EXPERIMENTAL SET-UP AND MATERIALS

4.7.1 SPECTRAL MEASUREMENTS LIGHT SOURCES

In addition to *Dunaliella salina* culture growth and maintenance in the MBB H floor growth room, experimental cultures were set up in arrange of apparatus including modified UV light box for the small scale algae growth, and big growth chamber designed by me for algal growth in 3L photobioreactor (for more information see Chapter 3 – Bioreactor design). Each experimental set up had its own lighting system, so the light intensities were different in each of them. Therefore, the spectra shown in Figure 4.4 were recorded in order to explain the range of light intensities and wavelengths that were used during the project. The lights used in the growth environments were as follows;

- **Modified UV light box**: UV light Philips TL8W/10 tubes and white lights were Philips 8W – T5 cool white
- **Closed system black box:** Mineralight Lamp Multiband UV – 254 (short band) / 365 (long band) nm. Model UVGL -58
- **Large growth chamber:** UV light – Philips TPX15-18 and white light GCL fluorescent tube 15W T8.

The intensities of the light sources were measured using the Ocean Optics spectrometer and SpectraSuite software, details of how to use the instrument were given in Chapter 2, Section 2.2.1.3 and 2.2.1.4 Absorbance and Emission Measurements. Other detailed information regarding the large growth chamber can be found in Chapter 3 Photobioreactor design.

4.7.2. COATING OF REACTORS

This part will not be covered in detail here, information about dye selection and dye coating procedures was described in detail in Chapter 2 – Fabrication of Wavelength Tuning Materials. The coating of the produced materials was done easily, there was no procedure for it because of easy appliance of the materials. The only things that needed to be done was placing the PDMS- dye wavelength shifting material on the reactor surface with care. The orientation and the location of the wavelength shifting material on the reactor surfaces was explained and illustrated fully in Chapter 3 – Bioreactor design, please see there for more information.

4.7.3. PHOTOBIOREACTOR CLEANING

Two different reactor formats (Figure 4.5) were used in order to perform all the experiments. One of them is 50 ml culture flasks (VWR (CAT no; 737 – 2311), made from polystyrene) for small scale *D. salina* growth to be used inside the modified UV light box. These culture flasks were ready to use directly, they were already sterilized, so no cleaning procedure was used. On the other hand, these flasks are not suitable to be autoclaved, unfortunately, they melted when they were the autoclaved.

For large scale algae growth, 3L photobioreactor was used and the cleaning procedure for this reactor was as follows. Before each experimental runs, the reactor was taken apart and rinsed with distilled water 4 times. The reactor body was filled with Virkon (Dupont) solution for more than 15 minutes and the separate small parts and the pipes were then sterilised in a bath of the same solution for the same period. Then, all items were rinsed with autoclaved distilled water 4 times, with the exception of the spargers and control valves. The reactor and the other parts were then left on the bench upside down for a while to dry. Next, the reactor was then reassembled using gloves and was ready to be used.

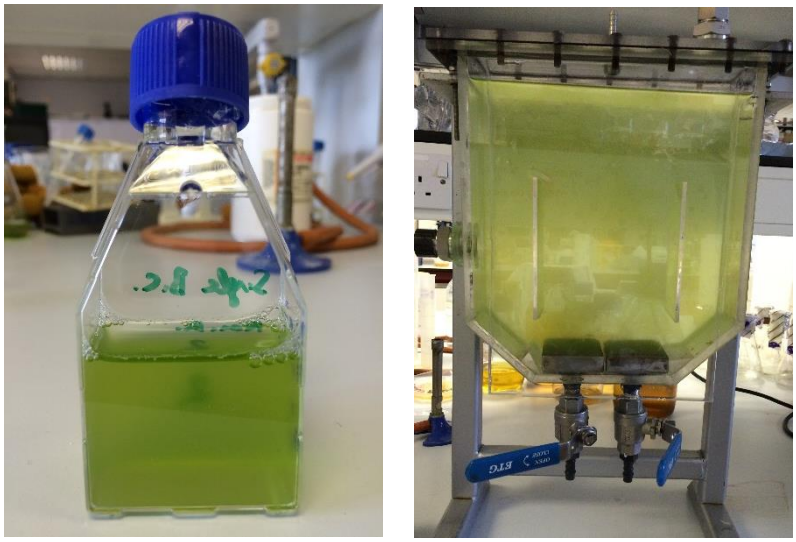

Figure 4. 5. Culture flask and the 3L photobioreactor used in the experiments

4.7.4. ALGAL GROWTH SYSTEM SET-UP

Fresh and actively growing algae are necessary for each growth set-up; hence, maintenance culture inoculations were done every 15- 30 days. Conical flasks (250 ml) were autoclaved, and then 100 ml of growth medium was poured into the flask, next 5 ml of actively growing culture was added. All sub-cultures were kept in the growth room on H-floor in the MBB department at a constant temperature of 25^{o}C as mentioned in Section 4.6.2.

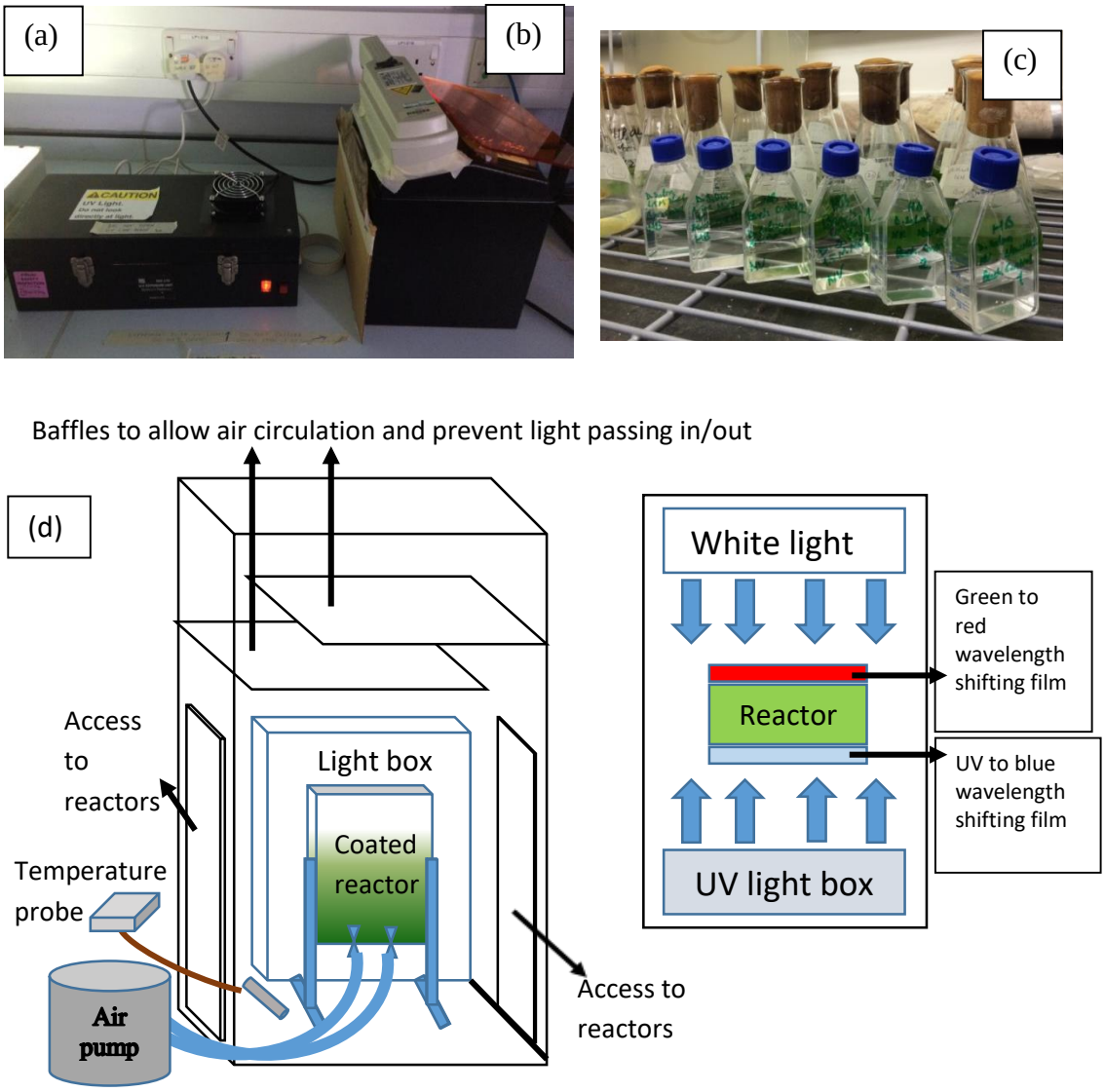

Figure 4. 6. Algae growth systems (a) UV light box, (b) closed system black box, (c) H-floor growth room and (d) scheme of large growth chamber and wavelength shifting orientations inside the chamber

Algae growth was carried out inside one of three different growth boxes; (1) modified UV light box (Modified RS-555-279 UV Exposure Unit), (2) closed system black box, and (3) large black box for 3L photobioreactor which is shown in Figure 4.6 (d), or some samples were grown in the H-floor growth room as control flasks. The custom modified UV light box includes a fused high transparency quartz diffuser (Instrument Glass – Optical white crown spectacle B270 Glass) with dimensions 250mm x 150mm x t1.15mm; 1 UV light; and 1 white light. For some experiments, algal growth was

performed separately under UV light only or white light only; thus, 2 UV or 2 white light bulbs were used accordingly. UV and white bulbs were used for UV to blue light conversion with Coumarin wavelength tuning material and green to red light conversion with Bestoil Orange 2G wavelength tuning material, respectively. The temperature of the box was measured with a thermometer (Farnell – Part no: TK-612) at several intervals. On the other hand, the black box has only a UV light for illumination which has short band (254 nm) and long band (365 nm) emission.

After arranging growth boxes, several set-ups were run with different wavelength tuning films. For all growth set-ups, initially, culture flasks were covered with aluminum foil except the underside where light penetrated. Then, 25 ml of 1.5M NaCl growth medium with single bio-carbonated $NaHCO_3$ amount as given in the medium recipe or double bio-carbonated $NaHCO_3$ amount double that given in the medium recipe were infused into each culture flask. Then, 0.3 - 1 ml of inocula (depending on inoculation density) were added to the flasks, and then first samples were taken for the zero-hour measurement. After that, the flasks were put into UV light box, black box and growth room with and without wavelength tuning material as illustrated in Chapter 3 – Photobioreactor design. Then, every 24 hours samples were taken and the optical density results were recorded (see Section 4.3.1).

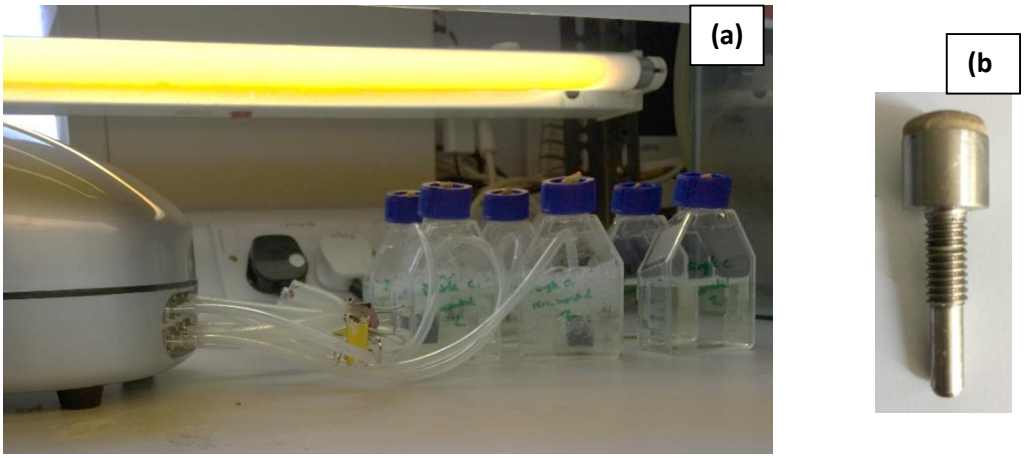

Figure 4. 7. Introducing fine-bubble technology to algal growth system (a) growth set-up and (b) sparger used in the experiment

The second part of the small scale algae growth in culture flasks applied with fine bubble injection into the growth system. Only a few set-ups were run to test the bubble effect on growth rate. The growth system incorporating fine-bubbles (Figure 4.7 (a)) was composed of a prototype sparger with 5mm diameter (or air stones), an air pump (5W, output stream is 7.2 L/min, supplier HAILEA), and a white light on the bench.

First, 5mm holes were drilled in the side of the flasks to pass the connecting pipework into the flasks; 3 mm holes were also drilled in the lids to assure ventilation. Meantime, the pipes and sparger / air stone (Figure 4.7 (b)) were put into an autoclave for sterilization. Next, the sparger / air stones were inserted into the flasks. After that, 30 ml of growth medium (either 1.5M NaCl single bio-carbonated or double bio-carbonated) were put into the culture flasks. Next, all flasks were put under UV light (BioMat 2) for sterilization for 45 min. This UV light chamber is different from equipment used for algal growth. Finally, 1 ml of inoculum was added and first samples were taken. The flasks were connected to a gas pump as in Figure 4.7, which was set to its minimum working rate of 17.2 L/min. Every 24 hours samples were taken and data recorded.

Large scale *D. salina* growth part of the project was completed using 3L flat plate photobioreactor inside a growth chamber as illustrated in Figure 4.6 and also explained in detail in Chapter 4 – Bioreactor design part. After the reactor was cleaned as described in Section 4.8.3, the autoclaved 1.5M NaCl *D. salina* medium (3 litres) was poured inside the reactor and approximately 150 - 200 ml of *D. salina* culture which was about 14 days old was inoculated. Initial inoculation OD was always arranged to be OD 0.068 at 595nm. Then the reactor was connected to air or CO_2 supply (shown in Figure 4.6) at different percentages (only air, 0.5% CO_2, 1% CO_2, 5% CO_2, and 10% CO_2) depending on the experimental set-up. The wavelength tuning materials were placed on the reactor as illustrated in Figure 4.5 and explained in Chapter 3. Then every 24 hours samples were taken in order to check the OD.

CHAPTER 5: ALGAE GROWTH WITH AIR SUPPLY

5.1. Introduction

An important parameter for algal biomass production is light, so to increase the useful light available wavelength shifting materials were produced as explained in Chapter 2, Section 2.2.1.2. Dye- PDMS Thin Films. Wavelength tuning materials chosen for *Dunaliella salina* 19/30 growth in small scale cell culture flasks were 20% Coumarin/PMMA + toluene coating, 1 (stock) Coumarin/THF + PDMS thin film and 1 (stock) Bestoil Orange 2G/THF + PDMS thin film. And the ones used for the large scale *D. salina* 19/30 growth in 3L photobioreactor were 1 (stock) Coumarin/THF + PDMS thin film and 1 (stock) Bestoil Orange 2G/THF + PDMS thin film. In order to determine how effective, the films used are at tuning the wavelength of the light, the absorbance and emission spectra of the films were measured as shown in Figure 5.1, and these wavelength shifting materials are referred to as C +PDMS and O+PDMS. Figure 5.1 given below indicates the absorption and emission properties of each wavelength shifting film.

The results discussed in this chapter include experiments where two different UV to blue light wavelength tuning films were used. The C coating (Coumarin dye coated on the glass) one was expected to be slightly better compared to C+PDMS (Coumarin dye and PDMS cured together) film because the percentage overlap of this material's emission and the algae's absorption is longer and larger. On the other hand, the absorption band of C+PDMS is larger than for the C coating. As mentioned previously, the O+PDMS thin film has less distinct absorption features which may cause less efficiency with respect to the C coating and the C+PDMS film.

On the other hand, supplying different amounts of carbon to the small scale *D. salina* cultures was tested by changing the bicarbonate amount in the algae growth media. Moreover, as an initial study for this project fine bubbling was incorporated into the small scale culture flasks in a similar manner to the pilot scale studies on microbubble generation for *D. salina* growth done by Zimmerman, et al.(2011).

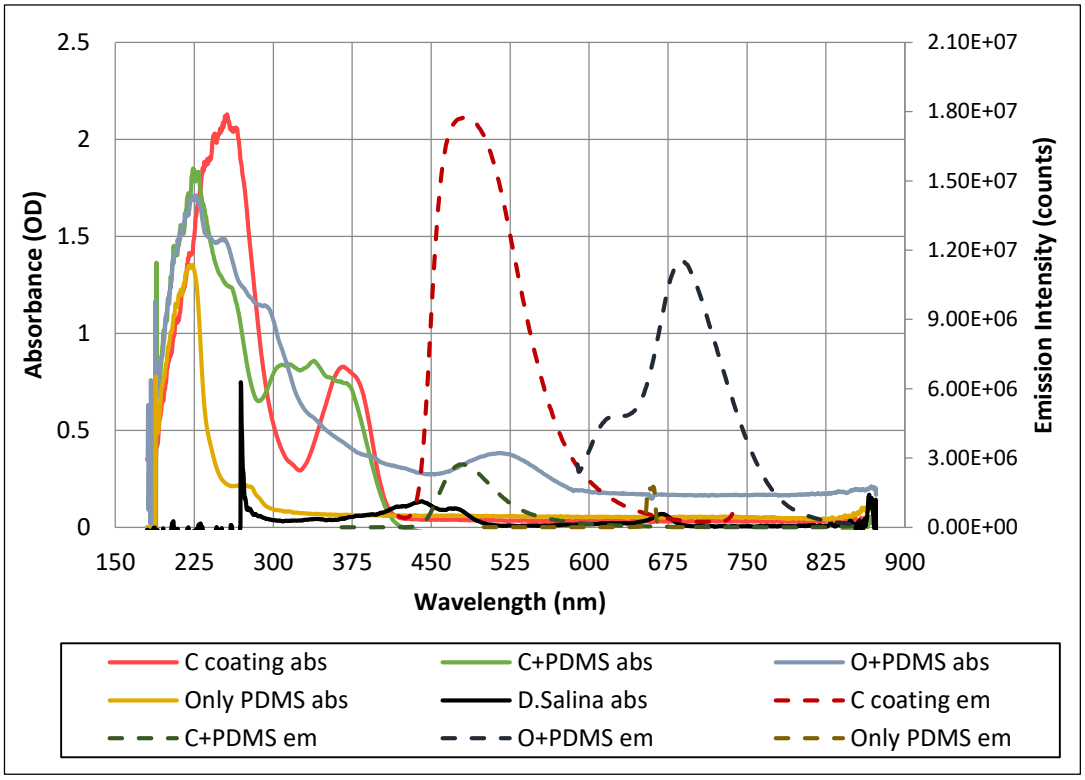

Figure 5. 1. Absorption/ emission spectra of the wavelength tuning materials used in the algae growth in cell culture flasks. C coating means that Coumarin- THF mixture was coated on the glass. C+ PDMS means that mixture of Coumarin and THF was combined and cured together with PDMS. O+PDMS means that mixture of Bestoil Orange 2G and THF was combined and cured together with PDMS.

The next step for air supplied *D. salina* growth was carried out in 3L photobioreactors using an air pump with inlet flow of 150 cc/min. Four sets of experiment were performed; control (without shifting materials), UV to blue light shifting using Coumarin PDMS film, green to red light shifting using Orange 2G PDMS film and both UV to blue and green to red light shifting using both Coumarin PDMS and Orange 2G PDMS films. At the end of the each run algae biomass was tested for lipid analysis.

The protocol in order to measure the lipid accumulated in the algal cell is not made to conform to a standard among the researchers since each researcher is using different methods so as to get precise and reliable results for the lipid accumulation in different algae species (Li et al., 2014). There are various techniques to determine lipid such as

gravimetric (Bligh and Dyer, 1959), NMR, calorimetric (Van Handel, 1985), Nile Red staining (fluorometric) (Alonzo and Mayzaud, 1999, Cooksey et al., 1987, Chen et al., 2009), etc. In this study Nile Red staining was used to determine the neutral lipid amount for different algal growth set-ups since it is recommended for in-situ algal lipid screening and is easy and cheap to apply. On the other side, the other methods have drawbacks e.g. gravimetric method is time consuming (Bertozzini et al., 2011) and also contains non-fatty acid lipids which will change the total lipid amount (Breuer, 2013).

While applying the Nile Red analysis to algae cells, many stress conditions were tried and described in the literature, such as, nutrient deprivation, nitrate depletion, temperature effect, and light exposure (Jiang et al., 2012, Roleda et al., 2013, Seunghye Park, 2013, Thompson, 1996). In this project, light exposure was used to stress the *D. salina* cells and the effect of the wavelength shifting materials on the lipid production was investigated. And also, the intracellular lipid was monetarized after each different light exposure experiment using Fluorescent light microscopy as explained in Chapter 4, Section 4.5.

5.2. Results of *Dunaliella salina* growth with air supply

In this part, the results of the *Dunaliella salina* 19/30 growth with only air supply to the system in order to make bubbling will be explained. The results of this part are divided into two main sections i.e. small scale *D. salina* growth in 50 ml culture flasks and large scale growth of the *D. salina* inside the 3L airlift photobioreactor.

5.2.1. *D. salina* growth in small scale using cell culture flasks

5.2.1.1. *D. salina* growth using normal growth media and doubled amount of bicarbonate in growth media

The properties of the growth systems and the light intensities of the light inside growth boxes are given in materials and methods, Section 4.7 and Figure 4.4, and using these systems several algae growth curves were measured. Firstly, algal growth was carried out using 1.5 M NaCl single bicarbonate growth medium (as described in the materials and methods section) growth medium and in the UV light box equipped with only UV light. The wavelength shifting materials consisting of the C coating and C+PDMS, were located between the flask and the light and for the control flasks where there is no shifting film applied were also tested. The analysis of this experiment is shown in Figure 5.2 (A), and algae growth, unfortunately, stops within 5 days in all trials. The reason for the cell deaths might be dissolved O_2 inhibition or a lack of carbon supplies ($NaHCO_3$). Another observation from the graph concerns the growth rates for each sample. According to the graph, it seems that all samples grow at an equal rate which is likely to be a result of the UV lights producing some emission over 400nm and/or day light entering the UV light box. Day light penetrating into UV light box through the lid seal could result in growth inside the control flasks.

In response to the problems faced in the previous experiment, a 3 mm hole was drilled in the lid of each flask in order to assist evacuation of accumulated O_2. Subsequently as shown in Figure 5.2 (B), samples with wavelength shifting material in the UV light box equipped with both UV and white light grew; whereas control flasks inside the closed system black box equipped with only UV light (longest wavelength – 365 nm) did not. Figure 5.2 (B) reveals that *D. salina* cannot grow under UV light without using any wavelength shifting film and dies in just 3 days. Unexpectedly the flasks with shifting film grew up to an OD 0.4, similar to previous experiment and then all growth ceased within 6 days. This was attributed to insufficient $NaHCO_3$.

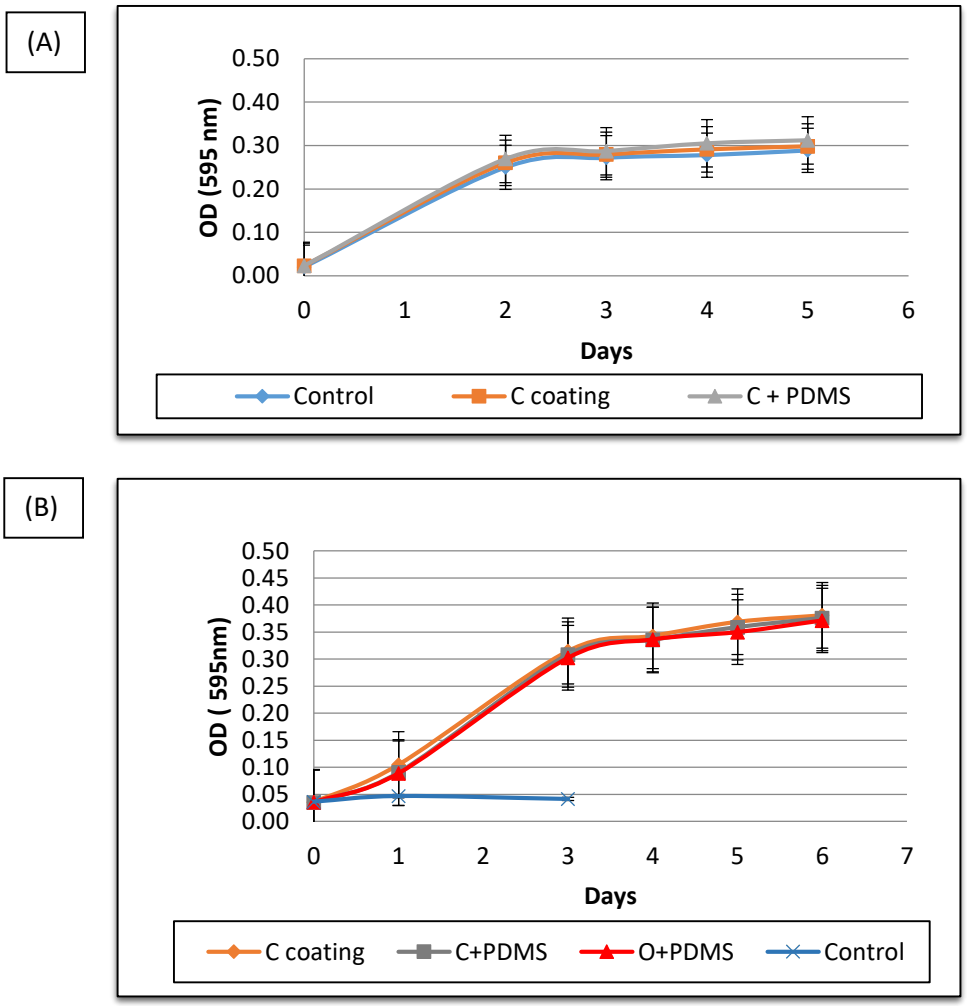

Figure 5. 2. Growth rate of *D. salina* under 24 h (A) only UV light and (B) both UV and white light illumination with and without wavelength shifting material

For the following experiment, the supplied $NaHCO_3$ amount was doubled and more replicates were put inside the box; with the control flasks being placed in the growth room on H-floor of the MBB department. Figure 5.3 demonstrates the growth pattern of this experiment which provides proof that the wavelength shifting materials are actively assisting algae generation. Maximum OD values are 0.934, 0.926, 0.864 and 0.770 for C coating, C+PDMS, O+PDMS and control, respectively. These results mean that in comparison to control, there is 17.6% and 11.2% growth increments for UV to blue wavelength tuning and green to red wavelength tuning, respectively.

Actually, the light tubes in the H-floor growth room have more power and the number of lights are more than UV light box; hence, the light intensity is higher for control flasks. If there was more space inside the UV light box, and the control flasks were put in it, it is assumed that the growth enhancement with wavelength tuning material would be greater than current results. Additionally, the temperature inside the UV light box is higher than the growth room, which is another reason for slow growth.

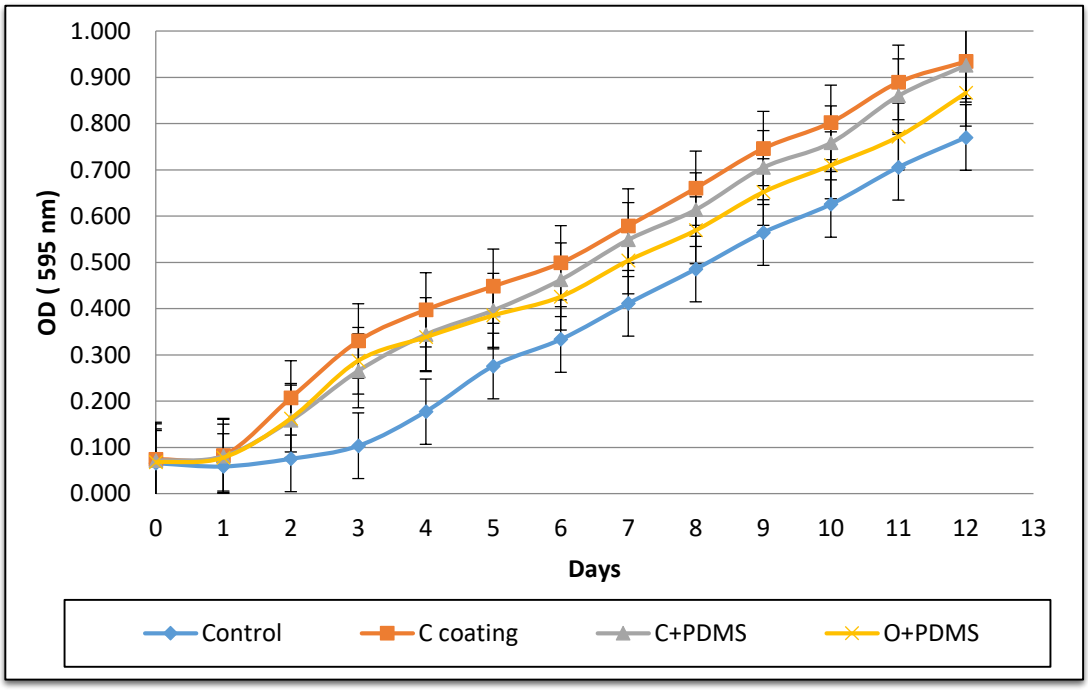

Figure 5. 3. Growth pattern of *D. salina* under 24h UV and white light illumination using double amount of $NaHCO_3$. C coating means that Coumarin- THF mixture was coated on the glass. C+ PDMS means that mixture of Coumarin and THF was combined and cured together with PDMS. O+PDMS means that mixture of Bestoil Orange 2G and THF was combined and cured together with PDMS.

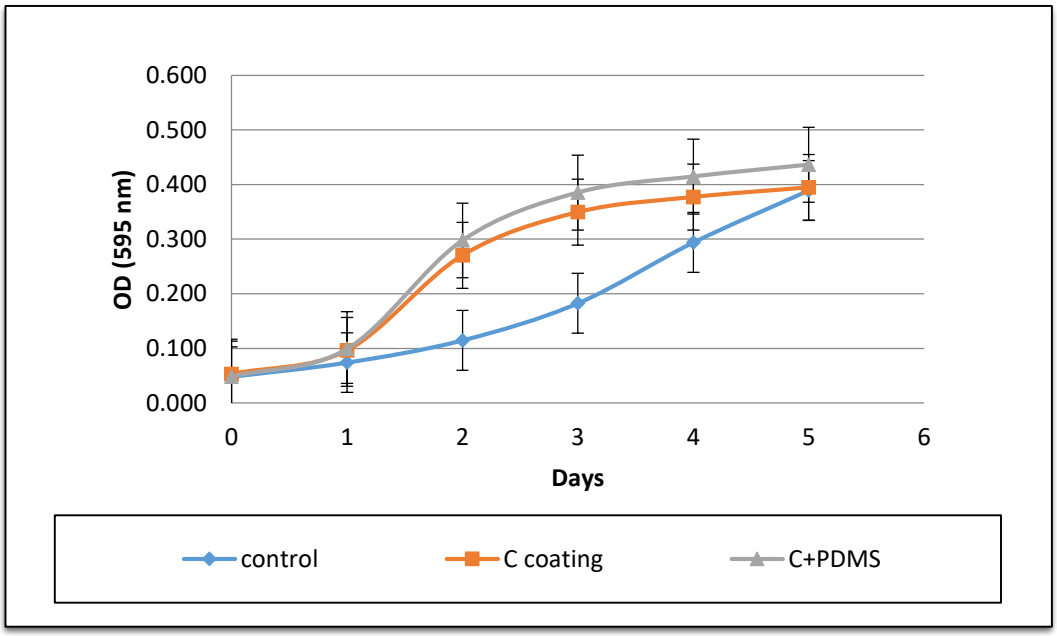

Figure 5. 4. Influence of high temperature on *D. salina* growth

Before performing more experiments with UV to blue light shifting material, the UV light box was modified by sealing the edges with a black sponge strip to prevent light coming inside the box through the lid joint. An unintended outcome of this sealing process was a significant increase in temperature to very high values, 36^{o}C, in which *D. salina* cannot survive. Figure 5.4 illustrates the cell deaths of the *D. salina* and growth of bacteria in the flasks. Under normal conditions, this bacterium and *D. salina* can live together. However, bacteria can invade the growth culture and cause fast decimation of *D. salina* at high temperatures. Samples were taken from this bacteria growth flask and inoculated (at different salinities) and images were captured to see

the density of bacteria. Figure 5.5 highlights that the inoculum with 1.5M NaCl is also contaminated but this bacteria type and *D. salina* can live happily together in a suitable environment. Nonetheless, when the temperature was unintentionally increased, it caused a rapid cell death (Figure 5.4 and 5.5). Additionally, the graph in Figure 5.4 shows the growth rates become almost equal at the end of the 5th day, although the control growth was slower at the beginning. This is the consequence of UV light used inside the box which emits over 400nm. A visible light filter that can cut out the light over 400 nm (see Appendix 5) was used for the next experiment. Nevertheless, growth experiments were not successful because of heating problem of the box. Some more modifications were done by adding more fans for cooling but the power of the fans was not sufficient to overcome the heating issues.

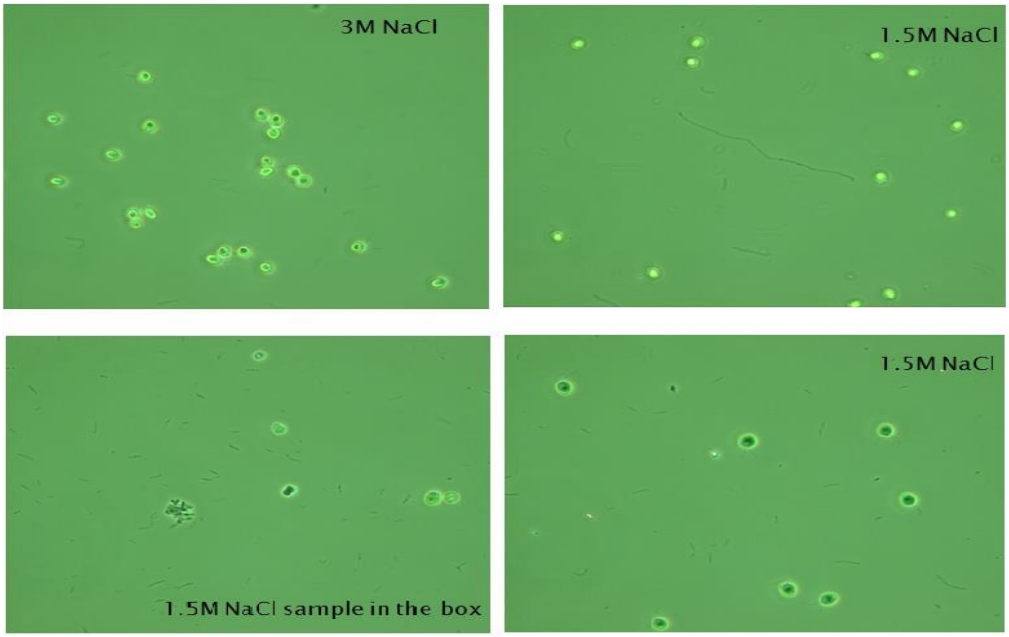

Figure 5. 5. Microscopic images of *D. salina* at different salinity. The image was taken using a Nikon Eclipse E400 Microscope (phase 2 – 40X) endowed with a Nikon DXM1200 Digital Camera. The camera was attached to a software programme named LUCIA G Software and images were saved using this software with parameters; Red: 44, Green: 68, Blue: 72, Gain: 0, Gamma: 1, Offset:0, Exposure: 64ms. Sample preparation method was the same as explained for the Fluorescence light microscope in Section 4.5 Materials and methods Chapter.

5.2.1.2. *D. salina* growth by adding fine bubble to the system

The final small scale experiment examines the influence of fine bubbles on algae growth. The experiment was carried out based on the Figure 4.7 in Chapter 3, Materials and Methods. Figure 5.6 shows that aeration results in a significant increase I the growth rate however, there is no significant variation in growth of single bicarbonate and double bicarbonate flasks when they are not aerated. Since normally, single bicarbonate medium is used, the focus will be on this flask, thus the maximum OD achieved during growth of aerated single bicarbonate is 1.051 OD while it is 0.419 for non-aerated single bicarbonate. The results show more than doubled growth increment with the application of aeration using microbubble technology. The experiment had to be stopped before stationary phase is completed because the volume of the medium fell below minimum working volume due to the number of samples taken during the experiment.

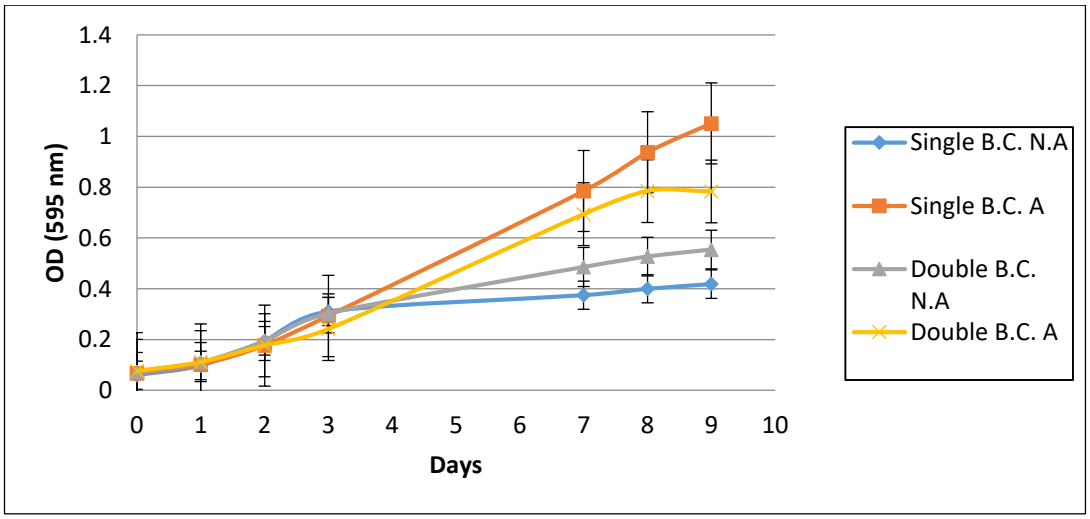

Figure 5. 6. Effect of fine bubbles and carbon amount on algae growth. B.C. represents bicarbonate; A. indicates aerated and N.A. indicates non-aerated.

5.2.2. *D. salina* growth in large scale - 3L photobioreactor

Dunaliella salina 19/30 CCAP was grown in an 3L airlift photobioreactor for the rest of the experiments. The reactor was put inside a big black chamber designed by me and the features of this box and the accessories used for the set-up are shown in Chapter 4, Section 4.7.4 Algal Growth System Set-up. After completing the algae growth in cell culture flasks, it was clear that both UV to blue light shifting materials, either Coumarin coating on glass or the Coumarin PDMS curing, had almost the same positive effect on the growth of *D. salina*. Therefore, when the easy cure of the PDMS inside the mould and basic application on the reactor as well were considered, it was decided to use the Coumarin PDMS shifting materials during the experiment with 3L photobioreactor. Thus, both shifting materials to convert UV to blue light and green to red light would be made from the same material, organic dye (Coumarin / Bestoil 2G) + PDMS. The emission spectrum of the fluorescent lamp inside the light boxes are given in Figure 5.7 and the transmission spectra of the light beams from uncoated and coated reactor are given in Figure 5.8. The transmission spectrum is obtained using Ocean Spectroscopy as shown in Figure 5.9. The UV is largely absorbed and there is no clearly light between 400 nm and 500 nm for the UV only illuminated Coumarin coated reactor. The change and the light illumination for the green to red dye is not so obvious. The main observation is that the total intensity is slightly reduced with the film present, but there is a subtle change in the spectral shape of the curve.

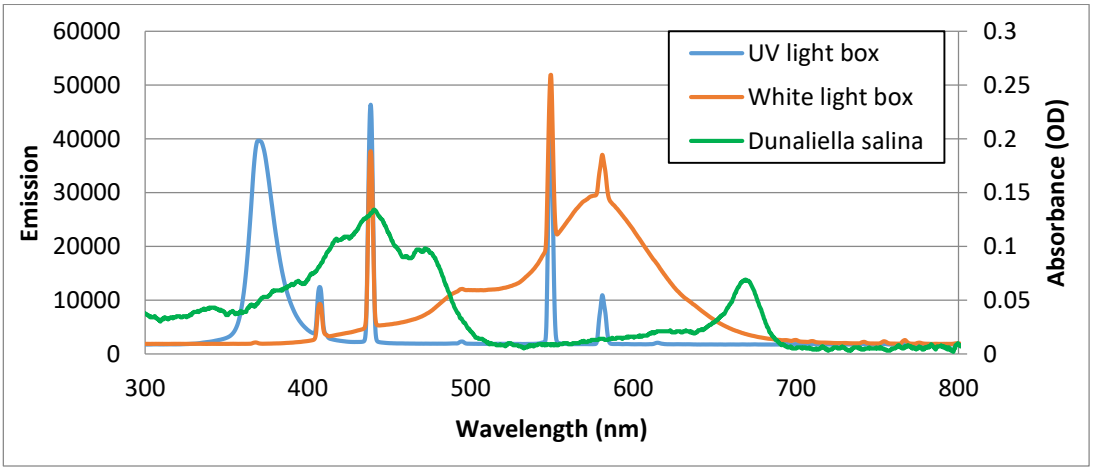

Figure 5. 7. Emission spectra of the white and UV light inside the light box

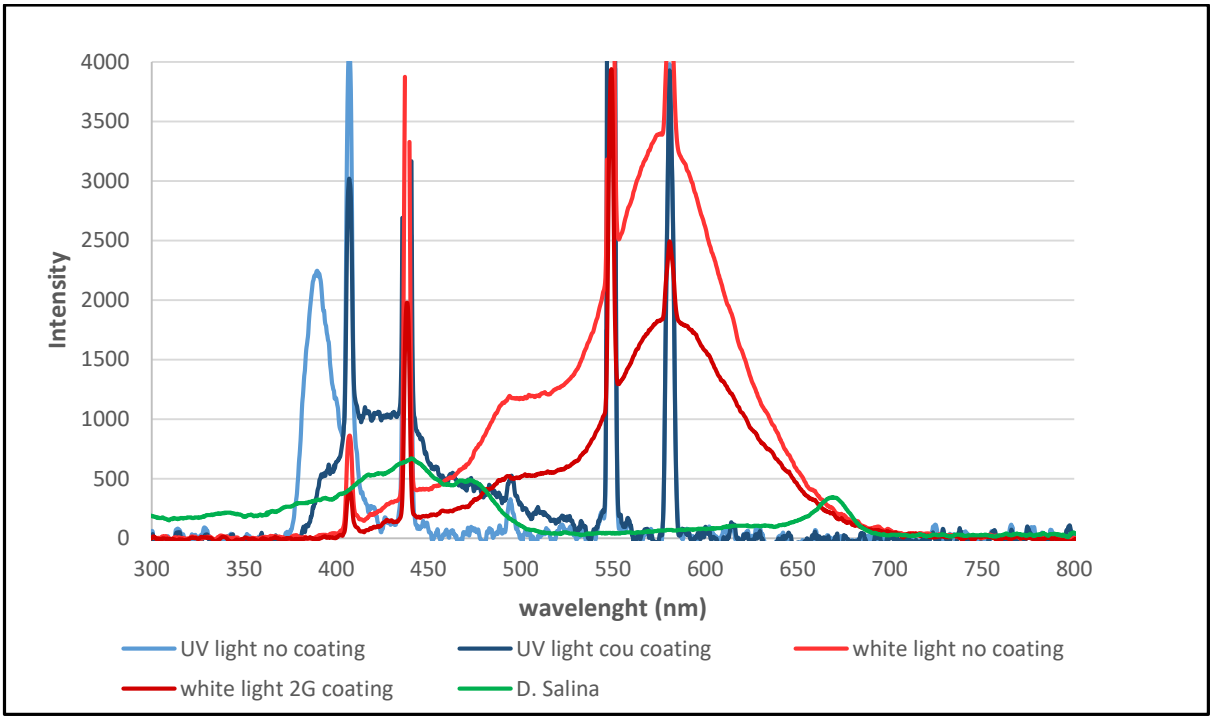

Figure 5. 8. Light transfer from the 3L photobioreactor with and without wavelength shifting materials.

Figure 5. 9. Measuring the light transmission of the reactor with coating either UV to blue shifting material or green to red shifting material.

As explained in Chapter 5, Materials and methods, all experimental sets started with the same initial OD (0.069 at 595nm) and the samples were taken every 24 hours to obtain OD based growth pattern. In order to obtain growth trend of *D. salina* supplying only air with inlet flow rate of 150 cc/min, 5 experimental set ups were run as a) Control 1 (see the UV light effect on *D. salina* growth using both UV and White light at the same time), b) Control 2 (only white light was used), c) UV to blue wavelength tuning (Coumarin – PDMS wavelength shifting material was used), d) green to red wavelength tuning (Bestoil Orange 2G – PDMS wavelength shifting material was used) and finally e) both UV to blue and green to red wavelength tuning.

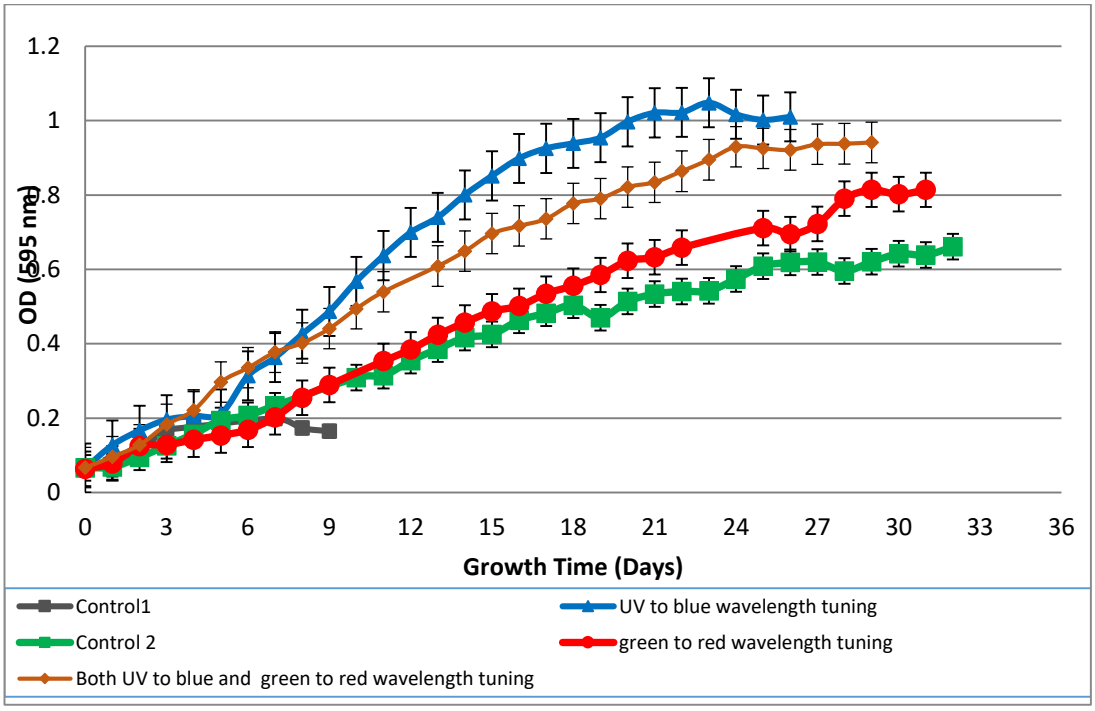

Figure 5. 10. Growth curves of control and coated reactors. Control1 is done without shifting material but using both UV and white light in order to see the UV light effect which causes cell death in a few days; Control2 is done without wavelength shifting materials and only with white light; UV to blue wavelength tuning is done with only Coumarin 1 material and both light sources on; green to red wavelength tuning is done with only Bestoil Orange 2G material and only white light on; and for the final one both Coumarin 1 and Bestoil Orange 2G materials used with both lights on.

Figure 5.10 demonstrates the growth pattern of each set-up which provides proof that wavelength tuning actively assists algae generation. The maximum OD values are recorded as 1.048, 0.814, 0.942, 0.173 and 0.661 at 595nm for UV to blue wavelength tuning film, green to red wavelength tuning film, both UV to blue + green to red wavelength tuning films and control 1 and control 2, respectively. These results mean that in comparison to control 2, there is 39.9% and 18.8% increase in the final OD growth increments for UV to blue wavelength tuning and green to red wavelength tuning, respectively. As mentioned previously in the introduction, there are two previous studies on wavelength tuning materials. One succeeded in reaching > 20% spectral conversion for green to red wavelength shifting (Wondraczek et al., 2013), the other one reached 10% enhancement on product rate using commercial UV to blue wavelength tuning material. Compared to these studies, the work described in this thesis shows more microalgae production for UV to blue wavelength tuning as indicated with high final OD results and high density in the algal culture (see Figure 5.11). Furthermore, Figure 5.10 shows the result of these experiments, and as it can be seen from the graph, UV light caused a distinct and fast cell death just within 6 days on *D. salina* CCAP 19-30 growth. On the other hand, every other experimental run continues for approximately 30 days until the growth reached the stationary phase. The growth with wavelength shifting material reaches to the more dense culture faster than the control experiments.

As illustrated in Figure 5.7, UV lamp used for the experiments also emits some visible light which is absorbed by the chlorophyll which helps the *Dunaliella* to survive but just for 7 days. The UV light clearly shows a harmful effect on *Dunaliella* growth. On the other hand, if only white light is used as in the Control 2 experiment, a final biomass of about 0.661 OD_{595} is obtained by the final day yet the growth time is longer than other wavelength tuning film set-ups. Figure 5.11 illustrates the growth achieved by *Dunaliella* cells in each experimental run, the starting and final day images of the reactors are shown. The reactor with UV to blue wavelength tuning is denser compared to control 2 and green to red wavelength tuning experiments.

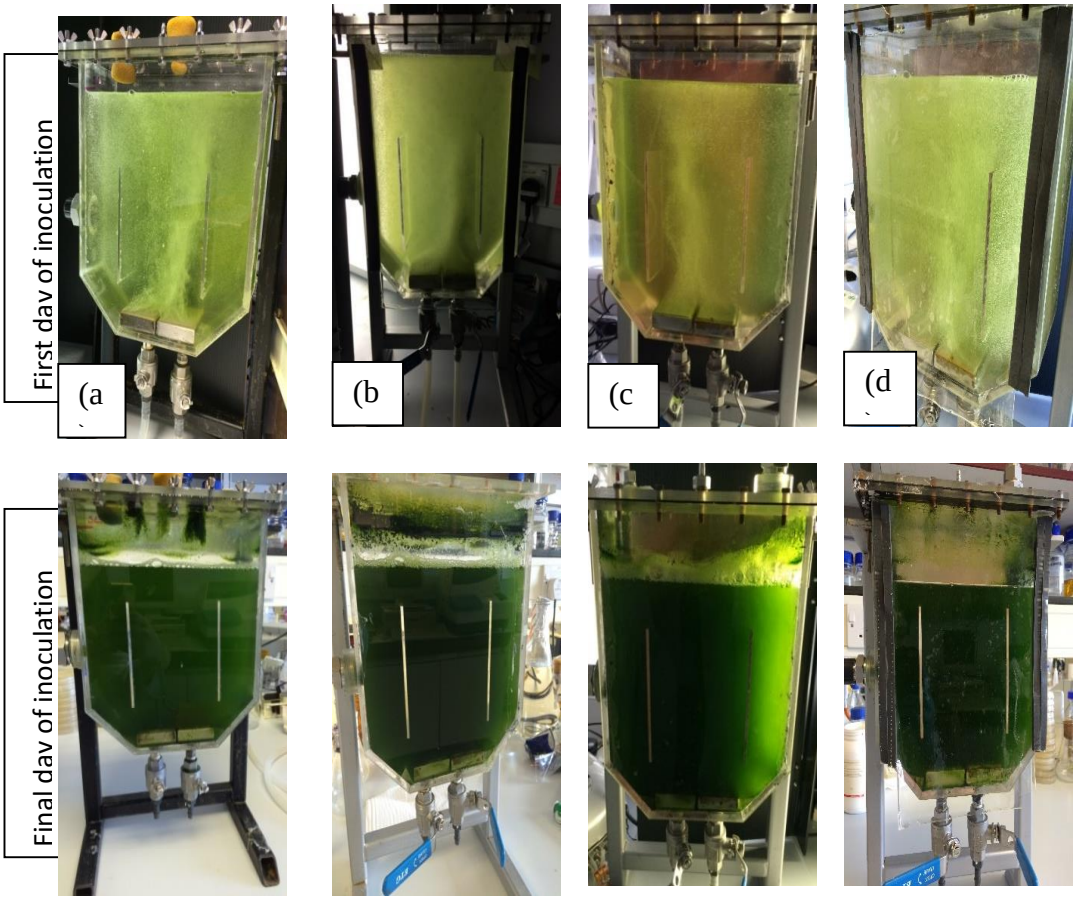

Figure 5. 11. Images of the experimental runs at the starting and final days: (a) Control 2, (b) UV to blue wavelength tuning, (c) green to red wavelength tuning (d) and both UV to blue and green to red wavelength tuning.

5.2.3. Determination of Neutral Lipid in 3L photobioreactor cultures using Nile Red

Although, in the literature, there are many application procedures for determination of the accumulated neutral lipid amount in algae biomass, it is still an uncertain process since researchers are applying different methods to different algae species. As explained in Section 5.1, there are many ways for lipid identification and using Nile Red dye is one of them. Depending on the published papers on Nile Red usage (Alonzo and Mayzaud, 1999, Cooksey et al., 1987, Chen et al., 2009) and owing to low biomass requirement, this method was used in the current work with the procedure clarified in Section 4.4.

Nile Red (NR, 9-diethylamino-5H-Benzo[α]phenoxazine-5-one or $C_{20}H_{18}N_2O_2$) is an effective lipid soluble fluorescent dye which has been utilised in order to detect the lipid amount inside various living organisms such as bacteria (Izard and Limberger, 2003), yeast (Sitepu et al., 2012), zooplankton (Alonzo and Mayzaud, 1999), and algae (Bertozzini et al., 2011, Elsey et al., 2007) using flow cytometry and fluorescence microscopy (Guzmán et al., 2010). The initial study showing the Nile Red penetration inside the neutral lipid and the fluorescence emission was announced by Smith and Thorpe at the beginning of 20^{th} century (Fowler, 1987).

Nile Red goes through the cell barriers including the cell wall, cell membrane and fusing inside the neutral lipid emitting a golden yellow fluorescence for neutral lipids, red for chlorophyll auto-fluorescence and polar lipids. However, the studies done by Chen et al. (2009) and Chen and Blankenship (2011) showed that the cell walls of some algae species have an effect on the dye penetration which causes a time delay for the dye to pass through the membrane and penetrate to the lipid droplets. Thus, the methods proposed by Chen et al. so as to decrease the retention and raise the reaction use dimethyl sulfoxide (DMSO) as solvent and additionally microwaving the samples at temperature 35-40^{o}C (Chen et al., 2009). DMSO was used in this study as suggested by Chen et al., however microwaving process was omitted since *D. salina* does not have a cell wall and has a fairly fragile structure (Ben-Amotz et al., 2009, FAY, 1983).

The efficiency of Nile Red for evaluating the neutral lipid amount depends upon the exact excitation and emission wavelength of the spectroscopy filter. The wavelengths used for the Nile Red measurements are characterized by the hydrophobicity of the solvent used to dissolve Nile Red. These wavelengths for excitation and emission, in general, are identified as 480 and 575 nm for the neutral lipids and 549 and 628 nm for the polar lipids, respectively (Chen and Blankenship, 2011, Storms et al., 2014). Moreover, if the wavelength is longer than 590 nm, then the lipid will not be detected by the Nile Red (Greenspan et al., 1985). On the other hand, the excitation and the emission wavelengths may vary depending on the microalga species. Dunaliella salina CCAP 19/30 was analysed under wavelengths given in Table 5.4 in Section 5.4.1.1 as 485nm and 580nm for excitation and emission, respectively.

Since the intensity of the Nile Red is changeable, the accurate neutral lipid determination in algae species like *D. salina 19/30*, can be obtained by optimizing two main determinants; algal cell concentration and Nile Red concentration.

5.2.3.1. Optimization of *Dunaliella salina* concentration

The optimization of the Nile Red staining peak time and the optimum concentration of the *D. salina* was determined based on the explanation in Material and Methods Chapter, Section 4.4.1.1. Different concentrations of *D. salina* (12.5, 25,32.5,50,62.5,75,87.5 and 100%) were tested and the optimum peak time and the best concentration was obtained depending upon the cell normalization values balanced with concentration and the measured staining times. Figure 5.12 shows the normalized results of the *D. salina* samples, and considering the times and standard deviation of the samples, 75% concentration and 15 minutes were chosen as the ideal concentration and time, respectively.

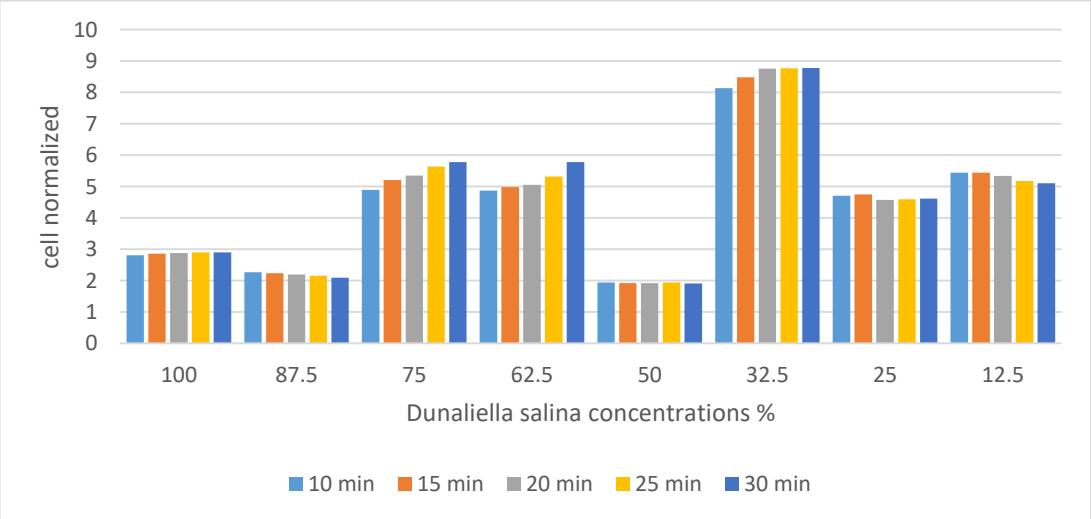

Figure 5. 12. Optimization of cell concentration of *D. salina* and the determination of Nile Red staining peak time. Each column symbolises the normalised value of every single concentration (100 (pure sample), 87.5, 75, 62.5, 50, 32.5, 25, 12.5 %)

5.2.3.2. Optimization of Nile Red concentration

The second part of the Nile Red analysis is defining the optimum Nile Red concentration in order to use the same concentration for all algae samples. For this reason, the experiment was done as described in Section 5.4.1.2 and Figure 6.13 gives the result of this experiment. It is obvious that the Nile Red concentration, 0.64 µg ml^{-1}, has highest fluorescent intensity for 15 minutes.

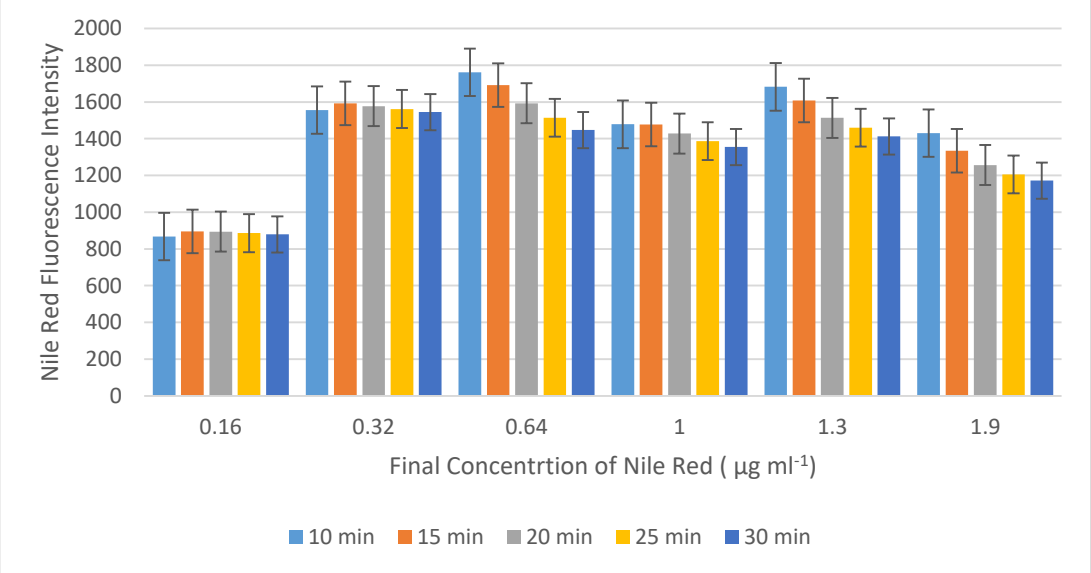

Figure 5. 13. Optimization of Nile Red dye concentration for staining 75% concentrated *D. salina* samples. Nile Red staining readings were taken at diverse times 10, 15, 20, 25 and 30 minutes. The error bars symbolise the technical repeats (3 replicates) of four stained and four unstained readings.

5.2.3.3. Effect of wavelength shifting material on the lipid content

The stress condition on the neutral lipid accumulation for this part of the project is changing the light intensity using different wavelength shifting materials. As explained in previous chapters, there are 3 different stress conditions i.e. increasing blue light intensity using Coumarin shifting material (convert UV to blue light), increasing the red light intensity using Bestoil 2G wavelength shifting material (convert green to red light) and increasing both light types using both shifting materials on each side of the reactor. The control experiment was under normal conditions without using any wavelength shifting material.

The neutral lipid analysis of each stress experiment set up was done at the end of the experimental run; therefore, the final times vary (see Table 5.1) depending on reaching the stationary phase. However, the time is approximately 30 days for each run (29 days +/- 3 days). The sample concentration used was 75% as determined in Section 6.2.3.1 and the Nile Red dye concentration used was 0.64 µg ml-1 as obtained in Section 6.3.2.2. The highest fluorescence intensity was obtained with Coumarin shifting material (2486.58) in the shortest experiment time period (26 days). On the other hand, Coumarin + 2G experimental run gives the lowest value with 267.08 fluorescence intensity.

Table 5. 1 Nile Red Fluorescence Intensity analysis of *D. salina* samples grown in 1.5M NaCl medium**.** Each Nile Red analysis for each experimental run has 3 replicates of four stained and four unstained readings.

	Control	**Coumarin**	**2G**	**Coumarin + 2G**
Fluorescence Intensity	845	2486.58	515.33	267.08
Total experiment days	32	26	31	29

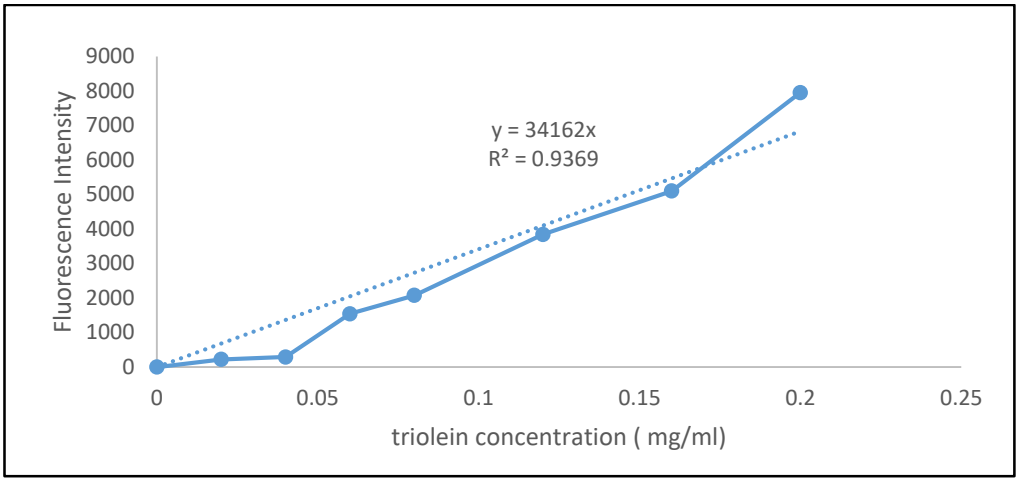

Figure 5. 14. Standard addition Triolein concentration versus Nile Red fluorescence intensity calibration curve

5.2.3.4. Correlation between OD and Cell Dry weight

In order to determine the percentage neutral lipid in the *D. salina* cultures, correlation between OD and cell dry weight was done. It was also necessary to plot a Triolein (standard neutral lipid) curve (Figure 5.14) in addition to the dry weight curve (Figure 5.15) so as to find out *x* values in the equation in both graphs and correlate them to each other which is explained in Chapter 5, materials and methods. By doing this correlation, the OD value of culture recorded every day, can be converted to optimized dry weight of the cells (mg /ml). After that, Triolein values will be divided by the dry weight and multiplied by 100 to get the percentage neutral lipid value.

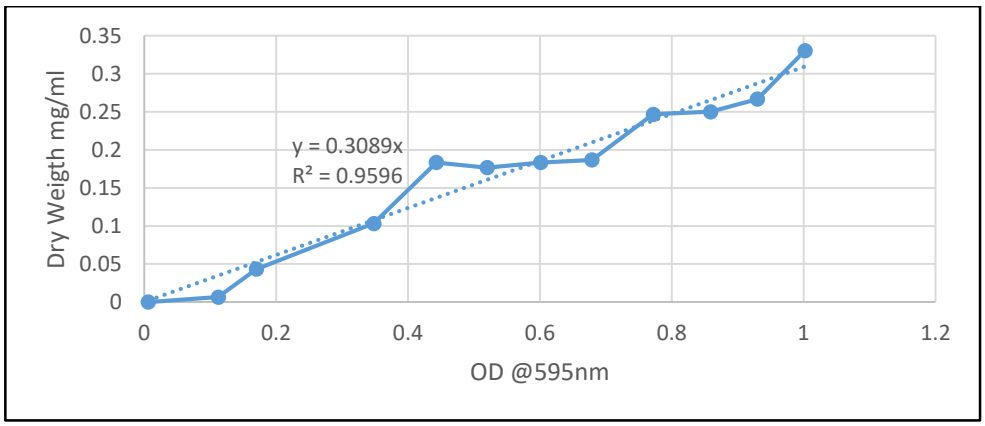

Figure 5. 15. Dry weight vs OD concentration calibration curve of *D. salina*

Depending on the dry weight *vs* OD graph, Figure 6.15, the optimum dry weight amount for 75% concentrated *D. salina* is 0.2312 µg ml^{-1} at OD 595 nm. Table 5.2 shows the calculated neutral lipid amounts and the percentage lipid amounts for the four different growth conditions. From the table it can be said that the highest lipid amount is obtained using the Coumarin shifting material which is 0.31 µg ml^{-1}.

Table 5. 2. Accumulated lipid amount of *D. salina* at normal and different stressed conditions.

Stress condition	Day	Fluorescent Intensity	Concentration mg/ml	Neutral Lipid amount µg/ml	Percentage Lipid Amount CDW %
Control	32	845.00	0.0247	0.1068	10.6766
Coumarin	26	2486.58	0.0728	0.3142	31.4181
2G	31	515.33	0.0151	0.0651	6.5112
Coumarin + 2G	29	267.08	0.0078	0.0337	3.3746

5.2.4. Fluorescence Microscope images to monitor lipid droplets

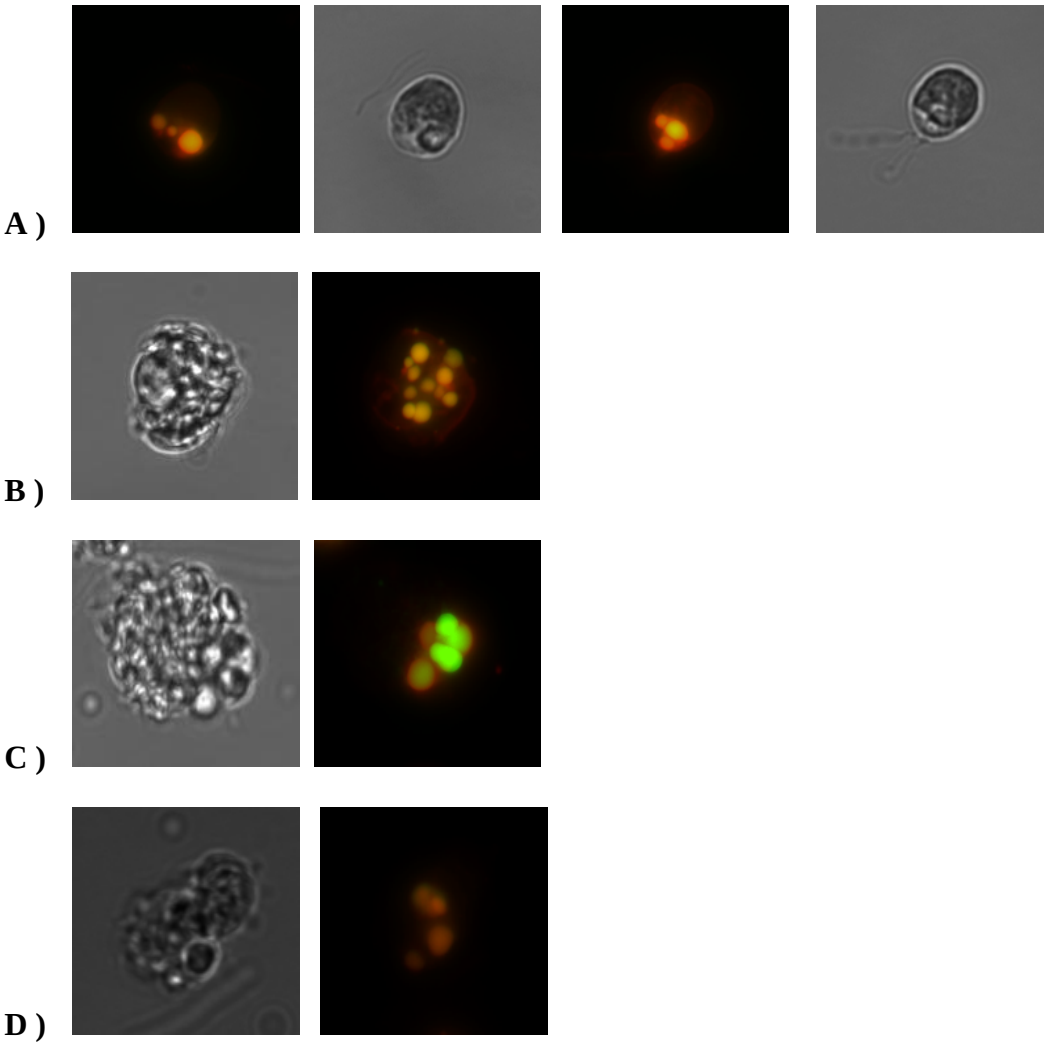

Figure 5. 16. Fluorescence microscopy images (both bright field and coloured) of *D. salina* stained with Nile Red after growth under different light intensities using different wavelength shifting materials. **A)** *D. salina* cells grown under normal condition without using any wavelength shifting material. **B)** *D. salina* cells grown under stress condition with more blue light using Coumarin shifting material. **C)** *D.salina* cells grown under more red light using Bestoil 2G wavelength shifting material. **D)** *D. salina* cells grown under more blue and red light using both Coumarin and Bestoil 2G wavelength shifting materials.

The fluorescence microscope was used to visually confirm the neutral lipid accumulation in the *D. salina* cells as visually. The Figure 5.16 shows the neutral lipid droplets inside the *D. salina* cells under various growth conditions i.e. control, Coumarin shifting material, Bestoil 2G shifting material and both Coumarin and Bestoil 2G shifting materials. The images were taken as explained in Section 4.5 using a fluorescence microscope; the grey captures represent bright field images and the colourful captures represent red and green lightening images. The yellowish droplets inside cells indicate the lipid droplets and as can be seen from the Figure 6.16 B, using Coumarin wavelength shifting materials increases the neutral lipid droplets number inside the cell. On the other hand, green droplets were observed in the Bestoil 2G wavelength shifting material used culture. As reported by Kleinegris et al. (2010, Kleinegris et al., 2011) , this is caused by the presence of β-carotene.

5.3. Discussion

Owing to the high CO_2 uptake properties of microalgae, they have been considered as an alternative way of reducing CO_2 emissions from industry by capturing CO_2 from factories flue gas. More microalgae growth results in more CO_2 capture. For this reason, the objectives of this project are to enhance microalgae (*D. salina*) growth by introducing wavelength shifting materials to the airlift photobioreactor (ALB). Wavelength shifting materials were prepared with fluorophores Coumarin and Bestoil Orange 2G and applied on the wall of photobioreactor in order to shift the light.

Since sunlight will be used as light source, the algae will be exposed to the UV light and PAR region at the same time. The effect of UV light on the living organisms has been reported many times by scientists. Exposure to ultraviolet radiation causes metabolic problems for photosynthetic organisms since the UV light is absorbed by the nucleic acids and proteins (White and Jahnke, 2002, Holzinger and Lütz, 2006). It is also responsible for photo inhibition by incorporating oxygen formation. Moreover,

the green light is not absorbed by the algae absorption pigments. Therefore, it is beneficial to convert these harmful and unused wavelength ranges to useful ones.

So far, some scientists have published work on how various light intensities effect the algae growth (see the table in Literature Review, Section 1.3.1). Furthermore, to this studies, Blair et al. (2014) published that *Chlorella vulgaris* cells have an improvement on the biomass production and growth rate under blue light (475nm) in comparison to green (510nm) and red (650nm) lights.

This section of the project examined the effect of wavelength shifting materials on *Dunaliella salina* CCAP 19/30 with air supply (where only %0.03 CO_2 is present) for bubbling inside cell culture flasks (as preliminary study) and 3L photobioreactor (as normal growth conditions inside a designed big black growth chamber). Based on the results obtained both after preliminary study (Sections 6.2.1.1) and the 3L photobioreactor (Section 6.2.2), it is definitely clear that the Coumarin wavelength shifting material which converts the harmful UV light to the utilised blue light, accelerates the *D. salina* growth more compared to the other growth conditions (control, green to red light conversion and both UV to blue and green to red conversion) with the final OD_{595nm} values of 0.934 (12 days) and 1.01 (26 days) for preliminary study and 3L photobioreactor, respectively. In many microalgae species blue light serves for enzyme activation during the photosynthesis and regulates gene transcription; thus the algae growth is enhanced (Matthijs et al., 1996). Furthermore, both study set ups illustrated the harmful effect of UV light during the control experiment without using any wavelength shifting materials or UV filter glass. However, it is also shown that the algae can survive after a couple of days lag phase after shutting off the UV light for the 3 L photobioreactor when it adapts itself to the new environment (Mohsenpour et al., 2012) . This might be because *Dunaliella* species produce β-carotene when they are exposed to more UV-A light in order to protect the cell from photo inhibition (White and Jahnke, 2002). Another observation is that using both wavelength shifting materials was not as effective as expected in increasing algal growth. There are two possible reasons for this: first, the green to red wavelength shifting material does not give perfect absorption and emission features as expected for a good overlap with chlorophyll absorption wavelengths; and second,

there might be photoinhibition because of high light intensity using both shifting materials at the same time which might be eliminated using a larger photobioreactor or doing some metabolic engineering to the light harvesting antennae (Hovel et al., 1979, Melis, 2009). Also the growth under green to red light shifting materials and control experiments are lower compared to blue light. Such a difference in results may be due to the fact that green light causes an inhibitory effect because the photon has less energy than a blue photon (Gaytán-Luna et al., 2016).

In order to further investigation higher algae growth under blue light, the Nile Red analysis and the screening of the *Dunaliella* cells under the fluorescent microscope were carried out. Depending on the findings in previous sections, it is concluded that these analyses also support the positive effects. Nile Red analysis shows the highest fluorescence intensity was obtained with Coumarin shifting material within 26 cultivation days as 2486.58 and it is about three fold higher than the control experiment. Besides this, the fluorescent light microscope images also indicate that the lipid droplets inside the cells grown in the Coumarin shifting material applied reactor are more than the others (Figure 5.16). And also in Figure 5.16, the light microscope images showed clear orange globules, the green fluorescence again was detected i.e. *D. salina* stores secondary carotenoids (predominantly β-carotene) in lipid globules in the chloroplast when cultivated under stress conditions. When the cells are stressed, the red fluorescence from chlorophyll partly disappears as the thylakoid membranes are broken down. At the same time, the cells start to produce carotenoid globules and green fluorescence appears simultaneously (Kleinegris et al., 2010, Kleinegris et al., 2011).

After the correlation of dry weight with the Nile Red analysis, it is concluded that the Coumarin shifting material applied reactor produce the most neutral lipid with the value 0.31 µg ml^{-1} which is about 31.42% lipid as a percentage of dry weight.

Bubbling technology is an important parameter for the algae growth in order to prevent O_2 accumulation and obtain well mixed cell and gas distribution inside the reactor. Therefore, an airlift photobioreactor was used for all large scale experiments. However, in the preliminary study, fine bubble supply to the system was investigated

in the second part of the initial experiments and the analysis indicates that incorporating fine bubbles in the system results in a more than double augmentation in algae growth.

Consequently, introducing wavelength shifting materials to the growth system increases the algal growth with UV to blue light conversion had the greater effect which was more than previously reported for the wavelength shifting materials and control conditions. Additionally, bubbling technology enhances the growth. Therefore, using both technologies at the same time for algae growth can provide even greater efficiency gains for algal biomass production.

CHAPTER 6: ALGAE GROWTH WITH CO_2 SUPPLY

6.1. Introduction

Similar to terrestrial plants, microalgae are also valuable living organisms for CO_2 fixation since they are the original CO_2/O_2 exchangers and initial biomass producers on the world (Pulz, 2001, Mohsenpour and Willoughby, 2016). CO_2 is an important driving force for algal photosynthesis as it is the main carbon source for RuBP carboxylation as explained in Section 1.2.1 (photosynthesis in microalgae). Much research has been done on how the amount of CO_2 affects microalgae growth; Ying et al. (2014)studied the effect of dissolved CO_2 amount on *D. salina* applying 3 different CO_2 concentrations (5%, 20% and 50%) and found out that extreme CO_2 levels (50%) cause inhibition of photosynthesis and becomes fatal for the algae species. Moreover, another study completed by Mohsenpour and Willoughby (2016) was on the effects of the diverse algae culture condition using pure air (0.03% CO_2), 5% and 15% CO_2 supply, and they concluded that the highest biomass content was obtained with 5% CO_2 aeration and at 15% growth at early stage is inhibited making the media more acidic.

The aim of this chapter is to show the effect of CO_2 supply on the system for *D. salina* CCAP 19/30 growth. Therefore, gas mixtures with different percentages of CO_2 (balanced with air) were introduced to the photobioreactor. The *D. salina* growth was initially measured using the 1% CO_2, then the 5% CO_2 was checked. After that 10% CO_2 was supplied since it is the closer to the levels found in fossil fuel power station fuel gas (~15% CO_2) and finally growth with 0.5% CO_2 was examined. In order to carry out the experiments the same 3L flat plate photobioreactor set-up explained in Figure 3.7 in Section 3.4.3. The wavelength tuning materials were also the same resulting in the same absorption and the emission spectrum was given in Figure 5.1 in Chapter 5. The reactors for the each experimental set up was inoculate using a 14 days old *D. salina* culture growth in a flask in the 25^{o}C growth room, H floor of MBB and the initial concentration of each reactor was arranged to OD 0.069 at 595nm. Every day, 1ml of sample was taken from the bottom of the reactor and the OD was measured at 595nm to discover the growth pattern of the *D. salina*. At the end of the experiment which is the stationary phase, approximately 400ml of the sample was taken to be used

in Nile red lipid analysis (see Section 4.4) and Fluorescent microscope imaging (see Section 4.5) as described in Chapter 4, Materials and Methods.

6.2. Results of *Dunaliella salina* growth with CO_2 supply

Dunaliella salina 19/30 CCAP was grown in an 3L airlift photobioreactor for the all experiments described in this chapter. The reactor was put inside a large black chamber designed by the author to control the illumination available to the algae and the features of this chamber and the accessories used for the set-up are shown in Chapter 4, Section 4.7.4 Algal Growth System Set-up. Initially four experiments were run with 1% CO_2 including a Control, UV to blue wavelength tuning (Coumarin – PDMS wavelength shifting material was used), green to red wavelength tuning (Bestoil Orange 2G – PDMS wavelength shifting material was used) and finally both UV to blue and green to red wavelength tuning.

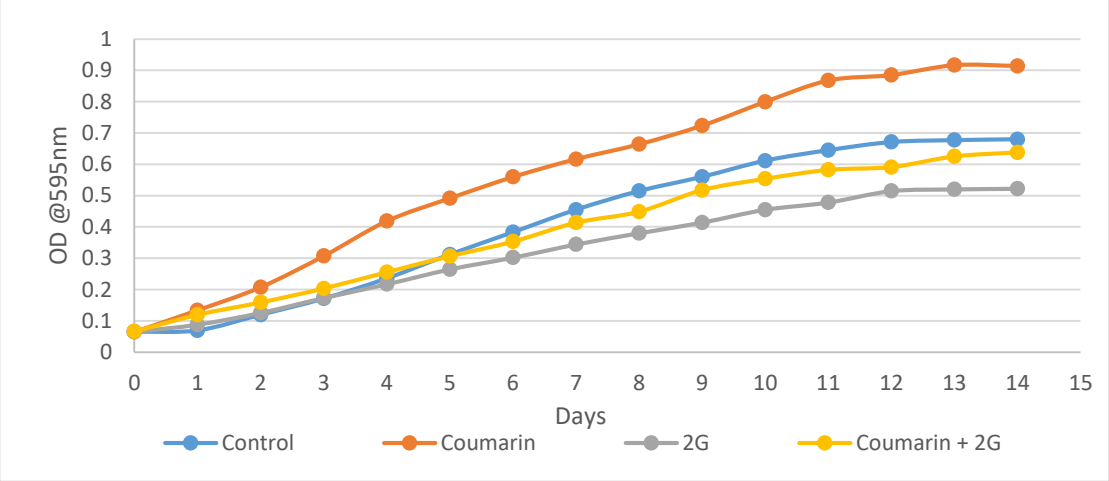

Figure 6. 1. Growth Curves of 1% CO_2 supplied control and coated reactors. The Control was measured without any wavelength shifting materials and only with white light; UV to blue wavelength tuning is measured with only Coumarin 1 material and both UV and white lights on; green to red wavelength tuning is measured with only Bestoil Orange 2G material and only white light on; and for the final one both Coumarin 1 and Bestoil Orange 2G materials were used with both lights on.

6.2.1. *D. salina* growth in 3L photobioreactor with 1% CO_2 supply

As initial experiment for the CO_2 dosing to the system, 1% CO_2 balanced with air was used. 4 experimental runs were carried out in a similar manner to the air supply experiments explained in Section 5.2.2. Each experimental run continues approximately 14 days until reach the stationary phase which is almost half time of the air supplied experiments. Figure 6.1 demonstrates the growth pattern of each set-up which provides proof that Coumarin wavelength tuning actively assists algae generation. The maximum OD values are recorded as 0.68, 0.914, 0.522 and 0.638 at 595nm for control, UV to blue wavelength tuning film, green to red wavelength tuning film and both wavelength material, respectively. These results mean that in comparison to the control, there is a 25% increase in the final OD growth increments for UV to blue wavelength tuning. These results support the key hypothesis of this thesis and also Figure 6.2 supports the growth curve data by illustrating the high density in the algal culture for UV to blue wavelength tuning.

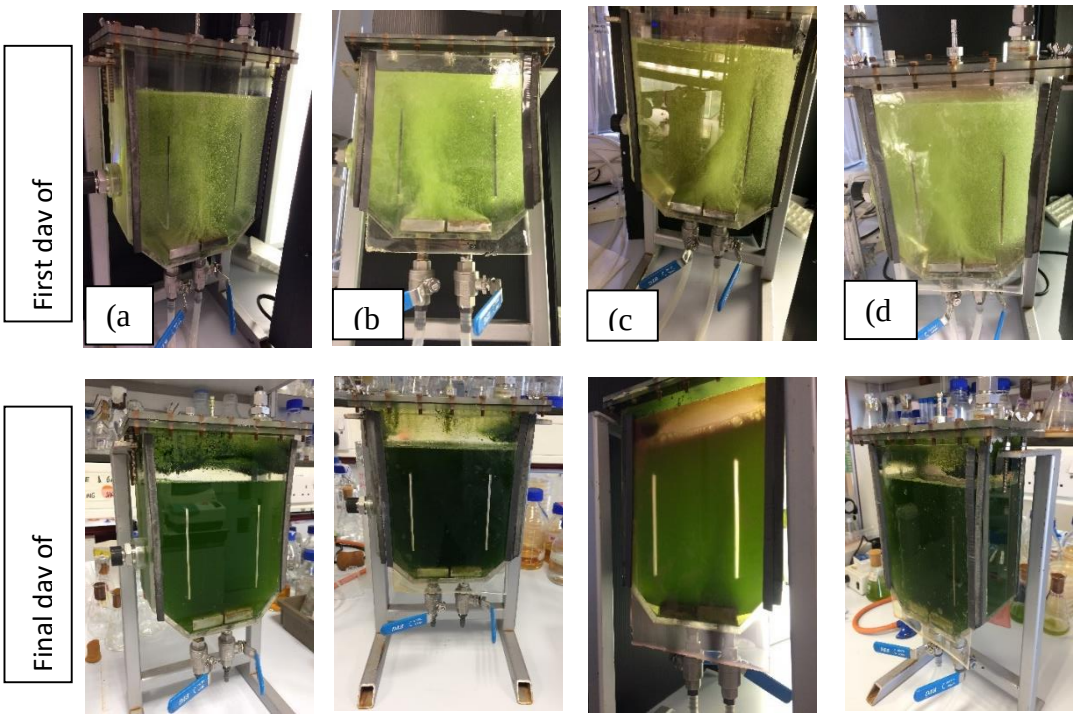

Figure 6. 2. Images of the experimental runs at the starting and final days: (a) Control, (b) UV to blue wavelength tuning, (c) green to red wavelength tuning (d) and both UV to blue and green to red wavelength tuning.

6.2.1.1. Neutral Lipid determination of 1% CO_2 supplied *D. salina* growth using Nile Red

As explained in previous chapters, there are 3 different stress conditions and the neutral lipid analysis of each stressed experiment set up were done at the end of the experimental run, in this case at day 14 (see Table 6.1). The sample concentration was 75% as determined in Section 5.2.3.1 and the optimum Nile Red dye concentration was used as 0.64 µg ml^{-1} as obtained in Section 5.3.2.2. The highest fluorescence intensity was obtained with the Control experiment as 207.58 despite the Coumarin showing the highest growth OD. On the other hand, Coumarin experimental run gives the lowest value with 81.33 fluorescence intensity. Thus, the highest percentage lipid amount, 2.62 % (0.0262 µg ml^{-1}), was obtained for the Control experiment on the contrary to the results observed for the air supplied experimental results.

Table 6. 1. Nile Red Fluorescence Intensity analysis and accumulated lipid amount of 1% CO_2 supplied *Dunaliella salina* samples grown in 1.5M NaCl medium**.** Each Nile Red analysis for each experimental run has 3 replicates of four stained and four unstained readings.

1 % CO_2 Stressed condition	**Day**	**Fluorescent Intensity**	**Concentration mg/ml**	**Neutral Lipid amount µg/ml**	**Percentage Lipid Amount CDW %**
Control	14	207.58	0.0061	0.0262	2.6228
Coumarin	14	81.33	0.0024	0.0103	1.0277
2G	14	164.92	0.0048	0.0208	2.0837
Coumarin + 2G	14	222.42	0.0065	0.0281	2.8102

6.2.1.2. Monitoring lipid droplets 1% CO_2 supplied *D. salina* with fluorescence microscope images

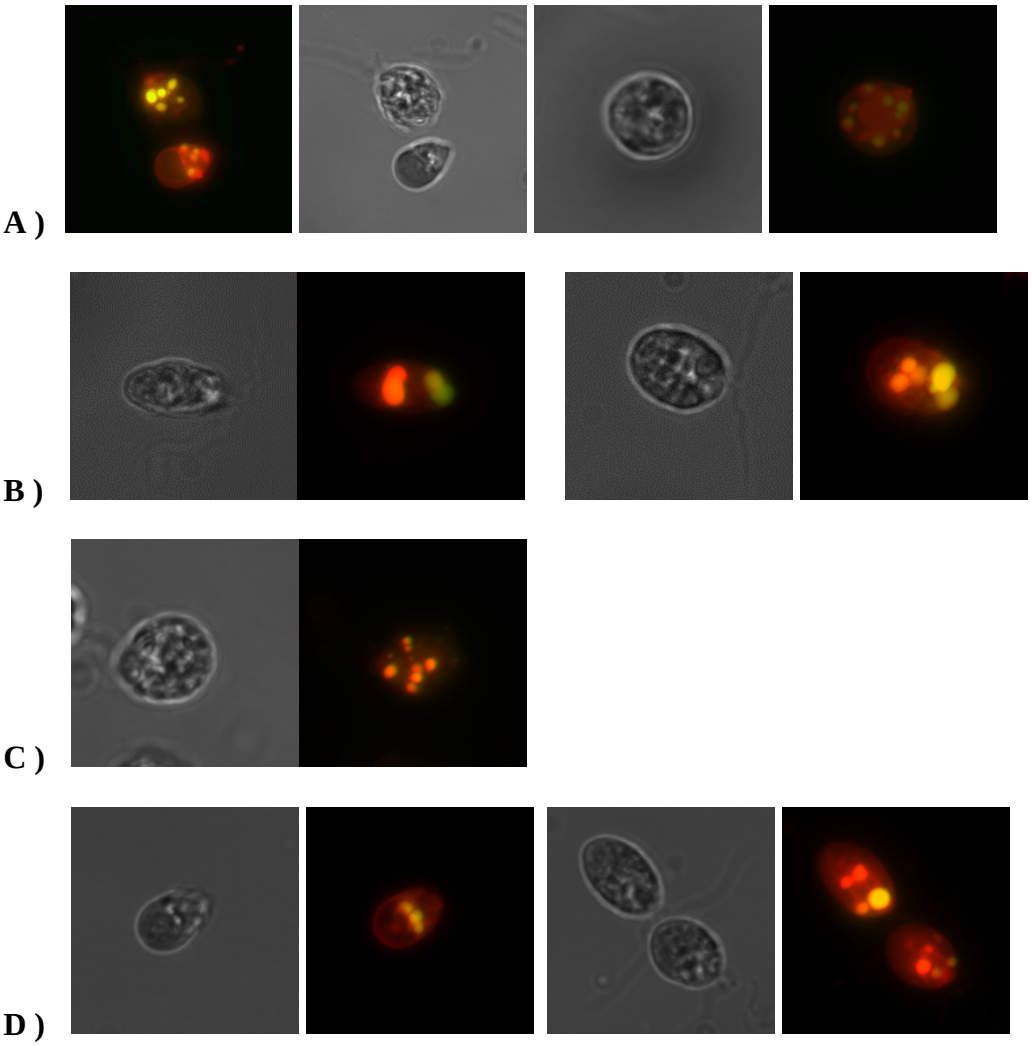

Figure 6. 3. Fluorescence microscopy images (both bright field and coloured) of 1% CO_2 supplied *Dunaliella salina* CCAP 19/30 stained with Nile Red after growth under different light intensities using different wavelength shifting materials. **A)** *D. salina* cells grown under normal condition without using any wavelength shifting material. **B)** *D. salina* cells grown under stress condition with more blue light using Coumarin shifting material. **C)** *D. salina* cells grown under more red light using Bestoil 2G wavelength shifting material. **D)** *D. salina* cells grown under more blue and red light using both Coumarin and Bestoil 2G wavelength shifting materials.

The fluorescence microscope images visually illustrate the neutral lipid accumulation in the *D. salina* cells. Figure 6.3 shows the neutral lipid droplets inside the 1% CO_2 supplied *D. salina* cells under various growth conditions. The images were taken as explained in Section 4.5 using a fluorescence microscope; the greyscale images represent bright field images and the colour images represent red and green fluorescence. The yellowish droplets inside the cells indicates the lipid droplets and as can be seen from Figure 6.3 A, Control experiment has more and smaller neutral lipid droplets number inside the cell which is also confirms the Nile Red and biomass correlation analysis in Section 6.2.1.1. On the other hand, greenish droplets were observed both in culture grown under the Control and Coumarin wavelength shifting conditions. As reported by Kleinegris et al. (2010, Kleinegris et al., 2011) , this green light is caused by β-carotene accumulation inside the cell.

6.2.2. *D. salina* growth in 3L photobioreactor with 5% CO_2 supply

For the second experimental set the CO_2 dosing to the system was increased to 5% CO_2 balanced with air. As before, 4 experimental runs were carried out as explained in Section 6.2.1. Figure 6.4 shows the growth curve of each set-up and again the growth increment when using the Coumarin film for wavelength tuning can be seen. The maximum OD values are recorded as 0.705, 0.939, 0.5725 and 0.6345 at 595nm for control, UV to blue wavelength tuning film, green to red wavelength tuning film and both wavelength material, respectively. These results mean that in comparison to control, there is a 25% increase in the final OD for UV to blue wavelength tuning. These results support the hypothesis of this thesis and also the Figure 6.5 supports the conclusion from the growth curve. The high density in the algal culture for UV to blue wavelength tuning as *D. salina* biomass is further illustrated by the observed attachment of algae onto the reactor wall can be seen in the photos. On the other hand, each experimental run continues approximately 15 days until reach the stationary phase which is almost half time of the air supplied experiments but is the same as for the 1% CO_2 supplied *D. salina* growth.

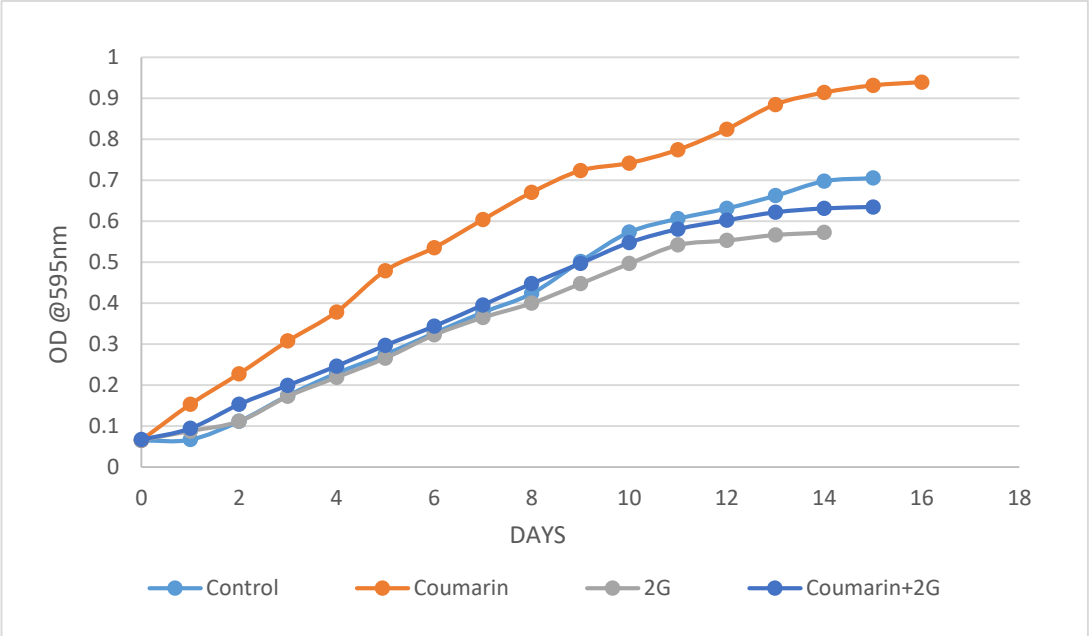

Figure 6. 4. Growth Curves of 5% CO_2 supplied control and coated reactors. Control is done without wavelength shifting materials and only with white light; UV to blue wavelength tuning is done with only Coumarin 1 material and both lights on; green to red wavelength tuning is done with only Bestoil Orange 2G material and only white light on; and for the final one both Coumarin 1 and Bestoil Orange 2G materials were used with both lights on.

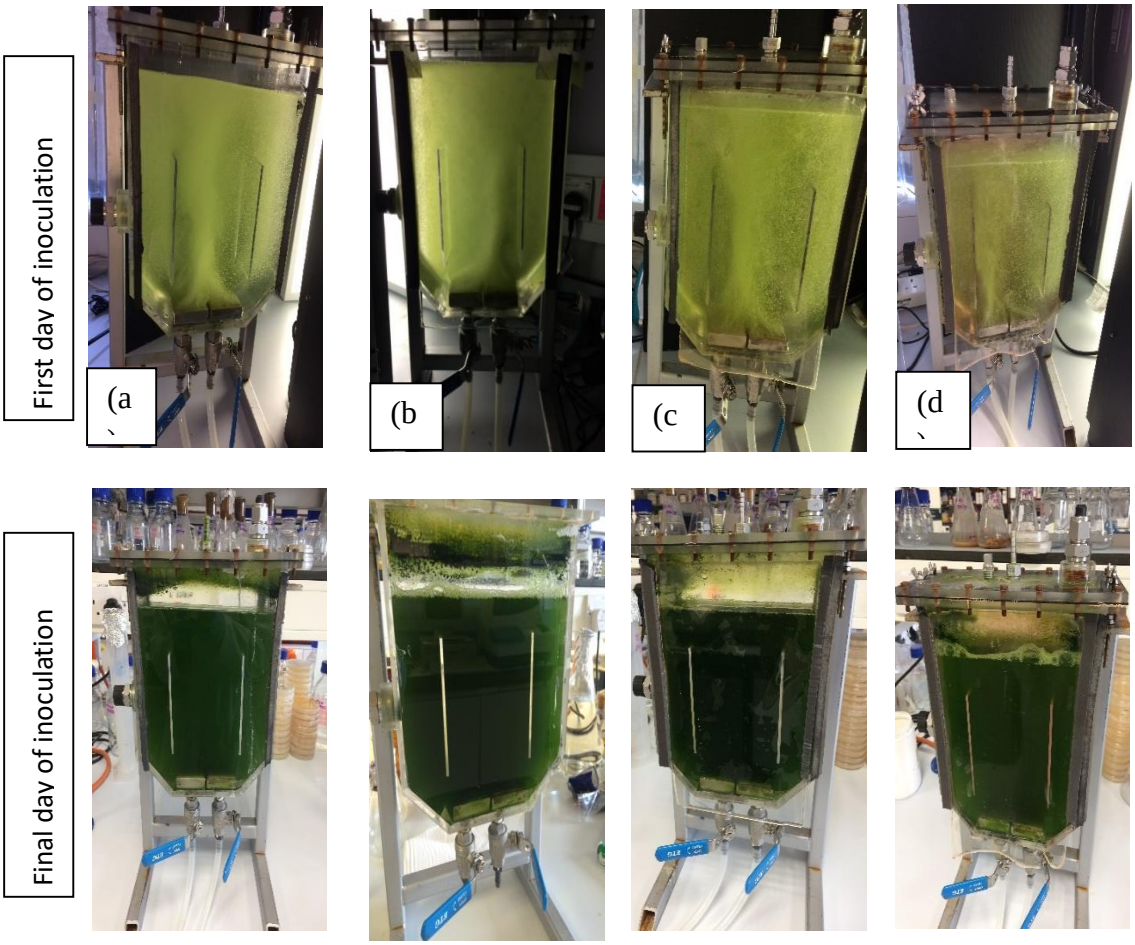

Figure 6. 5. Images of the experimental runs at the starting and final days: (a) Control, (b) UV to blue wavelength tuning, (c) green to red wavelength tuning (d) and both UV to blue and green to red wavelength tuning.

6.2.2.1. Neutral Lipid determination of 5% CO2 supplied *D. salina* growth using Nile Red

The neutral lipid analysis of the 3 stress conditions was again done at the end of the experimental run, after 15 days ±1 (see Table 6.2). The sample concentration was 75% as determined in Section 5.2.3.1 and the optimum Nile Red dye concentration was 0.64 µg ml^{-1} as obtained in Section 5.3.2.2. The highest fluorescence intensity was obtained with Coumarin shifting material at 180.75 and agrees with the Coumarin showing

highest growth OD. On the other hand, 2G experimental run gives the lowest value with 82.92 fluorescence intensity. Thus, the highest percentage lipid amount, 2.28 % (0.0228 µg ml^{-1}), was obtained for the Coumarin experiment which is contrary to the results found for 1% CO_2 supplied experimental results. In addition, this results agrees with the OD growth pattern of the diverse wavelength shifting material used experiments.

Table 6. 2. Nile Red Fluorescence Intensity analysis and accumulated lipid amount of 5% CO_2 supplied *Dunaliella salina* samples grown in 1.5M NaCl medium**.** Each Nile Red analysis for each experimental run has 3 replicates of four stained and four unstained readings.

5 % CO_2 Stressed condition	**Day**	**Fluorescent Intensity**	**Concentration mg/ml**	**Neutral Lipid amount µg/ml**	**Percentage Lipid Amount CDW %**
Control	15	109.67	0.0032	0.0139	1.3856
Coumarin	16	180.75	0.0053	0.0228	2.2838
2G	14	82.92	0.0024	0.0105	1.0477
Coumarin + 2G	15	63.83	0.0019	0.0081	0.8065

6.2.2.2. Monitoring lipid droplets 5% CO2 supplied *D. salina* with fluorescence microscope images

The fluorescence microscope images, in Figure 6.6, are used to show the visual neutral lipid accumulation in the 5% CO_2 supplied *Dunaliella salina* cells under various growth conditions. As in previous experiments, the images were taken as in Section 5.5 using a fluorescence microscope; the greyscale image represents the bright field images and the coloured images represent the red and green fluorescence images. Although the lipid droplet images are not very clear because of the smashed cell view due to harsh addition of lamella or vigorous mixing during sample preparation, the yellowish droplets inside cells can be seen from the Figure 6.6. It can be said that the cells from the Coumarin shifting material used experiment have more numerous and smaller sized neutral lipid droplets number inside the cells compared to other experimental runs. This also certifies the highest Nile Red and biomass accumulation of Coumarin as demonstrated in Section 6.2.2.1. On the other hand, shining green droplets caused by the β-carotene accumulation inside the cell were distinctively observed in the Coumarin + 2G wavelength shifting material used culture (Figure 6.6 D) (Kleinegris et al., 2010, Kleinegris et al., 2011).

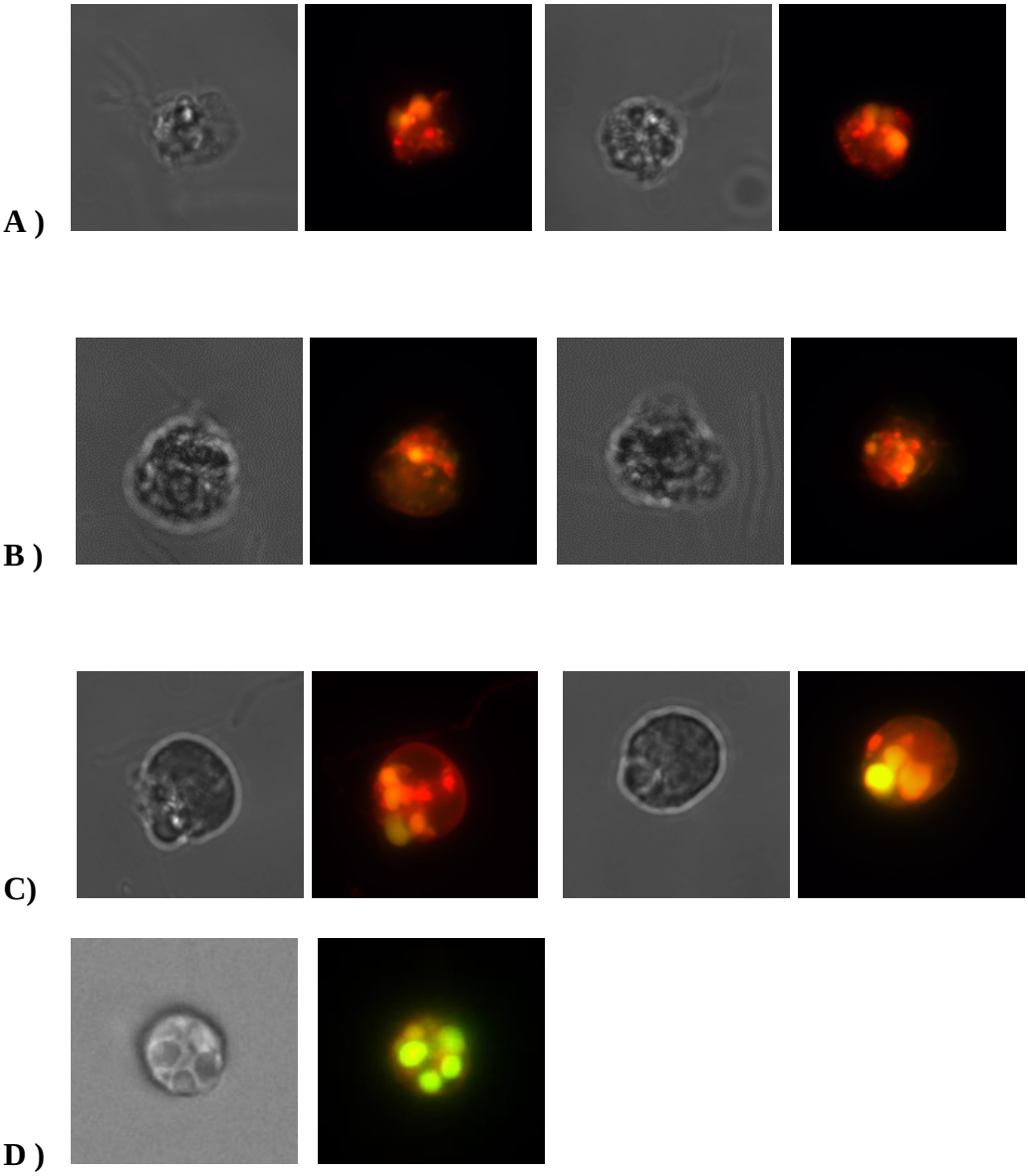

Figure 6. 6. Fluorescence microscopy images (both bright field and coloured) of 5% CO_2 supplied *Dunaliella salina* CCAP 19/30 stained with Nile Red after growth under different light intensities using different wavelength shifting materials. **A)** *D. salina* cells grown under normal condition without using any wavelength shifting material. **B)** *D. salina* cells grown under stress condition with more blue light using Coumarin shifting material. **C)** *D.salina* cells grown under more red light using Bestoil 2G wavelength shifting material. **D)** *D. salina* cells grown under more blue and red light using both Coumarin and Bestoil 2G wavelength shifting materials.

6.2.3. *D. salina* growth in 3L photobioreactor with 10% CO_2 supply

The third experimental set for the CO_2 dosing to the system, 10% CO_2 balanced with air was used. After getting the results of the previous CO_2 supply experiments, this time only control and Coumarin wavelength shifting material applied experiments were performed as explained in Section 6.2.1. The 2G and Coumarin+2G experiments were considered unnecessary because they repeatedly showed worse results compared to control experiment in the previous CO_2 experiment. This is thought to be due to the Bestoil 2G/PDMS wavelength shifting material not showing effective absorption/emission performance owing to aggregation within the film resulting scattering of the light and poor overlap of the 2G emission spectrum with the chlorophyll absorbance spectrum. Figure 6.7 shows the growth curve of each set-up and the maximum OD values are recorded as 0.7085 and 0.936 at 595nm for control and UV to blue wavelength tuning film, respectively. These results are also proof of growth increment when Coumarin wavelength tuning material is used and it means that in comparison to the control, there is approximately a 24% increase in the final OD for UV to blue wavelength tuning. Figure 6.8 supports the growth curve by illustrating high density in the algal culture for UV to blue wavelength tuning as *D. salina* biomass attachment on the reactor wall can be seen from the photos. Furthermore, each experimental run continued for 16 days until reaching the stationary phase which is about half the time of the air supplied experiments and but the same as previous CO_2 supplied *D. salina* cultures.

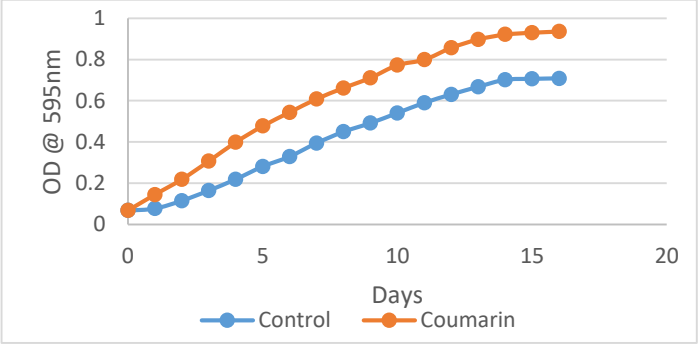

Figure 6. 7. Growth Curves of 10 % CO_2 supplied control and coated reactors. Control is done without wavelength shifting materials and only with white light; UV to blue wavelength tuning is done with only Coumarin 1 material and both light on.

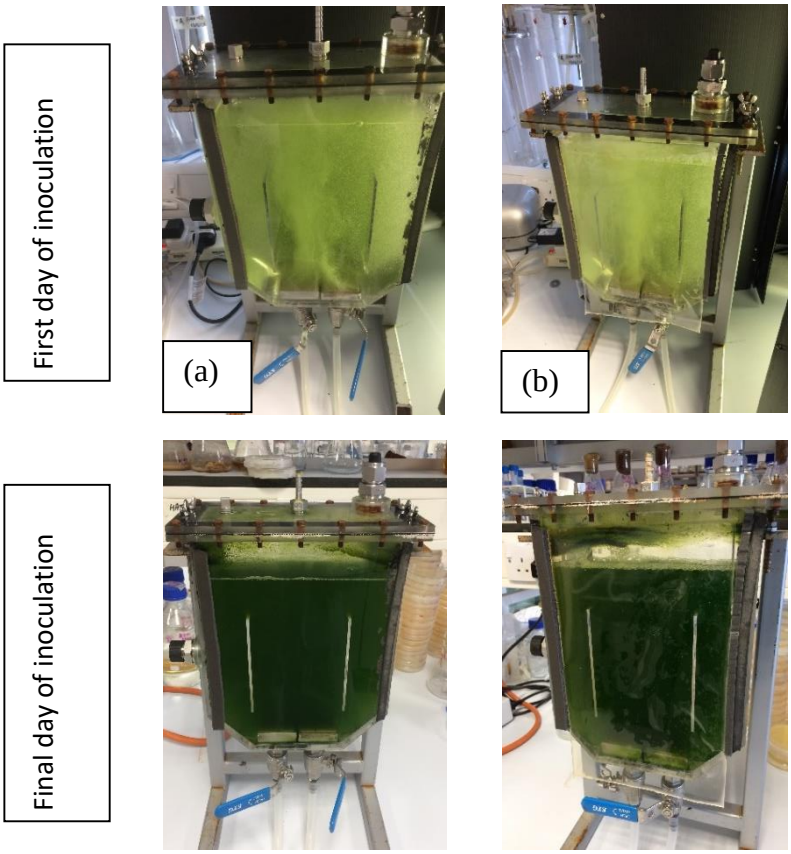

Figure 6. 8. Images of the experimental runs at the starting and final days: (a) Control, (b) UV to blue wavelength tuning.

Table 6. 3. Nile Red Fluorescence Intensity analysis and accumulated lipid amount of 10% CO_2 supplied *Dunaliella salina* samples grown in 1.5M NaCl medium**.** Each Nile Red analysis for each experimental run has 3 replicates of four stained and four unstained readings.

10 % CO_2 Stressed condition	**Day**	**Fluorescent Intensity**	**Concentration mg/ml**	**Neutral Lipid amount µg/ml**	**Percentage Lipid Amount CDW %**
Control	16	70.83	0.0021	0.0089	0.8950
Coumarin	16	76.92	0.0023	0.0097	0.9718

6.2.3.1. Neutral Lipid determination of 10% CO2 supplied *D. salina* growth using Nile Red

The neutral lipid analysis of control experiment and stress condition were done at the end of the experimental run, after 16 days in this case. The sample concentration used was 75% as determined in Section 5.2.3.1 and the optimum Nile Red dye concentration was 0.64 µg ml^{-1} as obtained in Section 5.3.2.2. As the Table 7.3 indicates the Nile Red analysis results, higher fluorescence intensity was obtained with Coumarin shifting material as 76.92 as expected since the Coumarin showed highest growth OD. Thus, the highest percentage lipid amount, 0.8950 % (0.0089 µg ml^{-1}), was obtained for the Coumarin experiment. In contrast to the previous 5% CO_2 supplied experiment results, this time the obtained lipid amount as well as the percentage lipid concentrations were very low. This might be because the acidity amount of the culture due to the CO_2 amount may increase the β-carotene amount instead of the neutral lipid.

6.2.3.2. Monitoring lipid droplets 10% CO2 supplied *D. salina* with fluorescence microscope images

The fluorescence microscope images, Figure 6.9, illustrate the neutral lipid accumulation visually in the 10% CO_2 supplied *D. salina* cells under control and Coumarin wavelength shifting material growth conditions. The images were captured as in Section 4.5 using fluorescence microscope like previous experiments; the greyscale images represent bright field images and the coloured images represent red and green fluorescence images. Although the images of control experiments are not very clear because of the smashed cell view due to the harsh addition of lamella or vigorous mixing during sample preparation, the lipid droplets inside the cells of all experimental run can be seen from the Figure 6.9. It is clear that there are a greater number of smaller sized neutral lipid droplets inside the cells of Coumarin shifting material experiment as more compared to the control runs which also supports the higher Nile Red and biomass accumulation of Coumarin in Section 6.2.3.1.

Nevertheless, both experimental set-up result in shining green droplets instead of desired yellowish droplets (neutral lipid) which is caused by the β-carotene accumulation inside the cell.

A)

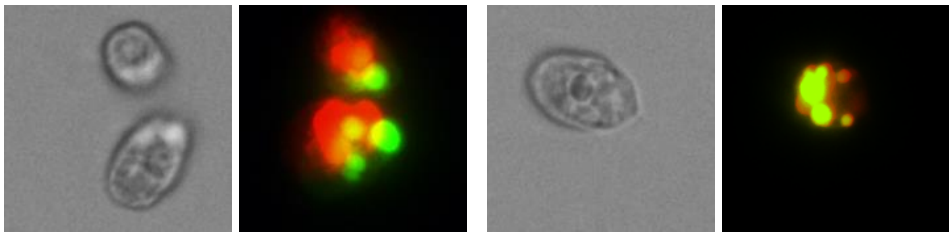

B)

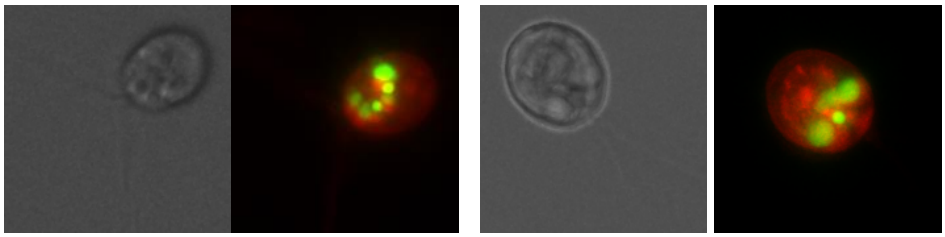

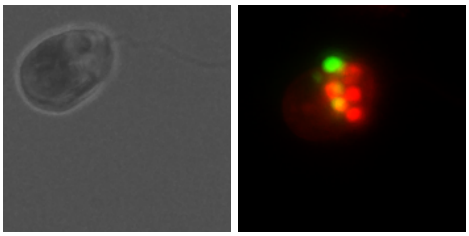

Figure 6. 9. Fluorescence microscopy images (both bright field and coloured) of 10 % CO_2 supplied *Dunaliella salina* CCAP 19/30 stained with Nile Red after growth under different light intensities using different wavelength shifting materials. **A)** *D. salina* cells grown under normal condition without using any wavelength shifting material. **B)** *D. salina* cells grown under stress condition with more blue light using Coumarin shifting material.

6.2.4. *D. salina* growth in 3L photobioreactor with 0.5% CO_2 supply

The final experimental set for the CO_2 dosing to the system, 0.5% CO_2 balanced with air was used. As for 10% CO_2 supply experiments, only control and Coumarin wavelength shifting material applied experiments were performed as explained in Section 6.2.1. For the same reason as explained in Section 6.2.3, 2G and Coumarin+2G experiments were not done. So, Figure 6.10 gives the result of Control and Coumarin wavelength shifting material growth curves and the maximum OD values are recorded as 0.7095 and 0.931 at 595nm for control and UV to blue wavelength tuning film, respectively. These results again prove the growth increment when wavelength tuning material are used and it means that in comparison to control, there is approximately a 24% increase in the final OD for UV to blue wavelength tuning much the same as for 10% CO_2 experiments. The images in Figure 6.11 support the evidence from the growth curve by showing the high density in the algal culture for UV to blue wavelength tuning as *D. salina* and biomass attachment on the reactor wall above the culture. Also shown in Figure 6.11(b) is the blue light emitted from the Coumarin wavelength shifting material demonstrating it is emitting blue light efficiently after absorbing the UV light. Furthermore, each experimental run continued for 15 days until reaching the stationary phase which is also about half the time period of the air supplied experiments but similar to previous CO_2 supplied *D. salina* cultures.

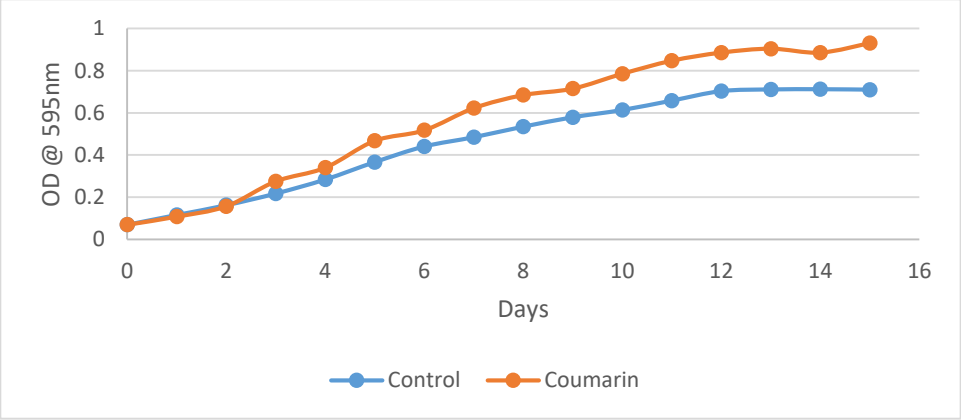

Figure 6. 10. Growth Curves of 0.5% CO_2 supplied control and coated reactors. Control is done without wavelength shifting materials and only with white light; UV to blue wavelength tuning is done with only Coumarin 1 material and both light on.

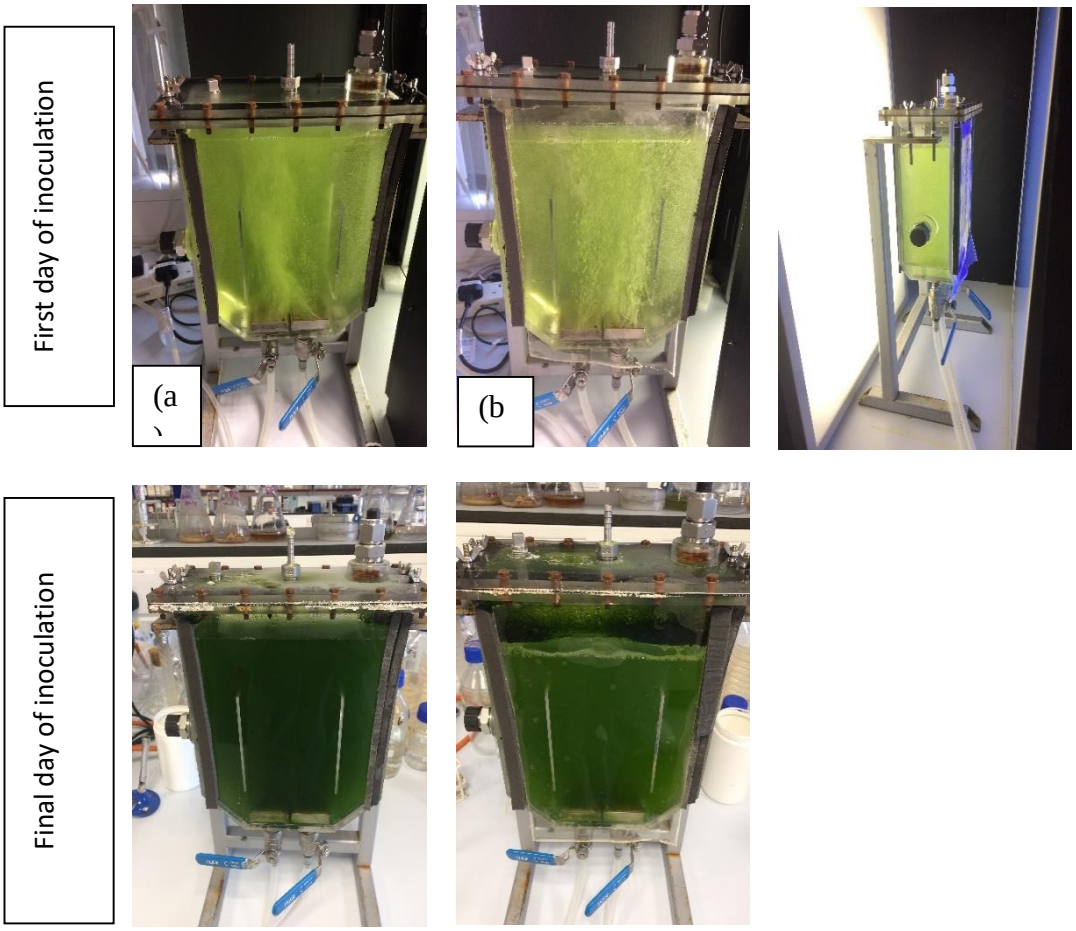

Figure 6. 11. Images of the experimental runs at the starting and final days: (a) Control, (b) UV to blue wavelength tuning,

6.2.4.1. Neutral Lipid determination of 0.5% CO_2 supplied *D. salina* growth using Nile Red

The neutral lipid analysis of the control experiment and the UV to blue light stress condition were performed at the end of the experimental run, after 15 days. The sample concentration was 75% as determined in Section 5.2.3.1 and the optimum Nile Red dye concentration was 0.64 µg ml^{-1} as obtained in Section 5.3.2.2. Table 6.4 displays the Nile Red analysis results; higher fluorescence intensity was achieved with Coumarin shifting material as 58.17 as expected since the Coumarin showed higher growth OD. Thus, the highest percentage lipid amount, 0.7349 % (0.0073 µg ml^{-1}), was obtained for the Coumarin experiment. Similar to the previous 10% CO_2 supplied

experiment results, obtained lipid amount as well as the percentage lipid concentrations were very low, too. This might be because the supplied CO_2 amount is not enough to produce neutral lipid.

Table 6. 4. Nile Red Fluorescence Intensity analysis and accumulated lipid amount of 10% CO_2 supplied *Dunaliella salina* samples grown in 1.5M NaCl medium**.** Each Nile Red analysis for each experimental run has 3 replicates of four stained and four unstained readings.

0.5 % CO_2 Stressed condition	**Day**	**Fluorescent Intensity**	**Concentration mg/ml**	**Neutral Lipid amount µg/ml**	**Percentage Lipid Amount CDW %**
Control	15	26.08	0.0008	0.0033	0.3296
Coumarin	15	58.17	0.0017	0.0073	0.7349

6.2.4.2. Monitoring lipid droplets 0.5% CO_2 supplied *D. salina* with fluorescence microscope images

The fluorescence microscope images, Figure 6.12, gives the visual neutral lipid accumulation in the 0.5% CO_2 supplied *D. salina* cells under control and Coumarin wavelength shifting material growth conditions. The images were captured as in Section 4.5 using fluorescence microscope like previous experiments; the greyscale image represent bright field images and the coloured image represent red and green fluorescence images. The yellowish lipid droplets inside cells of all experimental run can be seen in Figure 6.12, though there are some green lipid droplets in both control and Coumarin samples owing to the accumulated β-carotene. It is clear that the neutral lipid droplets are more numerous and smaller sized inside the cells of Coumarin shifting material experiment compared to control runs which also supports the higher Nile Red and biomass accumulation in the Coumarin experiment.

A)

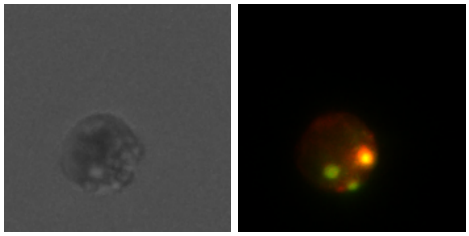

B)

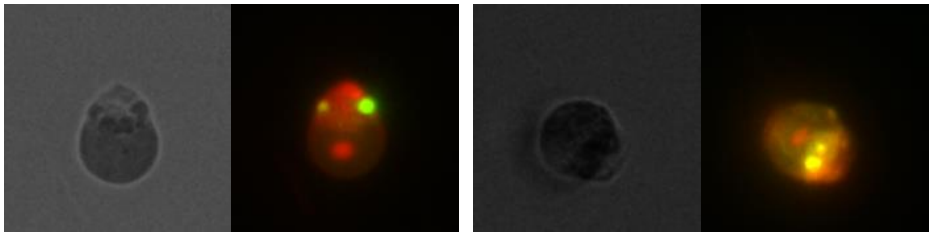

Figure 6. 12. Fluorescence microscopy images (both bright field and coloured) of 0.5 % CO_2 supplied *Dunaliella salina* CCAP 19/30 stained with Nile Red after growth under different light intensities using different wavelength shifting materials. **A)** *D. salina* cells grown under normal condition without using any wavelength shifting material. **B)** *D. salina* cells grown under stress condition with more blue light using Coumarin shifting material.

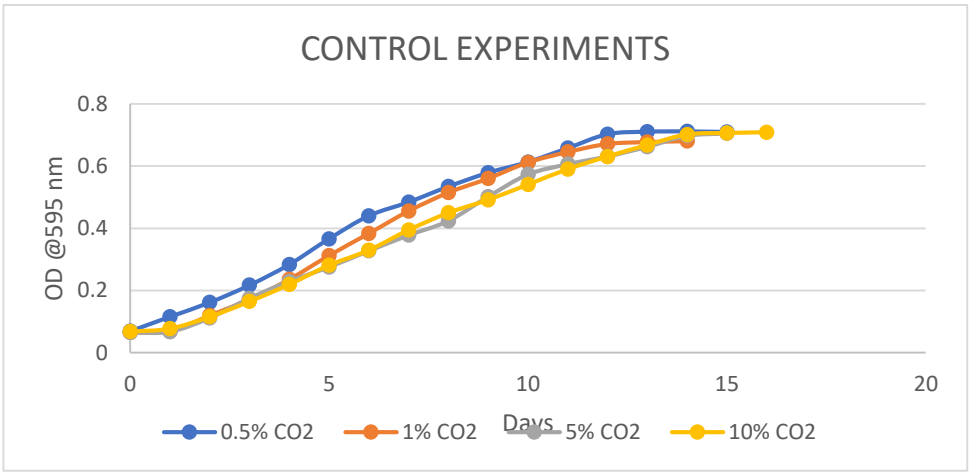

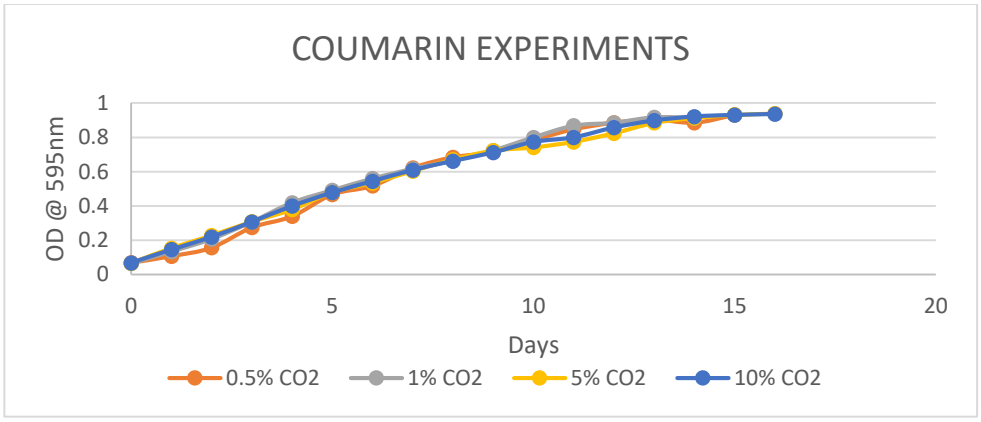

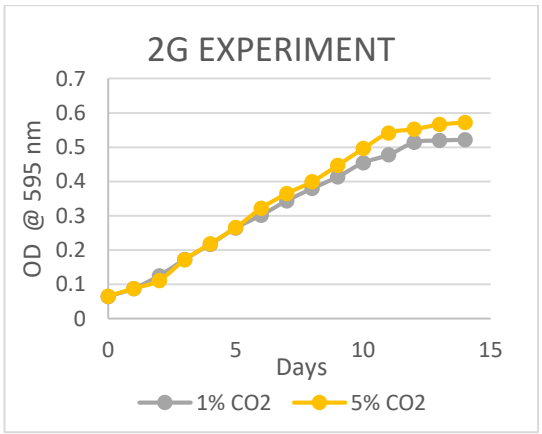

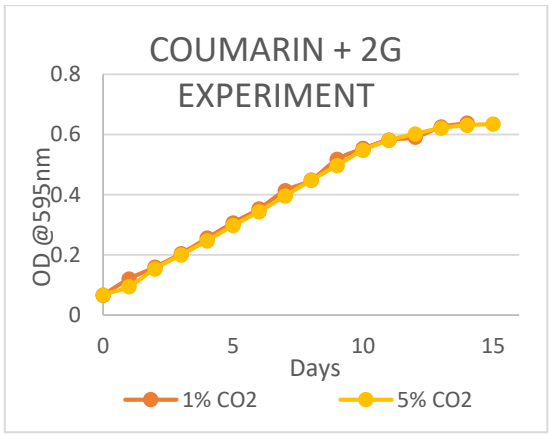

Figure 6. 13. *Dunaliella salina* growth with diverse percentages of CO_2 supply (0.5%, 1%, 5% and 10%). Control is done without wavelength shifting materials and only with white light; UV to blue wavelength tuning is done with only Coumarin 1 material and both lights on; green to red wavelength tuning is done with only Bestoil Orange 2G material and only white light on; and for the final one both Coumarin 1 and Bestoil Orange 2G materials were used with both light on.

6.3. Discussion

Since high CO_2 uptake property of *D. salina* was stated in the literature (Ying et al., 2014, Zimmerman et al., 2011), it was decided to examine different CO_2 concentrations for the *D. salina* growth over fairly short time periods in order to be used as an alternative way of decreasing CO_2 emissions released by factory chimneys. Hence, the aim of the current thesis is improving microalgae, *D. salina*, growth by coating the airlift photobioreactor (ALB) with wavelength shifting materials with an optimum CO_2 supply. For this reason, wavelength shifting materials were prepared with fluorophores Coumarin and Bestoil Orange 2G and applied on the wall of photobioreactor in order to shift the light (see Chapter 4, materials and methods) and the different CO_2 concentrations were dosed (air (0.03% CO_2) 0.5%, 1%, 5% and 10%) to the system.

As proposed in thesis goal, sunlight will be used as a light source for photosynthesis, so the *D. salina* will be exposed to both the UV light and PAR region simultaneously. Exposure to the ultraviolet radiation causes metabolic problems for organisms since the UV light is absorbed by the nucleic acids and proteins (White and Jahnke, 2002, Holzinger and Lütz, 2006). It is also responsible for photo inhibition by incorporating oxygen formation. Moreover, the green light is not absorbed by the algae absorption pigments. Therefore, it is beneficial to convert these harmful and unused wavelengths to useful ones. The effect of light intensities on algae growth has been studied by some scientists (Blair et al., 2014, Wondraczek et al., 2013, Delavari Amrei et al., 2014) (see the table in Literature Review, Section 1.3.1 for further information). Moreover, the effect of increased blue and red light on *D. salina* growth was examined and the results were given in previous Chapter.

Under saturated light intensities, the rate of CO_2 supply is vital for photosynthesis of microalgae because CO_2 is major source for the carboxylation of RuBP. Some studies were done by Mohsenpour and Willoughby (2016)and Ying et al. (2014) to show the effect of CO_2 concentration supplied to the system. They agreed that excess CO_2 amount (amount depending on the Algae species) has a fatal effect on the microalgae

growth. In this chapter, results are presented for the effects of the 0.5%, 1%, 5% and 10% CO_2 supply to the *D. salina* growth system inside the 3L photobioreactor.

The experimental results of each CO_2 concentration were given in the previous sections; on the other hand, Figure 7.13 gives the comparison of effect of each wavelength tuning materials at different CO_2 dosing. As it is seen from the graphs, all the stress conditions and the control experiments has the similar pattern for OD growth curve. Furthermore, the growth period was decreased to half the time compared to the air supplied *D. salina* growth given in the previous chapter. Also, the high algal density cultures of the Coumarin material (UV to blue wavelength shifting) were shown visually by giving the initial and the final photos of the reactor. As reported in the literature, in many microalgae species blue light serves for the enzyme activation during photosynthesis and regulates the gene transcription; thus the algae growth is enhanced (Matthijs et al., 1996, Mohsenpour and Willoughby, 2016), our experiments also give similar results to this literature explanation.

In order to further investigate the higher algae growth under blue light, the Nile Red analysis and the screening of the *Dunaliella* cells under fluorescent microscope were carried out. According to the findings reported in the previous sections, it is concluded that these analyses also support the growth experiments. Nile Red analysis shows the highest fluorescence intensity was obtained with Coumarin shifting material except from 1% CO_2 dosing. Also, the accumulated lipid amounts in the cells are shown in Figure 6.14. These summarized results of the lipid amounts indicate that Coumarin wavelength shifting materials best result for all CO_2 dosing except 1% CO_2 supplied one. Besides this, the fluorescent light microscope images also indicate that the lipid droplets inside the cells grown in Coumarin shifting material applied reactors are greater in number and smaller in size compared to the other stressed conditions and the control reactors. (Figure 6.3, 6.6, 6.9 and 6.12). And also, the fluorescence microscope images illustrated clear orange globules, the green lipid droplets were again detected indicating the *D. salina* stores secondary carotenoids (mainly β-carotene) in lipid bodies inside the chloroplast while cultivated under stress conditions. The red fluorescence emitted from chlorophyll vanishes because the thylakoid membranes are destroyed under stress condition. The cells, simultaneously, start to

generate carotenoids and green fluorescence appears at that time (Kleinegris et al., 2010, Kleinegris et al., 2011).

All in all, coating the reactor with wavelength shifting materials and dosing the CO_2 to the growth system increases the algal growth as well as decreases the experiment run time.

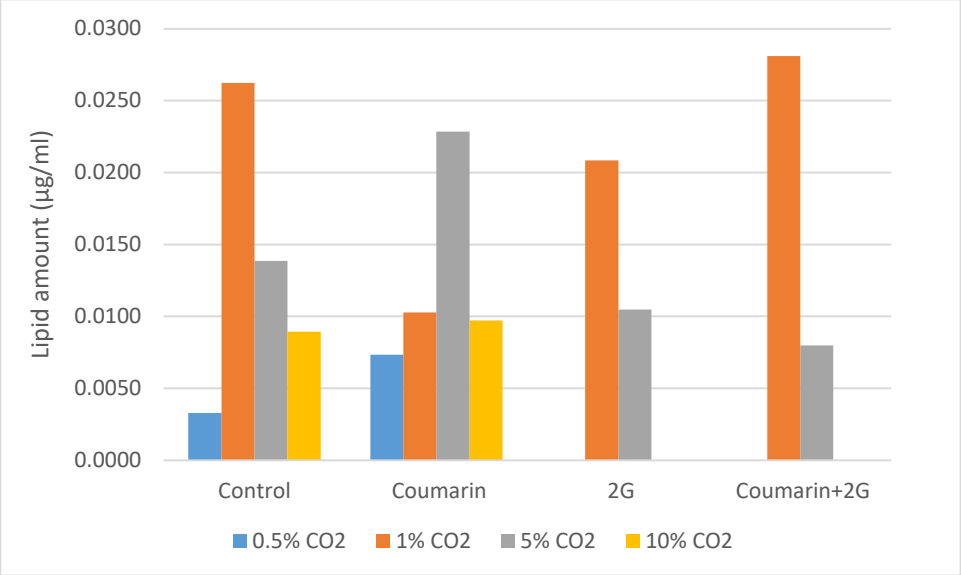

Figure 6. 14. Accumulated lipid amount of different CO_2 supplied (0.5%, 1%, 5% and 10%) *Dunaliella salina* samples grown in 1.5M NaCl medium depending on the correlation with Nile Red Fluorescence Intensity**.** Each analysis for each experiment has 3 replicates of four stained and four unstained readings.

CHAPTER 7: CONCLUSIONS AND FUTURE WORK

7.1. CONCLUSION

Each year, more than 80% of global energy is generated from fossil fuels; thus the CO_2 production increases a lot and is now higher than 24 gigatons annually (Hill et al., 2006, Melis, 2009). Therefore, it contributes to climate change, global warming and damages the world in which we live. Using a variety of renewable energy technologies is seen as the solution to this crisis, and biomass is one such technology. So far, researchers have mainly focused on producing fuel from first generation sources such as energy crops; however, the limitations of food storage for humanity and the lack of arable land availability makes it unsustainable and non-ecological. Consequently, new sources should be researched to protect the world, and microalgae is a very good option not only to produce biofuels as a third generation feedstock but also to reduce the CO_2 emissions via photosynthesis. As a result of algal growth, valuable biochemicals (e.g.hydrocarbons and lipids) are generated which can be used as food sources (for human, aquaculture and agriculture), biofuels, pharmaceuticals and for cosmetic applications. Algae were first used for commercial purposes in the 1940's as a source of food and biochemicals (Borowitzka et al., 1984).

Microalgae are photoautotrophic organisms which require light as an energy source to grow. This light is absorbed by the antenna complex which is made up chlorophyll and carotenoids pigments in green algae (see Literature review section 2.2.1 for more information) and then converted into chemical energy (ATP and NADPH) via electron transfer from reaction centres. Normally, green microalgae (e.g. *D. salina*) will absorb light in the ranges of 450– 475 nm (blue light) and 630–675 nm (red light) (Gaytán-Luna et al., 2016). If the absorbed light is too weak, photosynthesis cannot work efficiently and etiolation (loss of pigments) may occur. On the other hand, if the light is too intense, then oxygen radicals are generated which causes photo inhibition. Both possibilities significantly limit primary biomass productivity, see Section 2.2.2 for more information about photosynthesis limitation factors (Darko et al., 2014, Chen and Blankenship, 2011, Nakajima and Ueda, 1997). By using fluorophores in the *D. salina* growth with suitable excitation/emission properties, the light conditions for microalgae can be adjusted to match the absorption spectra of chlorophyll, in this way

microalgae can increase their photosynthetic activity (Xia et al., 2013, Mohsenpour et al., 2012).

As a consequence of the above mentioned criteria, the aim of this thesis was to develop an improved PBR design by coating it with wavelength shifting materials and by pumping in an optimum amount of CO_2 gas to the system to enhance the *D. salina* growth and biomass production (shorter time and denser culture). Thus, optimized wavelength shifting materials, made from organic dyes (Coumarin 1 for UV light to blue light conversion and Bestoil Orange 2G for green light to red light conversion) and PDMS (polymeric matrix) were tested. Moreover, bubbling from the bottom of the reactor was used to increase mass transfer and reduce O_2 accumulation and increase the mixing of growth medium.

In order to achieve our goals, the first step in the project was optimizing the wavelength shifting materials using various combinations of fluorophores, solvent and polymer matrixes. Chapter 2, Fabrication of wavelength shifting materials, explains how wavelength shifting materials used were produced and presents the absorption and emission spectra of the materials produced. The solvent/fluorophore/ polymer mixture graphs showed that the THF is the best solvent to dissolve both fluorophores and the polymers. From the spectrum patterns of the materials, it is obvious that the Coumarin is the best UV to blue light shifter which demonstrates the best overlap of the emission with the absorption spectrum of the *D. salina* chlorophyll pigments. Both Coumarin films produced either by spin coating or PDMS curing gave a similar spectrum, but PDMS curing was preferable because of the ease application to the 3L photobioreactor. However, Bestoil Orange 2G showed problems of light scattering and non-uniform material production. Figure 2.17 in Section 2.3.1.2 demonstrates that the material produced forms at different concentration. A uniform and clear material can be obtained with lower concentration but the absorption is low in that case. All in all, optimized wavelength shifting materials based on the absorption and emission spectra were used for the further *D. salina* growth experiment. Although, it is not shown inside the chapters, multi layered material production using sol-gel method was also tried to form better shifting material; however, we faced some problems during the experiments which needs further investigations. Producing second layer with spin

coating was successful but the next layers were come off when the third and fourth layer production was tried.

The next step, which is explained in Chapter 3, was the designing the small scale and 3L photobioreactor. The reactor designed by Krys Bangert (Bangert, 2013)was used as the basis of the 3L photobioreactor and other modification depending on the aim of *D. salina* growth for this thesis. And the scheme of the experimental set-up was shown in Figure 3.7. Considering the dye toxicity and the solubility of the material and the reflection problem, wavelength shifting materials were coated outside the reactors. As it is hypothesized that the supplemented blue light is activating cryptochrome (enzyme activation), a blue-light photoreceptor that mediates reduction of hypocotyl length in seedlings and it is well known for opening the stomata in plants; and also the red light enhancing the efficiency of the photosynthesis reaction centres (Matthijs et al., 1996). It would be beneficial to use both wavelength shifting materials at the same time for the *D. salina* growth (Darko et al., 2014, Wang et al., 2010). Initially, 50ml cell culture flasks were used and then scaled up to the designed 3L photobioreactor. The initial studies with small cell culture flasks (Chapter 5, Section 5.2.1) showed that the Coumarin shifting material which tunes the UV light to the blue light has the maximum OD growth value as 0.934 at 595nm which was a 17.6% growth increment for growth with a UV to blue wavelength tuning film compared to the control experiment (no wavelength shifting material). On the other hand, the importance of better medium mixing to achieve high cell concentration, avoiding cell attachment to the walls inside the PBR has been indicated in many articles. Good mixing can keep the cells in suspension, help nutrient distribution, decrease the shading and improve gaseous exchange by increasing area to volume ratio to let more light exposure to more algae cells (Al-Mashhadani et al., 2015, Lee and Palsson, 1994). Therefore, initial studies with fine bubbles were also carried out in the small cell culture flasks and it was seen that the bubbling doubled the algal biomass produced.

Furthermore, in Chapter 5, large scale *D. salina* cultures in the 3L photobioreactor with air supply were investigated. According to the results in Sections 5.2.2., 5.2.3 and 5.2.4, tests with the Coumarin wavelength shifting materials produced the highest biomass with a final OD_{595nm} value of 1.01 (26 days) among all other growth

conditions. Applied Nile Red analysis and the screening of the *Dunaliella* cells under fluorescent microscope showed that the highest fluorescence intensity was obtained with Coumarin shifting material (2486.58) and this correlated with the high biomass of the cultures grown with a Coumarin film. The fluorescence value is about three fold higher than the nearest high growth, control experiment. The fluorescent light microscope images also supported the result by showing that the lipid droplets inside cells grown in the reactor with Coumarin shifting material applied were more than the others (Figure 5.16). Moreover, the correlation of dry weight with the Nile Red analysis, showed that the reactor with Coumarin shifting material applied produced the most neutral lipid at 0.31 µg ml^{-1} which is about 31.42% lipid.

Additionally, both studies set up in Chapter 5 illustrated the harmful effect of UV light during the control experiment without using any wavelength shifting materials or UV filter glass. However, it is also shown that the algae can grow again after a few days lag phase once the UV light was switched off. These findings agreed with the reports saying that UV radiation has a detrimental effect on the living cells by affecting the DNA (Mohsenpour et al., 2012, Holzinger and Lütz, 2006, White and Jahnke, 2002). Also, it was noted that the extended UV light exposure changes the colour and function of the Coumarin wavelength shifting materials. The shifting material faded after about 6 months of use and needed to be renewed. The fading of the dyes when exposed to the sunlight were reported by Hovel et al. (1979).

The final step of the work described in this thesis was investigating different dosages of CO_2 (air i.e.0.03% CO_2, 0.5%, 1%, 5% and 10%) bubbled into to the growth system, Chapter 6. The results of these experiments were given in Figure 6.13 which compare the effect of each wavelength tuning materials at different CO_2 doses. Figure 6.13 illustrated that all stressed conditions and the control experiments has a similar pattern for OD growth curve at different concentrations. However, Coumarin material indicates the highest OD (biomass) in each dose as 0.931, 0.914, 0.939 and 0.936 at 595nm for 0.5%, 1%, 5% and 10%, respectively. Furthermore, the growth period was decreased by half compared to the air supplied *D. salina* cultures described in Chapter 5. Also, the high algal density growth of the Coumarin material cultures (UV to blue wavelength shifting) were shown visually by presenting the initial and final

photographs of the reactor. The highest Nile Red fluorescence intensity was consistently obtained with Coumarin shifting material cells except for the 1% CO_2 dosed culture. Apart from this, the summarized results of the lipid amounts (Figure 6.14) demonstrated that Coumarin wavelength shifting materials produced the best result over all other CO_2 doses. In addition, the fluorescent light microscope images showed the lipid droplets inside the cells from the reactor with the Coumarin shifting material applied are more numerous and smaller sized compared to the other stressed conditions and the control reactor.

All in all, it was observed that the Coumarin wavelength tuning material was showed the best performance in terms of OD and the high density achieved in the *D. salina* cultures can be seen from the before and after photographs of the reactors for each experiment. The fluorescence light microscope showed that the *D. salina* produces β-carotene under stressed conditions and this is seen as green lipid dots inside the cells (Kleinegris et al., 2010, Kleinegris et al., 2011, Chen et al., 2009). Increasing the CO_2 amount to 10% decreases the biomass and increases the β-carotene amount.

7.2. Future Work

As a result of the literature review presented and the experimental work described in this thesis, the following suggestions for future work are made in order to achieve even higher biomass production in shorter time than is achieved by conventional growth systems:

1. Finding a more suitable red dye and optimizing it with solvent and polymer in order to obtain a better green to red wavelength shifting material.

For the current thesis, Bestoil Red 5B and Bestoil Orange 2G were used to produce green to red wavelength material; however, these dyes did not work as well as expected. They did not dissolve very well inside the PDMS resulting in light scattering.

Therefore, it is important to try other solvents which may be more suitable to mix the dye and PDMS and cure to get an efficient, uniform green to red shifting material film. On the other hand, other red wavelength emitting dyes (e.g. Rhodamine derivatives as listed in Appendix xx) can be tried to obtain better wavelength shifting materials that emit in the red light region that overlaps with the *D. salina* absorption wavelength band.

2. Pilot scale photobioreactor design and optimization

Application of the wavelength shifting coating on a larger scale and different shaped bioreactors with dye/polymer mixtures is a challenging process. It may not be possible to produce a smooth, uniform and clean dye/PDMS materials for large reactors, so other coating methods (spraying or roll-to-roll) should be tried and their advantages and disadvantaged should be investigated completely. Moreover, the dimensions and material of the pilot scale PBR should be studied with simulation programmes and optimization should be done for efficient light penetration and elimination of reflection and scattering. Consequently, mathematical modelling of the reactor using modelling software should be done for pilot scale *D. salina* production with PBR.

3. Trying different algae species to obtain the highest efficiency and better algal biomass.

Currently *D. salina* CCAP 19/30 strain is used for this project but other algal strains should be examined depending on the desired algal biomass and application area. For instance, *Tetraselmis suecica* is one of the species of microalgae that is most extensively used in aquaculture as feed for larvae and postlarvae of shellfish, penaeid shrimp larvae and abalone larvae (Michels et al., 2014a, Michels et al., 2014b) and is considered to be an optimal source of long-chain PUFAs, and especially of eicosapentaenoic acid (EPA). Furthermore, most of the previous work on Tetraselmis *suecica* agrees on the predominance of the fatty acids 16:0 and of 18:1 in SATs and MUFAs, respectively, whereas the most abundant fatty acid in the PUFAs is 18:3ω-3 where the lipid content is determined based on the cultivation conditions. As indicated by Guzman et al. (2010), that enhancing the photon flux density causes an increase in content in PUFAs in various species of microalgae.

4. Algal biomass harvesting studies

Biomass harvesting studies have not been applied yet. Harvesting methods should be researched and then applied to the growth algal strains for lipid extractions.

5. Metabolic engineering

In order to harvest more light for the algae growth at the desired wavelength range, metabolic engineering should be considered. In all photosynthetic systems, however, over-absorption of bright sunlight and wasteful dissipation of most of it via non-photochemical quenching is the primary and most important source of the low efficiency and productivity. Therefore, it is important to improve regeneration of RuBP for CO_2 fixation (Melis, 2009).

6. Optimising microbubbles and CO_2 absorption

Microbubble production has been attracting the attention of researchers in chemical and biological areas due to their fundamental characteristics; which aid efficient mass, heat and momentum transport (Zimmerman et al., 2008, Al-Mashhadani et al., 2015). Microbubbles can be generated via three alternative ways. First, released air into the system is dissolved in liquid solution, and then it is evacuated towards a nozzle system, then nano-bubbles are produced. After that, nano-sized bubbles are dissolved in the supersaturated liquid in order to shift to micron size. Second, ultrasonic power is used to commence cavitation. Third, a low pressured air stream is broken with fluidic oscillation, mechanical vibration or flow focusing devices (Zimmerman et al., 2008). The fluidic oscillator (see Figure 8.1), improved by Prof. Zimmerman (2008), generates a pulse gas stream useful for generating uniform monodispersed microbubbles using the Coanda effect (an inclination of a fluid jet to be caught by a closer surface). It is easy and simple to build up since there are no moving parts and it is economic (no electrical supply needed) and robust. A feedback loop, the length of which affects the output stream frequency is used in the design. Incorporating microbubble technology inside the airlift photobioreactor will increase the stirring

effect and mass transfer compared to the conventional large bubbles because of high internal surface area.

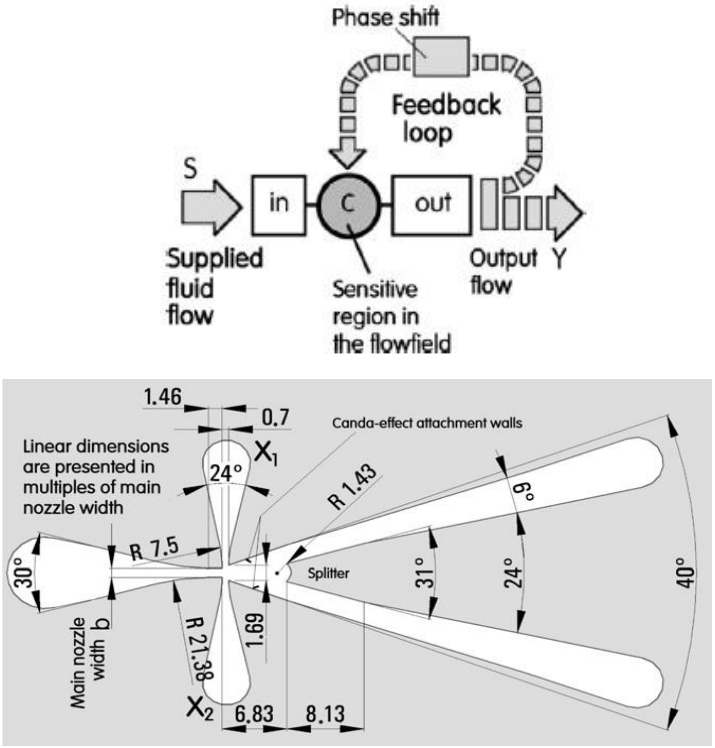

Figure 7. 1. Working principle and geometric shape of oscillator developed by Prof. Zimmerman

Zimmerman et al. (2011) embedded microbubble generation into a 250L photobioreactor and they obtained 30% higher algal growth compared to a non-aerated one. Ying et al. (2013) compared three systems (ALB with microbubble, ALB without microbubble and non-aerated flask) to see the effect of microbubbles and obtained 20-40% chlorophyll content enhancement in an ALB with microbubbles due to high mass transfer.

Microbubble production was tried as a final step for the work described in this thesis; however, the sparger inside the 3L reactor was not appropriate to produce microbubble. Because of the time limit of the PhD programme, further experiments could not be carried out. Thus, microbubble production with new spargers with diverse pore sizes is recommended as future work.

REFERENCES

ACIÉN FERNÁNDEZ, F. G., FERNÁNDEZ SEVILLA, J. M. & MOLINA GRIMA, E. 2013. Photobioreactors for the production of microalgae. *Reviews in Environmental Science and Bio/Technology,* 12**,** 131-151.

AL-MASHHADANI, M. K. H., WILKINSON, S. J. & ZIMMERMAN, W. B. 2015. Airlift bioreactor for biological applications with microbubble mediated transport processes. *Chemical Engineering Science,* 137**,** 243-253.

ALONZO, F. & MAYZAUD, P. 1999. Spectrofluorometric quantification of neutral and polar lipids in zooplankton using Nile red. *Marine Chemistry,* 67**,** 289-301.

ASTM, G.-. 2012. Standard Tables for Reference Solar Spectral Irradiances: Direct Normal and Hemispherical on 37° Tilted Surface. West Conshohocken, PA: ASTM International.

BANGERT, K. 2013. *Photo-bioreactor Modelling and Development of Methods for the Optimisation of Micro-algal Biodiesel Production.* PhD, University of Sheffield.

BARBER, J. 2009. Photosynthetic energy conversion: natural and artificial. *Chemical Society Reviews,* 38**,** 185-196.

BATAN, L., QUINN, J., WILLSON, B. & BRADLEY, T. 2010. Net Energy and Greenhouse Gas Emission Evaluation of Biodiesel Derived from Microalgae. *Environmental Science & Technology,* 44**,** 7975-7980.

BEN-AMOTZ, A. & AVRON, M. 1992. *Dunaliella: Physiology, Biochemistry, and Biotechnology*, Taylor & Francis.

BEN-AMOTZ, A., POLLE, J. E. W. & RAO, D. V. S. 2009. *The Alga Dunaliella*, Taylor & Francis.

BERTOZZINI, E., GALLUZZI, L., PENNA, A. & MAGNANI, M. 2011. Application of the standard addition method for the absolute quantification of neutral lipids in microalgae using Nile red. *Journal of Microbiological Methods,* 87**,** 17-23.

BLAIR, M. F., KOKABIAN, B. & GUDE, V. G. 2014. Light and growth medium effect on Chlorella vulgaris biomass production. *Journal of Environmental Chemical Engineering,* 2**,** 665-674.

BLANKENSHIP, R. E. 2002. *Molecular Mechanisms of Photosynthesis,* Oxford, Blackwell Science.

BLIGH, E. G. & DYER, W. J. 1959. A RAPID METHOD OF TOTAL LIPID EXTRACTION AND PURIFICATION. *Canadian Journal of Biochemistry and Physiology,* 37**,** 911-917.

BOROWITZKA, L. J., BOROWITZKA, M. A. & MOULTON, T. P. 1984. The mass culture of Dunaliella salina for fine chemicals: From laboratory to pilot plant. *Hydrobiologia,* 116-117**,** 115-121.

BOROWITZKA, M. A. 2013. High-value products from microalgae-their development and commercialisation. *Journal of Applied Phycology,* 25**,** 743-756.

BORSETTO, M., CARCANO, G. & CERIANI, M. 1996. Spin Coating Study for Thick Layers with High Viscosity Polyimide. *Microelectronics International: An International Journal,* 13**,** 30-32.

BREUER, G., EVERS, W. A., DE VREE, J. H., KLEINEGRIS, D. M., MARTENS, D. E., WIJFFELS, R. H., ET AL. 2013. Analysis of Fatty Acid Content and Composition in Microalgae. *J. Vis. Exp.,* 80.

BURRIS, J. E. 1977. *Photosynthesis, photorespiration, and dark respiration in eight species of algae*, Marine Biology.

CHAPMAN, R. L. 2013. Algae: The world's most important "plants"-an introduction. *Mitigation and Adaptation Strategies for Global Change,* 18**,** 5-12.

CHEN, M. & BLANKENSHIP, R. E. 2011. Expanding the solar spectrum used by photosynthesis. *Trends in Plant Science,* 16**,** 427-431.

CHEN, W., ZHANG, C., SONG, L., SOMMERFELD, M. & HU, Q. 2009. A high throughput Nile red method for quantitative measurement of neutral lipids in microalgae. *Journal of Microbiological Methods,* 77**,** 41-47.

CHIN-HANG, S., CHIEH-CHUNG, T., WEI-HSIU, L., KUN-YAN, C. & HAO-CHEN, H. 2012. Effects of light quality on the accumulation of oil in a mixed culture of Chlorella sp. and Saccharomyces cerevisiae. *Journal of Chemical Technology & Biotechnology,* 87**,** 601-607.

CHISTI, Y. 2007. Biodiesel from microalgae. *Biotechnology Advances,* 25**,** 294-306.

CHISTI, Y. 2008. Biodiesel from microalgae beats bioethanol. *Trends in Biotechnology,* 26**,** 126-131.

CHISTI, Y. 2010a. Dunaliella — A commercial microalga. *Biotechnology Advances,* 28**,** 197.

CHISTI, Y. 2010b. Fuels from microalgae. *Biofuels,* 1**,** 233-235.

CHISTI, Y. 2013. Constraints to commercialization of algal fuels. *Journal of Biotechnology,* 167**,** 201-214.

COOKSEY, K. E., GUCKERT, J. B., WILLIAMS, S. A. & CALLIS, P. R. 1987. Fluorometric determination of the neutral lipid content of microalgal cells using Nile Red. *Journal of Microbiological Methods,* 6**,** 333-345.

CRAGGS, R., SUTHERLAND, D. & CAMPBELL, H. 2012. Hectare-scale demonstration of high rate algal ponds for enhanced wastewater treatment and biofuel production. *Journal of Applied Phycology,* 24**,** 329-337.

DARKO, E., HEYDARIZADEH, P., SCHOEFS, B. & SABZALIAN, M. R. 2014. Photosynthesis under artificial light: the shift in primary and secondary metabolism. *Philosophical Transactions of the Royal Society B: Biological Sciences,* 369.

DELAVARI AMREI, H., RANJBAR, R., RASTEGAR, S., NASERNEJAD, B. & NEJADEBRAHIM, A. 2014. Using fluorescent material for enhancing microalgae growth rate in photobioreactors. *Journal of Applied Phycology*.

DUAN, Y. & SHI, F. 2014. Chapter 2 - Bioreactor design for algal growth as a sustainable energy source. *In:* SHI, F. (ed.) *Reactor and Process Design in Sustainable Energy Technology.* Amsterdam: Elsevier.

ELSEY, D., JAMESON, D., RALEIGH, B. & COONEY, M. J. 2007. Fluorescent measurement of microalgal neutral lipids. *Journal of Microbiological Methods,* 68**,** 639-642.

FAY, P. 1983. *The Blue Greens: Cyanophyta-cyanobacteria*.

FINK, M. 2009. Types of anti-reflective treatments and when to use them. *Feature.*

FOWLER, S. D. B., W J ; WARFEL, J ; GREENSPAN, P 1987. Use of nile red for the rapid in situ quantitation of lipids on thin-layer chromatograms. *Journal of lipid research,* 28**,** 1225-32.

FOX, M. 2010. *Optical properties od solids* Oxford, Oxford University Press.

GARDNER, R., PETERS, P., PEYTON, B. & COOKSEY, K. E. 2011. Medium pH and nitrate concentration effects on accumulation of triacylglycerol in two members of the chlorophyta. *Journal of Applied Phycology,* 23**,** 1005-1016.

GARDNER, R. D., COOKSEY, K. E., MUS, F., MACUR, R., MOLL, K., EUSTANCE, E., CARLSON, R. P., GERLACH, R., FIELDS, M. W. & PEYTON, B. M. 2012. Use of sodium bicarbonate to stimulate triacylglycerol accumulation in the chlorophyte Scenedesmus sp. and the diatom Phaeodactylum tricornutum. *Journal of Applied Phycology,* 24**,** 1311-1320.

GAYTÁN-LUNA, D. E., OCHOA-ALFARO, A. E., ROCHA-URIBE, A., PÉREZ-MARTÍNEZ, A. S., ALPUCHE-SOLÍS, Á. G. & SORIA-GUERRA, R. E. 2016. Effect of green and red light in lipid accumulation and transcriptional profile of genes implicated in lipid biosynthesis in Chlamydomonas reinhardtii. *Biotechnology Progress,* 32**,** 1404-1411.

GOETZ, V., LE BORGNE, F., PRUVOST, J., PLANTARD, G. & LEGRAND, J. 2011. A generic temperature model for solar photobioreactors. *Chemical Engineering Journal,* 175**,** 443-449.

GREENSPAN, P., MAYER, E. P. & FOWLER, S. D. 1985. Nile red: a selective fluorescent stain for intracellular lipid droplets. *The Journal of Cell Biology,* 100**,** 965-973.

GUSCHINA, I. A. & HARWOOD, J. L. 2006. Lipids and lipid metabolism in eukaryotic algae. *Progress in Lipid Research,* 45**,** 160-186.

GUZMÁN, H. M., DE LA JARA VALIDO, A., DUARTE, L. C. & PRESMANES, K. F. 2010. Estimate by means of flow cytometry of variation in composition of fatty acids from Tetraselmis suecica in response to culture conditions. *Aquaculture International,* 18**,** 189-199.

HAGFELDT, A., BOSCHLOO, G., SUN, L., KLOO, L. & PETTERSSON, H. 2010. Dye-sensitized solar cells. *Chemical Reviews,* 110**,** 6595-6663.

HARD, B. C. & GILMOUR, D. J. 1996. The uptake of organic compounds by Dunaliella parva CCAP 19/9. *European Journal of Phycology,* 31**,** 217-224.

HELENA, S., ZAINURI, M. & SUPRIJANTO, J. 2016. Microalgae Dunaliella salina (Teodoresco, 1905) Growth Using the LED Light (Light Limiting Dioda) and Different Media. *Aquatic Procedia,* 7**,** 226-230.

HERRMANN, H., HÄDER, D. P. & GHETTI, F. 1997. Inhibition of photosynthesis by solar radiation in Dunaliella salina: Relative efficiencies of UV-B, UV-A and PAR. *Plant, Cell and Environment,* 20**,** 359-365.

HILL, J., NELSON, E., TILMAN, D., POLASKY, S. & TIFFANY, D. 2006. Environmental, economic, and energetic costs and benefits of biodiesel and ethanol biofuels. *Proceedings of the National Academy of Sciences,* 103**,** 11206-11210.

HOLZINGER, A. & LÜTZ, C. 2006. Algae and UV irradiation: Effects on ultrastructure and related metabolic functions. *Micron,* 37**,** 190-207.

HOSKING, D. B. April, 2013. *Converting Unused Solar Radiation to Radiation Usable in Photosynthesis in Algal Bio-Reactors.* The University of Sheffield.

HOVEL, H. J., HODGSON, R. T. & WOODALL, J. M. 1979. The effect of fluorescent wavelength shifting on solar cell spectral response. *Solar Energy Materials,* 2**,** 19-29.

HU, X. & SCHULTEN, K. 1997. How nature harvests sunlight. *Physics Today,* 50**,** 28-34.

IZARD, J. & LIMBERGER, R. J. 2003. Rapid screening method for quantitation of bacterial cell lipids from whole cells. *Journal of Microbiological Methods,* 55**,** 411-418.

JIANG, Y., YOSHIDA, T. & QUIGG, A. 2012. Photosynthetic performance, lipid production and biomass composition in response to nitrogen limitation in marine microalgae. *Plant Physiology and Biochemistry,* 54**,** 70-77.

KARATAY, S. E. & DÖNMEZ, G. 2011. Microbial oil production from thermophile cyanobacteria for biodiesel production. *Applied Energy,* 88**,** 3632-3635.

KIRK, J. T. 1994. *Light and Photosynthesis in Aquatic Ecosystems [online]*, Cambridge University Press.

KITAJIMA, Y., EL-SHISHTAWY, R. A., UENO, Y., OTSUKA, S., MIYAKE, J. & MORIMOTO, M. 1998. Analysis of Compensation Point of Light Using Plane-Type Photosynthetic Bioreactor. *In:* ZABORSKY, O., BENEMANN, J., MATSUNAGA, T., MIYAKE, J. & SAN PIETRO, A. (eds.) *BioHydrogen.* Springer US.

KLAMPAFTIS, E., ROSS, D., MCINTOSH, K. R. & RICHARDS, B. S. 2009. Enhancing the performance of solar cells via luminescent down-shifting of the incident spectrum: A review. *Solar Energy Materials and Solar Cells,* 93**,** 1182-1194.

KLEINEGRIS, D. M. M., VAN ES, M. A., JANSSEN, M., BRANDENBURG, W. A. & WIJFFELS, R. H. 2010. Carotenoid fluorescence in Dunaliella salina. *Journal of Applied Phycology,* 22**,** 645-649.

KLEINEGRIS, D. M. M., VAN ES, M. A., JANSSEN, M., BRANDENBURG, W. A. & WIJFFELS, R. H. 2011. Phase toxicity of dodecane on the microalga Dunaliella salina. *Journal of Applied Phycology,* 23**,** 949-958.

KNUD-HANSEN, C. F. 1998. *Pond fertilization: ecological approach and practical applications.* PHd, Oregon State University.

KOC, K., TEPEHAN, F. Z. & TEPEHAN, G. G. 2005. Antireflecting coating from Ta2O5 and SiO2 multilayer films. *Journal of Materials Science,* 40**,** 1363-1366.

KOHEN, E., SANTUS, R. & HIRSCHBERG, R. G. 1995. Photobiologhy. London: Academia Press.

KOKU, H., EROĞLU, İ., GÜNDÜZ, U., YÜCEL, M. & TÜRKER, L. 2002. Aspects of the metabolism of hydrogen production by Rhodobacter sphaeroides. *International Journal of Hydrogen Energy,* 27**,** 1315-1329.

KRUSE, O., RUPPRECHT, J., MUSSGNUG, J. H., DISMUKES, G. C. & HANKAMER, B. 2005. Photosynthesis: a blueprint for solar energy capture and biohydrogen production technologies. *Photochemical & Photobiological Sciences,* 4**,** 957-970.

LAKOWICZ, J. 2006. *Principles of fluorescence spectroscopy,* New York, Springer.

LEE, C.-G. & PALSSON, B. Q. 1994. High-density algal photobioreactors using light-emitting diodes. *Biotechnol. Bioeng.,* 44**,** 1161-1167.

LEE, E., PRUVOST, J., HE, X., MUNIPALLI, R. & PILON, L. 2014. Design tool and guidelines for outdoor photobioreactors. *Chemical Engineering Science,* 106**,** 18-29.

LEE, J. N., PARK, C. & WHITESIDES, G. M. 2003. Solvent Compatibility of Poly(dimethylsiloxane)-Based Microfluidic Devices. *Analytical Chemistry,* 75**,** 6544-6554.

LEE, S. W., MAO, C., FLYNN, C. E. & BELCHER, A. M. 2002. Ordering of quantum dots, using genetically engineered viruses. *Science,* 296**,** 892-895.

LI, Y., GHASEMI NAGHDI, F., GARG, S., ADARME-VEGA, T. C., THURECHT, K. J., GHAFOR, W. A., TANNOCK, S. & SCHENK, P. M. 2014. A comparative study: the impact of different lipid extraction methods on current microalgal lipid research. *Microbial Cell Factories,* 13**,** 14.

MAO, X.-Y., MIYAKE, J. & KAWAMURA, S. 1986. Screening photosynthesis bacteria for hydrogen production from organic acids. *Journal of Fermentation Technology,* 64**,** 245-249.

MATA, T. M., MARTINS, A. A. & CAETANO, N. S. 2010. Microalgae for biodiesel production and other applications: A review. *Renewable and Sustainable Energy Reviews,* 14**,** 217-232.

MATTHIJS, H. C. P., BALKE, H., VAN HES, U. M., KROON, B. M. A., MUR, L. R. & BINOT, R. A. 1996. Application of light-emitting diodes in bioreactors: Flashing light effects and energy economy in algal culture (Chlorella pyrenoidosa). *Biotechnology and Bioengineering,* 50**,** 98-107.

MELIS, A. 2002. Green alga hydrogen production: progress, challenges and prospects. *International Journal of Hydrogen Energy,* 27**,** 1217-1228.

MELIS, A. 2009. Solar energy conversion efficiencies in photosynthesis: Minimizing the chlorophyll antennae to maximize efficiency. *Plant Science,* 177**,** 272-280.

MICHELS, M. H. A., SLEGERS, P. M., VERMUË, M. H. & WIJFFELS, R. H. 2014a. Effect of biomass concentration on the productivity of Tetraselmis suecica in a pilot-scale tubular photobioreactor using natural sunlight. *Algal Research,* 4**,** 12-18.

MICHELS, M. H. A., VASKOSKA, M., VERMUË, M. H. & WIJFFELS, R. H. 2014b. Growth of Tetraselmis suecica in a tubular photobioreactor on wastewater from a fish farm. *Water Research,* 65**,** 290-296.

MIYAKE, J. & KAWAMURA, S. 1987. Efficiency of light energy conversion to hydrogen by the photosynthetic bacterium Rhodobacter sphaeroides. *International Journal of Hydrogen Energy,* 12**,** 147-149.

MOHSENPOUR, S. F., RICHARDS, B. & WILLOUGHBY, N. 2012. Spectral conversion of light for enhanced microalgae growth rates and photosynthetic pigment production. *Bioresource Technology,* 125**,** 75-81.

MOHSENPOUR, S. F. & WILLOUGHBY, N. 2013. Luminescent photobioreactor design for improved algal growth and photosynthetic pigment production through spectral conversion of light. *Bioresource Technology,* 142**,** 147-153.

MOHSENPOUR, S. F. & WILLOUGHBY, N. 2016. Effect of CO2 aeration on cultivation of microalgae in luminescent photobioreactors. *Biomass and Bioenergy,* 85**,** 168-177.

MOLINA, E., FERNÁNDEZ, J., ACIÉN, F. G. & CHISTI, Y. 2001. Tubular photobioreactor design for algal cultures. *Journal of Biotechnology,* 92**,** 113-131.

MOLINA GRIMA, E., ACIÉN FERNÁNDEZ, F. G., GARCÍA CAMACHO, F., CAMACHO RUBIO, F. & CHISTI, Y. 2000. Scale-up of tubular photobioreactors. *Journal of Applied Phycology,* 12**,** 355-368.

MOLINA GRIMA, E., BELARBI, E. H., ACIÉN FERNÁNDEZ, F. G., ROBLES MEDINA, A. & CHISTI, Y. 2003. Recovery of microalgal biomass and metabolites: process options and economics. *Biotechnology Advances,* 20**,** 491-515.

MOLINA GRIMA, E., FERNÁNDEZ, F. G. A., GARCíA CAMACHO, F. & CHISTI, Y. 1999. Photobioreactors: light regime, mass transfer, and scaleup. *Journal of Biotechnology,* 70**,** 231-247.

NAKADA, E., NISHIKATA, S., ASADA, Y. & MIYAKE, J. 1998. Light Penetration and Wavelength Effect on Photosynthetic Bacteria Culture for Hydrogen Production. *In:* ZABORSKY, O., BENEMANN, J., MATSUNAGA, T., MIYAKE, J. & SAN PIETRO, A. (eds.) *BioHydrogen.* Springer US.

NAKAJIMA, Y. & UEDA, R. 1997. Improvement of photosynthesis in dense microalgal suspension by reduction of light harvesting pigments. *Journal of Applied Phycology,* 9**,** 503-510.

OHANIAN, H. C. 1989. Reflection,Refraction, and Polarization. *Physics.* 2nd ed., expanded. ed. ed.: New York: Norton.

OILGAE 2013. Comprehensive oilgae report - Energy from algae: products, market, processes and strategies. India: Oilgae.

PICK, U. & RACHUTIN-ZALOGIN, T. 2012. Kinetic anomalies in the interactions of Nile red with microalgae. *Journal of Microbiological Methods,* 88**,** 189-196.

PROKOP, A., QUINN, M. F., FEKRI, M., MURAD, M. & AHMED, S. A. 1984. Spectral shifting by dyes to enhance algae growth. *Biotechnology and Bioengineering,* 26**,** 1313-1322.

PRUVOST, J., CORNET, J. F., LE BORGNE, F., GOETZ, V. & LEGRAND, J. 2015. Theoretical investigation of microalgae culture in the light changing conditions of solar photobioreactor production and comparison with cyanobacteria. *Algal Research,* 10**,** 87-99.

PULZ, O. 2001. Photobioreactors: Production systems for phototrophic microorganisms. *Applied Microbiology and Biotechnology,* 57**,** 287-293.

QINGNA, Z., YUHONG, D., PENG, W. & XIUJIAN, Z. 2007. CeO2-TiO2/SiO2 Anti-Reflecting and UV-Shielding Double-Functional Films Coated on Glass Substrates Using Sol-Gel Method. *Journal of Rare Earths,* 25**,** 64-67.

RANJBAR, R., INOUE, R., KATSUDA, T., YAMAJI, H. & KATOH, S. 2008. High efficiency production of astaxanthin in an airlift photobioreactor. *Journal of Bioscience and Bioengineering,* 106**,** 204-207.

REBHUN, S. & BEN-AMOTZ, A. 1986. Effect of NaCl concentration on cadmium uptake by the halophilic alga Dunaliella salina. *Marine Ecology Progress Series,* 30**,** 215-219.

REBHUN, S. & BEN-AMOTZ, A. 1988. Antagonistic effect of manganese to cadmium toxicity in the alga Dunaliella salina. *Marine Ecology Progress Series,* 42**,** 97-104.

ROLEDA, M. Y., SLOCOMBE, S. P., LEAKEY, R. J. G., DAY, J. G., BELL, E. M. & STANLEY, M. S. 2013. Effects of temperature and nutrient regimes on biomass and lipid production by six oleaginous microalgae in batch culture employing a two-phase cultivation strategy. *Bioresource Technology,* 129**,** 439-449.

ROWAN, B. C., WILSON, L. R. & RICHARDS, B. S. 2008. Advanced material concepts for luminescent solar concentrators. *IEEE Journal on Selected Topics in Quantum Electronics,* 14**,** 1312-1322.

SÁNCHEZ MIRÓN, A., CONTRERAS GÓMEZ, A., GARCíA CAMACHO, F., MOLINA GRIMA, E. & CHISTI, Y. 1999. Comparative evaluation of compact photobioreactors for large-scale monoculture of microalgae. *Journal of Biotechnology,* 70**,** 249-270.

SAYRE, R. 2010. Microalgae: The Potential for Carbon Capture. *BioScience,* 60**,** 722-727.

SEUNGHYE PARK, Y. L. A. E. J. 2013. Comparison of the responses of two Dunaliella strains, Dunaliella salina CCAP 19/18 and Dunaliella bardawil to light intensity with special emphasis on carotenogenesis. *ALGAE,* 28**,** 203-211.

SIGMA ALDRICH. *Quantum dots* [Online]. Available: http://www.sigmaaldrich.com/materials-science/nanomaterials/quantum-dots.html 2015].

SITEPU, I. R., IGNATIA, L., FRANZ, A. K., WONG, D. M., FAULINA, S. A., TSUI, M., KANTI, A. & BOUNDY-MILLS, K. 2012. An improved high-throughput Nile red fluorescence assay for estimating intracellular lipids in a variety of yeast species. *Journal of Microbiological Methods,* 91**,** 321-328.

SMYTH, C. 2014. *Controlling the Wavelengths of Solar Radiation to Maximise Algal Growth within Algae Photobioreactors.* Fourth Year Research Project, The University of Sheffield.

STAHL, W., SCHWARZ, W. & SIES, H. 1993. Human serum concentrations of all-trans β- and α-carotene but not 9-cis β-carotene increase upon ingestion of a natural isomer mixture obtained from Dunaliella salina (Betatene). *Journal of Nutrition,* 123**,** 847-851.

STEPHENSON, P. G., MOORE, C. M., TERRY, M. J., ZUBKOV, M. V. & BIBBY, T. S. 2011. Improving photosynthesis for algal biofuels: Toward a green revolution. *Trends in Biotechnology,* 29**,** 615-623.

STORMS, Z. J., CAMERON, E., DE LA HOZ SIEGLER, H. & MCCAFFREY, W. C. 2014. A simple and rapid protocol for measuring neutral lipids in algal cells using fluorescence. *Journal of Visualized Experiments*.

THOMPSON, G. A. 1996. Lipids and membrane function in green algae. *Biochimica et Biophysica Acta (BBA) - Lipids and Lipid Metabolism,* 1302**,** 17-45.

TREDICI, M. R. & MATERASSI, R. 1992. From open ponds to vertical alveolar panels: the Italian experience in the development of reactors for the mass cultivation of phototrophic microorganisms. *Journal of Applied Phycology,* 4**,** 221-231.

TROSCH, W., SCHMID-STAIGER, ARMINZASTROW, RETZE, A. & BRUCKER, F. 2003. *Photobioreactor with improved supply of light by surface enlargement, wavelength shifter bars or light transport*.

UYAR, B., EROGLU, I., YÜCEL, M., GÜNDÜZ, U. & TÜRKER, L. 2007. Effect of light intensity, wavelength and illumination protocol on hydrogen production in photobioreactors. *International Journal of Hydrogen Energy,* 32**,** 4670-4677.

VADIVELOO, A., MOHEIMANI, N. R., COSGROVE, J. J., BAHRI, P. A. & PARLEVLIET, D. 2015. Effect of different light spectra on the growth and productivity of acclimated Nannochloropsis sp. (Eustigmatophyceae). *Algal Research,* 8**,** 121-127.

VAN HANDEL, E. 1985. *Rapid determination of total lipids in Mosquito*, Journal of the American Mosquito Control Association.

VAN SARK, W. G. J. H. M., MEIJERINK, A., SCHROPP, R. E. I., VAN ROOSMALEN, J. A. M. & LYSEN, E. H. 2005. Enhancing solar cell efficiency by using spectral converters. *Solar Energy Materials and Solar Cells,* 87**,** 395-409.

WANG, B., LAN, C. Q. & HORSMAN, M. 2012. Closed photobioreactors for production of microalgal biomasses. *Biotechnology Advances,* 30**,** 904-912.

WANG, W. J., SUN, X. T., WANG, G. C., XU, P., WANG, X. Y., LIN, Z. L. & WANG, F. J. 2010. Effect of blue light on indoor seedling culture of Saccharina japonica (Phaeophyta). *Journal of Applied Phycology,* 22**,** 737-744.

WEYER, K., BUSH, D., DARZINS, A. & WILLSON, B. 2010. Theoretical maximum algal oil production. *Bioenergy Research* 3**,** 204-213.

WHITE, A. L. & JAHNKE, L. S. 2002. Contrasting effects of UV-A and UV-B on photosynthesis and photoprotection of β-carotene in two Dunaliella spp. *Plant and Cell Physiology,* 43**,** 877-884.

WONDRACZEK, L., BATENTSCHUK, M., SCHMIDT, M. A., BORCHARDT, R., SCHEINER, S., SEEMANN, B., SCHWEIZER, P. & BRABEC, C. J. 2013. Solar spectral conversion for improving the photosynthetic activity in algae reactors. *Nat Commun,* 4.

XIA, Q., BATENTSCHUK, M., OSVET, A., RICHTER, P., HÄDER, D. P., SCHNEIDER, J., BRABEC, C. J., WONDRACZEK, L. & WINNACKER, A. 2013. Enhanced photosynthetic activity in Spinacia oleracea by spectral modification with a photoluminescent light converting material. *Optics Express,* 21**,** A909-A916.

XU, L., WEATHERS, P. J., XIONG, X. R. & LIU, C. Z. 2009. Microalgal bioreactors: Challenges and opportunities. *Engineering in Life Sciences,* 9**,** 178-189.

YING, K., GILMOUR, D. J. & ZIMMERMAN, W. B. 2014. Effects of CO2 and pH on growth of the microalga Dunaliella salina. *Journal of Microbial and Biochemical Technology,* 6**,** 167-173.

YING, K. G., D.; SHI, S.; AND ZIMMERMAN, W. 2013. Growth Enhancement of Dunaliella salina by Microbubble Induced Airlift Loop Bioreactor (ALB)—The Relation between Mass Transfer and Growth Rate. *Journal of Biomaterials and Nanobiotechnology,* 4 No. 2A**,** 1-9.

ZHU, X.-G., LONG, S. P. & ORT, D. R. 2008. What is the maximum efficiency with which photosynthesis can convert solar energy into biomass? *Current Opinion in Biotechnology,* 19**,** 153-159.

ZIMMERMAN, W. B., HEWAKANDAMBY, B. N., TESAŘ, V., BANDULASENA, H. C. H. & OMOTOWA, O. A. 2009. On the design and simulation of an airlift loop bioreactor

with microbubble generation by fluidic oscillation. *Food and Bioproducts Processing,* 87**,** 215-227.

ZIMMERMAN, W. B., TESAR, V., BUTLER, S. & BANDULASENA, H. C. H. 2008. Microbubble Generation. *Recent Patents on Engineering,* 2**,** 1-8.

ZIMMERMAN, W. B., ZANDI, M., HEMAKA BANDULASENA, H. C., TESAŘ, V., JAMES GILMOUR, D. & YING, K. 2011. Design of an airlift loop bioreactor and pilot scales studies with fluidic oscillator induced microbubbles for growth of a microalgae Dunaliella salina. *Applied Energy,* 88**,** 3357-3369.

APPENDIX

Appendix 1. Rhodamine derivatives

Name of organic dye	**Absorption and emission wavelengths**	**Application area**
Rhodamine B solution		ready-to-use spray and dip reagent for chromatography
Rhodamine B	λ_{ex} 554 nm; λ_{em} 627 nm (Acidic EtOH)	H_2O: soluble1 mg/mL
Rhodamine B isothiocyanate	λ_{max} 555 nm absorption	methanol: soluble10 mg/mL
Rhodamine 6G	λ_{ex} 528 nm; λ_{em} 551 nm in methanol	suitable for fluorescence
	λ_{max} 524 nm abs	Suitable as laser dye
Rhodamine 123		Useful as a laser dye
5(6)-Carboxy-X-rhodamine	λ_{ex} 570 nm; λ_{em} ~595 nm	bioreagent / fluoroscence in nucleic acid
5(6)-Carboxy-X-rhodamine *N*-succinimidyl ester	λ_{ex} 575 nm; λ_{em} 605 nm	bioreagent / fluoroscence
5(6)-Carboxytetramethylrhodamine (TAMRA)	λ_{ex} 543 nm; λ_{em} 572 nm in methanol	bioreagent / fluoroscence
5(6)-Carboxytetramethylrhodamine *N*-succinimidyl ester	λ_{ex} 543 nm; λ_{em} 576 nm in methanol	bioreagent / fluoroscence
5-Carboxy-X-rhodamine *N*-succinimidyl ester	λ_{ex} 575 nm; λ_{em} 600 nm	bioreagent / fluoroscence
Tetramethylrhodamine B isothiocyanate	λ_{ex} 529 nm; λ_{em} 596 nm in DMSO	suitable for fluorescence

Tetramethylrhodamine ethyl ester perchlorate	λ_{ex} 540 nm; λ_{em} 595 nm in DMSO	suitable for fluorescence
Sulforhodamine 101 acid chloride	λ_{ex} 586 nm; λ_{em} 605 nm in H_2O	
Sulforhodamine 101	λ_{ex} 586 nm; λ_{em} 605 nm in H_2O	
Rhodamine 110 chloride	λ_{ex} 498 nm; λ_{em} 520 nm in methanol	suitable for fluorescence
Rhodamine 6G perchlorate	λmax 528 nm abs	Suitable as laser dye
Rhodamine B octadecyl ester perchlorate	λ_{ex} 554 nm; λ_{em} 575 nm in methanol	Suitable as laser dye
Rhodamine 19 perchlorate	λ_{max} 517 nm abs; λem 544 nm in E	Laser dye
Rhodamine 800	λ_{ex} 682 nm; λ_{em} 712 nm in methanol	Suitable as laser dye
Sulforhodamine G	λ_{max} 529 nm abs	Laser dye
Sulforhodamine B	λ_{max} 554 nm	
Fluorescent Red Mega 520	λ_{ex} 527 nm; λ_{em} 663 nm in 0.1 M phosphate pH 7.0	suitable for fluorescence

Appendix 2. Reflection and transmission graphs of Bestoil Red 5B

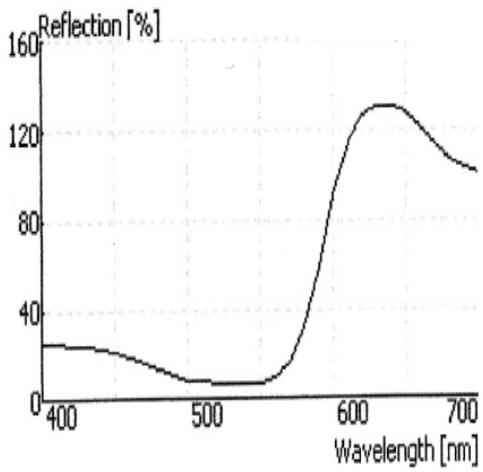

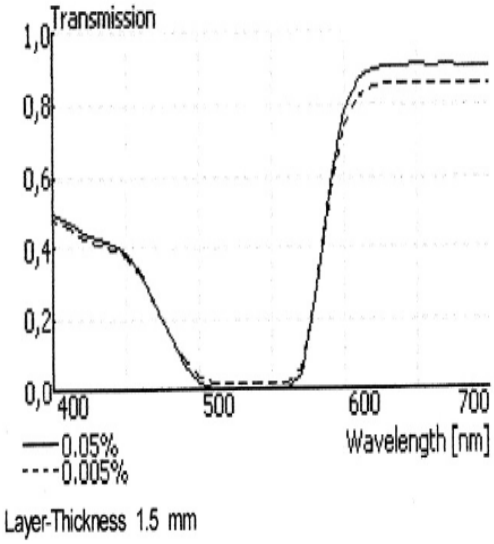

Appendix 3. Reflection and transmission graphs of Bestoil Orange 2G

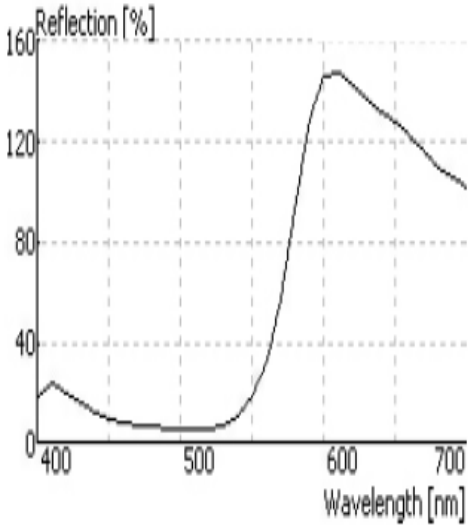

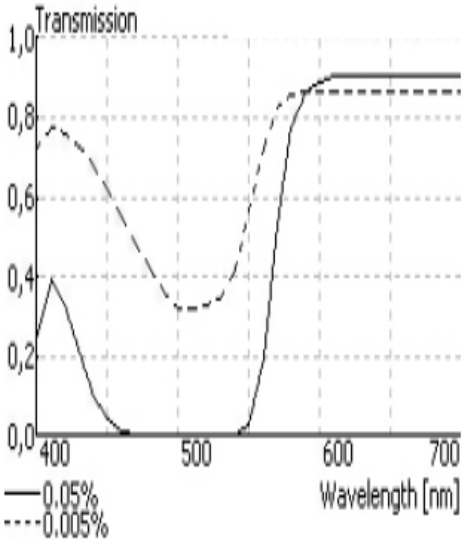

Appendix 4. Organic dyes, polymer material and equipments used for dye coating

- Coumarin 1($C_{14}H_{17}NO_2$) – used as laser dye and supplied from Sigma-Aldrich (Product No: D87759)
- 1,2-Diphenylacetylene ($C_6H_5C{\equiv}CC_6H_5$) – supplied from Sigma-Aldrich (Product No: D204803)
- Bestoil Red 5B - Fluorescent Red and supplied from FastColours (CAS No: 522-75-8). See Appendix 2 for reflection and transmission wavelengths.
- Bestoil Orange 2G - Fluorescent Orange and supplied from FastColours (CAS No: 16294-75-0). See Appendix 3 for reflection and transmission wavelengths.
- THF (Tetrahydrofuran) (C_4H_8O) – Fisher (CAS no: 109-99-9)
- Toluene (C_7H_8) – Fisher (CAS no: 109-88-3)
- Chlorobenzene (99%) (C_6H_5Cl) – Sigma- Aldrich (Product no: 101389)
- PMMA ($[CH_2C(CH_3)(CO_2CH_3)]_n$) – UV transparent polymer base supplied from Sigma-aldrich (Product no: 182265)
- Polystyrene (PS) ($[CH_2CH(C_6H_5)]_n$) - UV transparent polymer base supplied from Sigma- Aldrich (Product no 441147)
- Glass microscope slides - J. Melvin Freed Brand Premium Plain Glass Microscope Slides 2950WX- 003. Dimensions: 75mm x 25mm x 1mm.
- Spin Coater - Technologies Corporation Model WS-400BZ-6NPP/LITE
- Other laboratory equipments are vials, pipette, and balance.

Instruments used for spectral testing are in the following;

- UV/VIS Spectrometer - Ocean Optics USB2000+UV-VIS-ES UV/VIS spectrometer used for absorption wavelength measurement
- UV/VIS Light Source - Ocean Optics UV-VIS-NIR Deuterium Tungsten Halogen with Shutter Light Source. Model DT-MINI-2-G**S**
- SpectraSuit Spectrometer Operating Software – Ocean Optics (Document Number 000-20000-300-02-0607). Parameters are set-up as; integration time – 15, Scans to average – 4, Boxcar width – 4.
- FluoroMax®-4 Spectrofluorometer– Horiba Scientific (Part number 810005 version B) used for emission wavelength measurement.

Appendix 5. Transmission graph of 320 bandpass colour glass filter

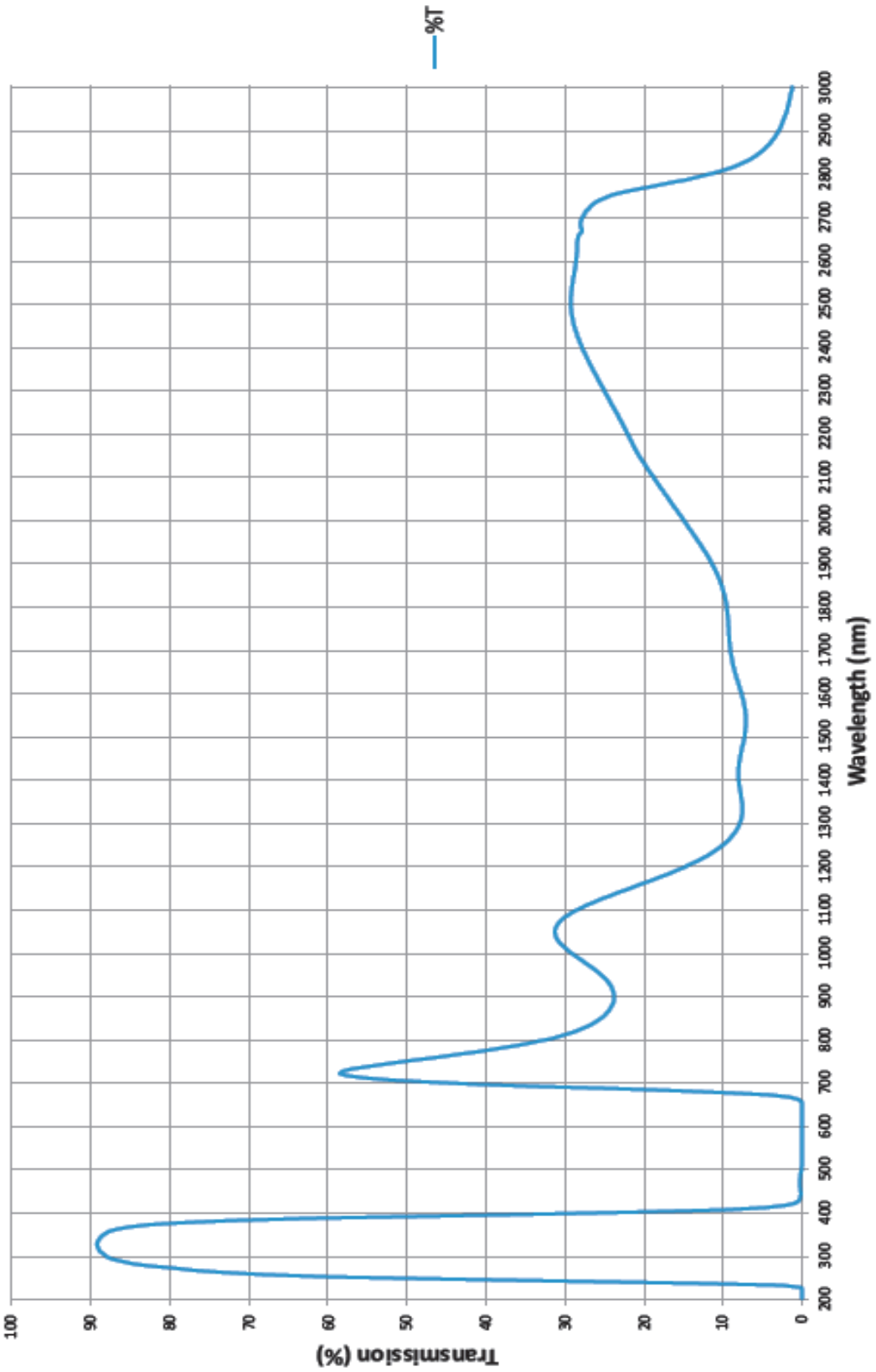

Appendix 6. Proposed aeration system for small scale enclosed air stones to the flasks